

1. Report No. FHWA/TX-86/13+368-1F		2. Government Accession No.		3. Recipient's Catalog No.	
4. Title and Subtitle IN SITU DETERMINATION OF ELASTIC MODULI OF PAVEMENT SYSTEMS BY SPECTRAL-ANALYSIS-OF-SURFACE-WAVES METHOD: PRACTICAL ASPECTS				5. Report Date August 1985	
				6. Performing Organization Code	
7. Author(s) Soheil Nazarian and Kenneth H. Stokoe II				8. Performing Organization Report No. Research Report 368-1F	
9. Performing Organization Name and Address Center for Transportation Research The University of Texas at Austin Austin, Texas 78712-1075				10. Work Unit No.	
				11. Contract or Grant No. Research Report 368-1F	
12. Sponsoring Agency Name and Address Texas State Department of Highways and Public Transportation; Transportation Planning Division P. O. Box 5051 Austin, Texas 78763				13. Type of Report and Period Covered Final	
				14. Sponsoring Agency Code	
15. Supplementary Notes Study conducted in cooperation with the U. S. Department of Transportation, Federal Highway Administration. Research Study Title: "Nondestructive Measurement of Thickness and Elastic Stiffness of Pavement Layers"					
16. Abstract  <p>The Spectral-Analysis-of-Surface-Waves (SASW) method is an in situ testing method for determining shear wave velocity profiles of soil sites and stiffness profiles of pavement systems. The method is non-destructive, is performed from the ground surface, and generally requires no boreholes. The key elements in SASW testing are the generation and measurement of surface waves. Two receivers are located on the ground surface and a transient impact containing a large range of frequencies is transmitted to the soil by means of a simple hammer. One of the most important steps in SASW testing is the inversion process, an analytical technique for reconstructing the shear wave velocity profile.</p> <p>Data collection and analysis used in the SASW technique are discussed in detail. Several case studies are presented to illustrate the utility and versatility of the SASW method. In each case, the results are compared with those of other well-established testing methods performed independently at the same locations. Generally, the shear wave velocity and Young's moduli profiles from these independent methods compare closely.</p>					
17. Key Words Spectral Analysis of Surface Waves, SASW, shear wave velocity profiles, soil sites, stiffness profiles, data collection, analysis, case studies			18. Distribution Statement No restrictions. This document is available to the public through the National Technical Information Service, Springfield, Virginia 22161.		
19. Security Classif. (of this report) Unclassified		20. Security Classif. (of this page) Unclassified		21. No. of Pages 190	22. Price

IN SITU DETERMINATION OF ELASTIC MODULI OF PAVEMENT SYSTEMS  
BY SPECTRAL-ANALYSIS-OF-SURFACE-WAVES METHOD:  
PRACTICAL ASPECTS

by

Soheil Nazarian  
Kenneth H. Stokoe, II

Research Report Number 368-1F

Nondestructive Measurement of Thickness and  
Elastic Stiffness of Pavement Layers  
Research Project 3-8-84-368

conducted for

Texas State Department of Highways and Public Transportation

in cooperation with the  
U. S. Department of Transportation  
Federal Highway Administration

by the

CENTER FOR TRANSPORTATION RESEARCH  
THE UNIVERSITY OF TEXAS AT AUSTIN

August 1985

The contents of this report reflect the views of the authors, who are responsible for the facts and the accuracy of the data presented herein. The contents do not necessarily reflect the official views or policies of the Federal Highway Administration. This report does not constitute a standard, specification, or regulation.

There was no invention or discovery conceived or first actually reduced to practice in the course of or under this contract, including any art, method, process, machine, manufacture, design or composition of matter, or any new and useful improvement thereof, or any variety of plant which is or may be patentable under the patent laws of the United States of America or any foreign country.

## PREFACE

This report is the first report in a series of three reports on the Spectral-Analysis-of-Surface-Waves (SASW method). The second report will be issued on Project 437 and will be a detailed description of the theoretical aspects employed in the SASW technique. The third report will consist of a manual for an interactive computer program called INVERT. This program is essential for determining the stiffnesses of the different layers from the in situ data. In this volume, (Report 1), the practical aspects of SASW testing are described. Many practical examples are provided so that a person not familiar with the method can understand and apply it.

The division of reports on Projects 368 and 437 into three volumes was necessary so that readers with different levels of knowledge or interest could easily access the required material. However, this report has been prepared in a manner that the overall approach and the diversified application of the SASW method can be fully followed without referring to the other reports.

This page replaces an intentionally blank page in the original.

-- CTR Library Digitization Team

## ACKNOWLEDGEMENT

This work was supported by the Texas State Department of Highways and Public Transportation under Research Project 3-8-84-368. The technical assistance and funding support provided by the organization are gratefully acknowledged. The writers specifically wish to thank Messers Gerald Peck, Richard B. Rogers and Kenneth Hankins for their interest, advice and support.

Appreciation is extended to Drs. Alvin H. Meyer, Clark R. Wilson, Roy O. Stearman, Stephen G. Wright and W.R. Hudson for their advice and interest in this work. The writers would also like to thank Tony Ni, Glenn Rix, Ignacio Sanchez, J.C. Sheu, Waheed Uddin and other graduate students at the University of Texas whose valuable assistance during the course of this study accelerated greatly the advancements.

Several other organizations have contributed to the advancement of the technique by their financial and technical assistance. The authors wish to thank,

- T.L. Youd and Mike Bennett from the United States Geological Survey,
- Andy Vicksne and Jerry Wright from the United States Bureau of Reclamation, and
- Captains Joe Amend and J.D. Wilson from the United States Air Force.

This page replaces an intentionally blank page in the original.

-- CTR Library Digitization Team

## ABSTRACT

The Spectral-Analysis-of-Surface-Waves (SASW) method is an in situ testing method for determining shear wave velocity profiles of soil sites and stiffness profiles of pavement systems. The method is non-destructive, is performed from the ground surface, and requires no boreholes. However, if the type of materials is also of interest, one borehole is needed. Measurements are made at strains below 0.001 percent where elastic properties of the materials are independent of strain amplitude. The key elements in SASW testing are the generation and measurement of surface waves. Two receivers are located on the ground surface and a transient impact containing a large range of frequencies is transmitted to the soil by means of a simple hammer. The surface waves are captured and recorded by the receivers using a spectral waveform analyzer. The analyzer is used to transform the waveforms into the frequency domain and then to perform spectral analyses on them. The points of interest from this operation are the phase information of the cross power spectrum and the coherence function. By evaluating the coherence function during testing, the range of frequencies which is not contaminated with random background noise can be quickly identified, so that the quality of the signals being saved for further data reduction is insured. Phase information from the cross power spectrum is indicative of the relative phase shift of each frequency propagating between the two receivers. By knowing the distance between receivers and the phase shift for each frequency, phase velocity and wavelength associated with that frequency are calculated. With this information a dispersion curve can be constructed. A dispersion curve is a plot of phase velocity versus wavelength. By applying an inversion process, an analytical technique for reconstructing the shear wave velocity profile from the dispersion curve, layering and the shear wave velocity and Young's modulus of each layer can be readily obtained. One of the most important steps in SASW testing is the inversion process which has been the missing link in engineering applications.

Data collection and analysis used in the SASW technique are discussed in detail. Several case studies are presented to illustrate the utility and versatility of the SASW method. In each case, the results are compared with those of other well-established testing methods performed independently at the same locations. Generally, the shear wave velocity and Young's moduli profiles from these independent methods compare closely.

## SUMMARY

In this report, improvements in the practical aspects of the Spectral-Analysis-of-Surface-Waves (SASW) method since Research Report 256-4 are presented. The SASW method is used to determine the shear wave velocity and elastic modulus profiles of pavement sections and soil sites. With this method, a transient vertical impulse is applied to the surface, and a group of surface waves with different frequencies are generated in the medium. These waves propagate along the surface with velocities that vary with frequency and the properties of the different layers comprising the medium. Propagation of the waves are monitored with two receivers a known distance apart at the surface. By analysis of the phase information of the cross power spectrum and by knowing the distance between receivers, phase velocity, shear wave velocity and moduli of each layer are determined.

This report contains a comprehensive description of the in situ testing technique and the in-house data reduction procedure used in conducting SASW tests.

This page replaces an intentionally blank page in the original.

-- CTR Library Digitization Team

## IMPLEMENTATION STATEMENT

The Spectral-Analysis-of-Surface-Waves (SASW) method has many applications in material characterization of pavement systems. With this method, elastic moduli and layer thicknesses of pavement systems can be evaluated in situ. The method can be utilized as a tool for quality control during construction and during regular maintenance inspections.

The method can be implemented to evaluate the integrity of flexible and rigid pavements. Reduction of the experimental data collected in situ is fully automated. The inversion process is not automated, as yet. The method has been employed at more than 35 pavement sites to study the precision and reliability of the method. From this study it can be concluded that the thicknesses of different layers are generally within ten percent of those measured from boreholes and the moduli are, on the average, within 20 percent of moduli measured with other independent methods employing in situ seismic techniques.

This page replaces an intentionally blank page in the original.

-- CTR Library Digitization Team

## TABLE OF CONTENTS

	<u>Page</u>
PREFACE	iii
ACKNOWLEDGEMENT	v
ABSTRACT	vii
SUMMARY	ix
IMPLEMENTATION STATEMENT	xi
LIST OF SYMBOLS	xvii
LIST OF TABLES	xix
LIST OF FIGURES	xxi
<b>CHAPTER ONE</b>	
INTRODUCTION	1
1.1 Problem Statement	1
1.2 Organization	2
1.3 Objectives	2
<b>CHAPTER TWO</b>	
BACKGROUND	5
2.1 Introduction	5
2.2 Wave Propagation in a Layered Half-Space	5
1 Seismic Waves	5
2 Characteristics of Surface Waves	5
3 Elastic Constants and Seismic Wave Velocities	8
2.3 Factors Affecting Elastic Moduli	8
1 Soil (or Subgrade)	8
2 Base and Subbase	10
3 Asphalt-Cement Concrete	12
4 Concrete Material	12
2.4 In Situ Methods	14
1 Nondestructive Testing of Pavements	14
2 Seismic Methods	17
2.5 Summary	18
<b>CHAPTER THREE</b>	
HISTORICAL DEVELOPMENTS	19
3.1 Past Investigations	19
3.2 Summary	25

	<u>Page</u>
<b>CHAPTER FOUR</b>	
FIELD PROCEDURE	27
4.1 Introduction	27
4.2 Field Testing	27
1 Advantages of Signal Averaging	29
2 Advantages of Reversing the Source	30
3 Source-Receiver Arrays	30
4.3 Field Equipment	40
<b>CHAPTER FIVE</b>	
IN-HOUSE DATA REDUCTION	43
5.1 Introduction	43
5.2 Construction of a Dispersion Curve	43
1 Theoretical Considerations	43
5.3 Automated Data Reduction	44
5.4 Summary	60
<b>CHAPTER SIX</b>	
INVERSION PROCESS	61
6.1 Introduction	61
6.2 Inversion Process	61
6.3 Comparison with previous Inversion Models	71
6.4 Summary	75
<b>CHAPTER SEVEN</b>	
CASE STUDIES	77
7.1 Introduction	77
7.2 Soil Sites	77
1 Effectiveness of Compaction	78
7.3 Flexible Pavement	83
1 McDill Air Force Base	83
2 Embankment Site	90
7.4 Rigid Pavements	100
1 Columbus Site	100
<b>CHAPTER EIGHT</b>	
SUMMARY, CONCLUSIONS AND RECOMMENDATIONS	113
8.1 Summary	113
8.2 Conclusions	113
8.3 Recommendations for Future Research	114
REFERENCES	117
<b>APPENDIX A</b>	
EQUIPMENT USED IN SASW TESTING	123
A.1 Source	123
A.2 Receivers	126
A.3 Recording Device	131
A.4 Power Supply	140
A.5 Summary	142

	<u>Page</u>
<b>APPENDIX B</b> CONSTRUCTION OF A DISPERSION CURVE FOR A FLEXIBLE PAVEMENT SITE	143
<b>APPENDIX C</b> COMPARISON OF THEORETICAL AND EXPERIMENTAL DISPERSION CURVES AFTER COMPLETION OF INVERSION PROCESS AT WILDLIFE SITE	149
<b>APPENDIX D</b> COMPARISON OF THEORETICAL AND EXPERIMENTAL DISPERSION CURVES AFTER COMPLETION OF INVERSION PROCESS AT A FLEXIBLE PAVEMENT SITE	155

This page replaces an intentionally blank page in the original.

-- CTR Library Digitization Team

## LIST OF SYMBOLS

E	= Young's Modulus
exp	= Exponential
f	= Frequency
FFT	= Fast Fourier Transform
G	= Shear Modulus
i	= $\sqrt{-1}$
$L_{ph}$	= Wavelength
m	= Integer
n	= Integer
$s_n$	= $(k^2 - k_n^2)$
t	= Time
$T_o$	= Fundamental Period
$V_p$	= Compression Wave Velocity
$V_s$	= Shear Wave Velocity
$V_{ph}$	= Phase Velocity
$V_R$	= Rayleigh Wave Velocity
X	= Distance between Receivers
$z_n$	= Depth to Interface n
$\chi^2(f)$	= Coherence Function
$\chi_t$	= Total Unit Weight
$\gamma$	= Shear Strain
$\Delta f$	= Increment of Frequency
$\Delta t$	= Increment of Time
$\epsilon$	= Normal Strain
$\nu$	= Poisson's Ratio
$\pi$	= Pi = 3.14159...
$\rho$	= Mass Density
$\phi_R$	= Raw Phase
$\phi$	= Phase

This page replaces an intentionally blank page in the original.

-- CTR Library Digitization Team

## LIST OF TABLES

<u>Table</u>		<u>Page</u>
2.1	Parameters Affecting Shear Modulus	9
2.2	Characteristics of Common Nondestructive Testing Devices Used on Pavements	15
5.1	Example of Determination of Dispersion Data from Phase Information of Cross Power Spectrum	51
7.1	Comparison of Young's Moduli from SASW and Crosshole Tests	89
7.2	Comparison of Young's Moduli from SASW and Crosshole Methods at at Embankment Site	99
7.3	Comparison of Young's Moduli from SASW and Crosshole Tests at Columbus Site	111

This page replaces an intentionally blank page in the original.

-- CTR Library Digitization Team

## LIST OF FIGURES

<u>Figure</u>		<u>Page</u>
2.1	Variation in Young's Modulus with Strain Amplitude at Different Confining Pressures of an Unsaturated Clay Subgrade	11
2.2	Variation in Normalized Young's Modulus with Strain Amplitude of an Unsaturated Clay Subgrade	11
2.3	Effect of Temperature on Young's Modulus of Asphaltic Concrete Material	13
3.1	Wave Velocity as a Function of Approximate Depth, Showing the Softening of a Base Course by Water (II) and Its Gradual Recovery on Draining (III)	21
3.2	Shear Wave Velocity versus Depth Profile in Rock	22
3.3	Comparison of Theoretical and Experimental Dispersion Curves for a Concrete Layer over Soil	24
4.1	Schematic Diagram of Spectral-Analysis-of-Surface-Waves (SASW) Method	28
4.2	Comparison of Using 5 and 25 Averages to Obtain Representative Spectral Measurements	31
4.3	Schematic of Forward and Reverse Profiles	32
4.4	Comparison of Phase Information of Cross Power Spectrum from Forward and Reverse Profiles	34
4.5	Common Source Geometry	36
4.6	Common Receivers Midpoint Geometry	37
4.7	Dispersion Curves from SASW Tests Performed Using Common Source Geometry at Walnut Creek Site	38
4.8	Dispersion Curves from SASW Tests Performed Using Common Receivers Midpoint Geometry at Walnut Creek Site	39

<u>Figure</u>		<u>Page</u>
4.9	Comparison of Phase Information of Cross Power Spectrum for Different Source-to-Near-Receiver Spacings	41
5.1	Schematic of Automated Data Transfer	45
5.2	Typical Coherence Function and Cross Power Spectrum from Wildlife Site	47
5.3	Unfolded Phase Information of Cross Power Spectrum	48
5.4	Phase Information of Cross Power Spectrum in the Range of Frequencies of 10 to 80 Hz	50
5.5	Dispersion Curve Constructed from Phase Information of Cross Power Spectrum Shown in Figure 7.2b	52
5.6	Dispersion Curve Data After Filtering	53
5.7	Coherence Function and Phase Information of Cross Power Spectrum Measured from Reverse Profile	54
5.8	Comparison of Cross Power Spectra from Forward and Reverse Profiles	56
5.9	Comparison of Dispersion Curves from Forward and Reverse Profiles	57
5.10	Dispersion Curve from All Receiver Spacings for Wildlife Site	58
5.11	Comparison of Dispersion Curves from Two Directions	59
6.1	Example of Output from Computer Program INVERT	64
6.2	Division of Dispersion Curves into Layers for Estimation of Initial Shear Wave Velocity Profile	66
6.3	Initial and Improved Shear Wave Velocity Profiles from First Stage of Inversion	67
6.4	Comparison of Theoretical and Experimental Dispersion Curves from the First Stage of the Inversion Process	68

<u>Figure</u>		<u>Page</u>
6.5	Comparison of Theoretical and Experimental Dispersion Curves after Completion of Inversion Process at Wildlife Site	70
6.6	Shear Wave Velocity Profile from Wildlife Site after Completion of Inversion Process	72
6.7	Comparison of Theoretical and Experimental Dispersion Data from a Site in Nevada Tested by Ballard (1964).	74
7.1	Dispersion Curves from SASW Tests at Compaction Site before Excavation	79
7.2	Shear Wave Velocity Profiles from SASW and Crosshole Tests at Compaction Site before Excavation	80
7.3	Dispersion Curve from SASW Tests at Compaction Site after Backfilling	81
7.4	Comparison of Shear Wave Velocity Profiles at Compaction Site before and after Compaction	82
7.5	Location of Sites Tested at McDill Air Force Base	84
7.6	Composite Profile of Site 3 at McDill Air Force Base	85
7.7	Comparison of Shear Wave Velocity Profiles from SASW and Crosshole Tests at McDill Air Force Base	86
7.8	Comparison of Young's Modulus Profiles from SASW and Crosshole Tests at McDill Air Force Base	88
7.9	Comparison of Shear Wave Velocity Profiles Based on the Second and Third Generations of the Inversion Process	91
7.10	Dispersion Curve from SASW Tests at Embankment Site	91
7.11	Comparison of Shear Wave Velocity Profiles from SASW and Crosshole Tests at Compaction Site	92
7.12	Dispersion Curve from SASW Tests at Embankment Site after Replacement of the Pavement	95

<u>Figure</u>		<u>Page</u>
7.13	Comparison of Dispersion Curves from SASW Tests Performed on Old and New Pavements	96
7.14	Comparison of Shear Wave Velocity Profiles from SASW Tests Performed on Old and New Pavements at Embankment Site	97
7.15	Comparison of Young's Modulus Profile from SASW Tests on New and Old Pavements at Embankment Site	98
7.16	Location of Sites on SH71	101
7.17	Plan View of Testing Locations	102
7.18	Material Profile of Sites Tested at SH71	103
7.19	Dispersion Curves from SASW Tests in May 1982 and August 1984 on CRCP	104
7.20	Shear Wave Velocity Profile at CRCP Site Determined by Initial Inversion Process	106
7.21	Dispersion Curve from SASW Test on CRCP Section in August, 1984	107
7.22	Comparison of Shear Wave Velocities from 1982 and 1984 Tests at Columbus Site	108
7.23	Comparison of Young's Moduli from 1982 and 1984 Tests at Columbus Site	110
A.1	Sources Used in SASW Tests	125
A.2	Elements of a Geophone	127
A.3	Typical Responses of Geophones with Different Damping Ratios	128
A.4	Typical Response of an Accelerometer	130
A.5	Receivers Used in SASW Tests	132
A.6	Hewlett-Packard 5423A Structural Dynamics Analyzer	133
A.7	Default Measurement State of Analyzer	135
A.8	A Typical Measurement State Used in SASW Tests	135

<u>Figure</u>		<u>Page</u>
A.9	Phase Information of Cross Power Spectra from Different Bandwidths	137
A.10	Effect of Bandwidth on Time Domain Records	138
A.11	Effect of Sensitivity of Recording Channels on Time Records	139
A.12	Effect of Pretriggering Delay on Signals	141
B.1	Typical Spectral Analysis Measurements on a Flexible Pavement Site	144
B.2	Dispersion Curve Constructed from Phase Information of Cross Power Spectrum at Pavement Site (from Fig. B.1b)	145
B.3	Comparison of Dispersion Curve from Forward and Reverse Profiles at Pavement Site	146
B.4	Dispersion Curve from All Receiver Spacings for Flexible Pavement Site	147
C.1	Comparison of Theoretical and Experimental Dispersion Curves after Completion of Inversion Process at Wildlife Site (Range of Wavelengths of 3 to 10 ft)	150
C.2	Comparison of Theoretical and Experimental Dispersion Curves after Completion of Inversion Process at Wildlife Site (Range of Wavelengths of 10 to 20 ft)	151
C.3	Comparison of Theoretical and Experimental Dispersion Curves after Completion of Inversion Process at Wildlife Site (Range of Wavelengths of 20 to 35 ft)	152
C.4	Comparison of Theoretical and Experimental Dispersion Curves after Completion of Inversion Process at Wildlife Site (Range of Wavelengths of 35 to 50 ft)	153
C.5	Comparison of Theoretical and Experimental Dispersion Curves after Completion of Inversion Process at Wildlife Site (Range of Wavelengths of 50 to 100 ft)	154

<u>Figure</u>		<u>Page</u>
D.1	Comparison of Theoretical and Experimental Dispersion Curves after Completion of Inversion Process at Pavement Site (Range of Wavelengths of 0.80 to 1.30 ft)	156
D.2	Comparison of Theoretical and Experimental Dispersion Curves after Completion of Inversion Process at Pavement Site (Range of Wavelengths of 1.30 to 1.80 ft)	157
D.3	Comparison of Theoretical and Experimental Dispersion Curves after Completion of Inversion Process at Pavement Site (Range of Wavelengths of 1.50 to 4.50 ft)	158
D.4	Comparison of Theoretical and Experimental Dispersion Curves after Completion of Inversion Process at Pavement Site (Range of Wavelengths of 4 to 8 ft)	159
D.5	Comparison of Theoretical and Experimental Dispersion Curves after Completion of Inversion Process at Pavement Site (Range of Wavelengths of 5 to 20 ft)	160
D.6	Shear Wave Velocity Profile of the Flexible Pavement Site after Completion of Inversion	161

## CHAPTER ONE INTRODUCTION

### 1.1 PROBLEM STATEMENT

In transportation engineering, Young's moduli of pavement systems are utilized in characterizing materials, assessing structural adequacy and evaluating rehabilitation needs. In the last two decades the analytical power employed in the design of major projects has improved substantially. Unfortunately, the capability of determining material properties in situ has not followed this pattern. Very sophisticated constitutive models are incorporated in large finite element programs. However, the lack of accurate material properties many times creates doubts about the feasibility of and justification for employment of these analytical advancements.

The state-of-the-art in measurement of the stiffness of materials consists of laboratory methods such as the resonant column, and cyclic triaxial (resilient modulus) or in situ methods such as the crosshole and downhole seismic tests for soils and the Dynaflect and Falling Weight Deflectometer tests for pavements. The results from laboratory tests usually suffer from factors such as sample disturbance, alteration of state of stress and nonrepresentative samples. Therefore, it is preferable to measure the properties in situ. Seismic methods are under-utilized because of economic, time and personnel considerations. On pavements, nondestructive methods are quite feasible for collecting data in situ, but data reduction techniques have major drawbacks such as nonuniqueness in the results and representation of a dynamic load by a static one.

A seismic method for in situ measurement of shear wave velocity and elastic moduli profiles of soil deposits and pavement systems at small strains (less than 0.001 percent) is presented herein. In this range of strain, moduli are independent of the strain amplitude. The method is called the Spectral-Analysis-of-Surface-Waves (SASW) method. The SASW method is a seismic technique tailored for engineering applications and is based upon generation and detection of elastic stress

waves. The method is fast, economical and requires no boreholes. In addition, the method has the potential for full automation; hence, the need for specialized personnel to perform the test is minimized.

## 1.2 ORGANIZATION

The theoretical background on the propagation of seismic waves in elastic media is presented in Chapter Two. Both body waves and surface waves are presented, but the emphasis is placed on surface waves as generation and detection of surface waves is the basis of this study. In addition, relationships for determining propagation velocities and elastic constants of material along with factors affecting elastic moduli of soils and pavement layers are presented. A literature review of past applications of surface waves is presented in Chapter Three.

A recommended procedure for employment of SASW tests in situ is discussed in Chapter Four. Required equipment and measurement techniques for optimum use are presented in Appendix A.

The data reduction process consists of two phases: construction of an experimental dispersion curve from data collected in situ (considered as raw data), and inversion of the dispersion curve to determine the shear wave velocity profile and eventually elastic moduli. Construction of the experimental dispersion curve and the inversion process are discussed in detail with several illustrative examples for better understanding of the complete process in Chapters Five and Six, respectively.

The SASW method has been employed at over 60 sites nationwide during the last three years. Several illustrative cases are selected and discussed in Chapter Seven to show the versatility and shortcomings of the method.

A brief summary and conclusions along with recommendations for further enhancement of the method are presented in Chapter Eight.

## 1.3 OBJECTIVES

The main objective of this study was to develop a rigorous inversion process. In the past, and even now, an over-simplified process

is used in civil engineering applications. This approximate process is performed by changing the axes of the dispersion curve; the velocity axis is multiplied by a constant in the range of 1 to 1.10 and the wavelength axis is divided by 2 or 3. The results from this process are significantly in error except in the case of near-uniform profiles as shown by work of Heisey (1981) on pavements as well as earlier investigations by the Corps of Engineers and others as reviewed in Chapter Three. The rigorous inversion was successfully developed, as discussed in Chapters Seven and Eight.

Another objective was to apply the SASW method at sites with different properties to investigate experimentally the inversion process which was developed. Over 60 soil and pavement sites and a concrete dam have been tested. From these tests, a new testing pattern was developed to reduce scatter in the experimental dispersion curve. Also, during the course of this study, the process of transferring data collected in the field to the computer has been fully automated.

This work illustrates the applicability of the method for engineering purposes. However, more work is needed to refine this process further in aspects concerning the required equipment and the inversion process in the region of high velocity contrasts.

This page replaces an intentionally blank page in the original.

-- CTR Library Digitization Team

## **CHAPTER TWO BACKGROUND**

### **2.1 INTRODUCTION**

A comprehensive discussion of the theoretical background required to fully understand the various aspects of SASW testing includes discussions of: 1. wave propagation in a layered medium; 2. Fourier transforms and spectral analyses; 3. descriptions of alternative testing techniques; and 4. theoretical characteristics of surface waves (which the study is based upon). Such a discussion is presented in an accompanying report (Nazarian and Stokoe, 1985a). Herein, a brief overview of essential topics is included for completeness. Should more information be required on each topic, the reader is referred to Nazarian and Stokoe (1985a).

### **2.2 WAVE PROPAGATION IN A LAYERED HALF-SPACE**

For engineering purposes, many soil and most pavement sites can be approximated by a layered half-space with reasonable accuracy; especially over short lateral distances. With this approximation, the profiles are assumed to be homogeneous and to extend to infinity in two horizontal directions while being heterogeneous in the vertical direction. This heterogeneity is often modelled by a number of layers with constant properties within each layer. In addition, it is assumed that the material in each layer is elastic and isotropic. The waves are assumed to be plane. A medium characterized by these assumptions is called an ideal medium.

#### **2.2.1 Seismic Waves**

Wave motion created by a disturbance within an ideal whole-space can be described by two kinds of waves: compression waves and shear waves. These waves are collectively called body waves as they travel within the body of the medium. Compression (P) and shear (S) waves can be distinguished by the direction of particle motion relative to the direction of wave propagation.

In a half-space, other types of waves occur in addition to body waves. These waves are called surface waves or Rayleigh waves. Rayleigh waves propagate near the surface of the half-space. Rayleigh waves (R-waves) propagate at a speed of approximately  $90\pm 5$  percent of S-waves. Particle motion associated with R-waves is composed of both vertical and horizontal components, which, when combined, form a retrograde ellipse close to the surface.

### 2.2.2 Characteristics of Surface Waves

In a homogeneous, isotropic, elastic, half-space, the velocity of surface waves does not vary with frequency. However, since the properties of earth materials typically exhibit variations with depth (are not homogeneous vertically), surface wave velocities vary with frequency. This frequency dependency of wave velocity in a heterogeneous medium is termed dispersion, and surface waves are thus said to be dispersive. A plot of wave velocity versus frequency (or wavelength) is called a dispersion curve.

The dispersive characteristic of a wave can be demonstrated by means of phase velocity. Phase velocity is defined as the velocity with which a seismic disturbance of a given frequency is propagated in the medium over the horizontal distance between the source and receivers.

The study of dispersion of waves in a horizontally-layered half-space relies upon derivation of the so-called dispersion function (i.e., the relationship between phase velocity and frequency). Thomson (1950) and Haskell (1953) introduced the first matrix solution to this problem.

In the classical approach, the dispersion function and wavelengths (or frequencies) are obtained by vanishing a determinant whose elements are functions of mass densities and elastic moduli of the layers as well as phase velocity and frequency.

The Haskell-Thomson technique builds up the (surface wave) dispersion function as the product of layer matrices which relate the displacement components as well as the stress components acting on the interface to those associated with the next interface. The product of

these layer matrices then relates the stress and displacement components of motion at the deepest interface to those at the free surface. However, the Haskell-Thomson solution exhibits numerical difficulties at high frequencies. Dunkin (1965) presented a new approach to circumvent these numerical difficulties. Thrower (1965) also proposed an approach which is more appropriate for determination of dispersion curves in layered media such as pavements where the layers become gradually softer. The last two approaches are used in this study. These different approaches are discussed in full detail in Nazarian and Stokoe (1985a).

The shape of a dispersion curve is affected by three independent properties of the material composing each layer for a given profile. These properties are: (i) shear wave velocity, (ii) Poisson's ratio, and (iii) mass density. It is demonstrated (Nazarian and Stokoe, 1985a) that the effect of the last two parameters on dispersion of waves is quite small. Therefore, only the effect of shear wave velocity is discussed herein.

In an elastic medium, surface waves are dispersive only if a velocity contrast exists in the layering. At short wavelengths, the phase velocities are close to the R-wave velocity of the top layer. In other words, for waves with short wavelengths (relative to the height of the layers) the half-space has very little effect on the dispersion curve. For these short wavelengths, the top layer acts like a half-space by itself.

The other extreme involves long wavelengths. In this case phase velocities are quite close to the R-wave velocity of the last layer which means that the top layers do not have an appreciable affect on the dispersion curve. However, between these two extremes there is a transition zone in which the phase velocity is bound between the R-wave velocities of the least stiff and stiffest layers in the profile. The extent of this transition zone in the intermediate wavelengths depends on the velocity contrast between the layers.

The topics introduced in this section are detailed in Nazarian and Stokoe (1985a). It is recommended that the reader refer to that reference for more information on these matters.

### 2.2.3 ELASTIC CONSTANTS AND SEISMIC WAVE VELOCITIES

In transportation engineering for material characterization and the design of overlays, Young's moduli of the different layers should be measured. Calculation of elastic moduli from propagation velocities is, thus, important.

Shear wave velocity,  $V_s$ , is used to calculate shear modulus,  $G$ , by:

$$G = \rho \cdot V_s^2 \quad (2.1)$$

in which  $\rho$  is the mass density. Mass density is equal to,  $\gamma_t/g$ , where  $\gamma_t$  is total unit weight of the material and  $g$  is gravitational acceleration. If Poisson's ratio (or compression wave velocity) is known, other moduli can be calculated for a given  $V_s$ . Young's and shear moduli are related by:

$$E = 2G (1 + \nu) \quad (2.2)$$

## 2.3 FACTORS AFFECTING ELASTIC MODULI

### 2.3.1 Soil (or Subgrade)

Based upon numerous laboratory tests, Hardin and Drnevich (1972) proposed many parameters that affect the moduli of soils. These parameters, along with their degree of importance in affecting moduli, are tabulated in Table 2.1. They suggested that state of stress, void ratio, and strain amplitude are the main parameters affecting moduli measured in the laboratory. However, for this study dealing with measurement of moduli in situ, the main factors affecting the elastic moduli and wave velocities are void ratio and state of stress (confining stress).

Table 2.1. Parameters Affecting Shear Modulus (from Hardin and Drnevich, 1972).

Parameter	Importance <sup>a</sup>	
	Clean Sands	Cohesive Soils
Strain Amplitude	V	V
Effective Mean Principle Stress	V	V
Void Ratio	V	V
Number of Cycles of Loading	R <sup>b</sup>	R
Degree of Saturation	R	V
Overconsolidation Ratio	R	L
Effective Strength Envelope	L	L
Octahedral Shear Stress	L	L
Frequency of Loading	R	R
Other Time Effects (Thixotropy)	R	L
Grain Characteristics	R	R
Soil Structure	R	R
Volume Change Due to		
Shear Strain	V	R

a) V means Very Important, L means Less Important, R means Relatively Unimportant, and U means relative importance is not known at the time.

b) Except for saturated clean sand where the number of cycles of loading is a less Important Parameter.

Strain amplitude has essentially no effect on the in situ tests because the measurements are performed at very low strains. Up to a strain amplitude of about 0.01 percent, moduli are nearly constant, with a slight decrease in the range from 0.001 to 0.01 percent. This constant modulus is called the elastic modulus, or maximum modulus. Above a strain level of 0.01 percent, moduli decrease significantly. A typical example of the variation in Young's modulus,  $E$ , with normal strain,  $\epsilon$ , for a stiff clay is shown in Figs. 2.1 and 2.2. An undisturbed sample of stiff clay from San Antonio, Texas was tested using the resonant column method (Richart et al, 1970). The variation of  $E$  with  $\log \epsilon$  at several confining pressures is shown in Fig. 2.1. As the confining stress increases, the low-amplitude modulus increases, as shown in this figure. Also, it is evident that below strain levels of 0.001,  $E$  is constant and independent of strain at each pressure.

The effect of strain on modulus is easily seen by plotting the variation of normalized modulus,  $E/E_{\max}$ , versus  $\log \epsilon$  as shown in Fig. 2.2. In this figure,  $E_{\max}$  is taken as the maximum value of Young's modulus at each confining pressure. It can be seen that normalized modulus is constant below a strain of about 0.001 percent and is equal to  $E_{\max}$ . Also, all modulus-strain curves are nearly independent of confining pressure once they are normalized. If a normalized modulus-strain curve such as that shown in Fig. 2.2 is available for the material, then moduli at higher strains can be determined once  $E_{\max}$  has been measured.

### 2.3.2 Base and Subbase

Two types of base and subbase materials are usually used, granular or treated materials. Granular base and subbase materials demonstrate the same characteristic as natural soil deposits. The base or subbase material are sometimes treated by additives such as cement, bitumen, or lime. In this situation, the moduli of the layer depends on additional factors such as type of aggregate and percentage of additive. Typical values of Young's moduli for granular and treated layers are in the range of 15 to 110 ksi (100 to 750 MPa) and 50 to 2000 ksi (350

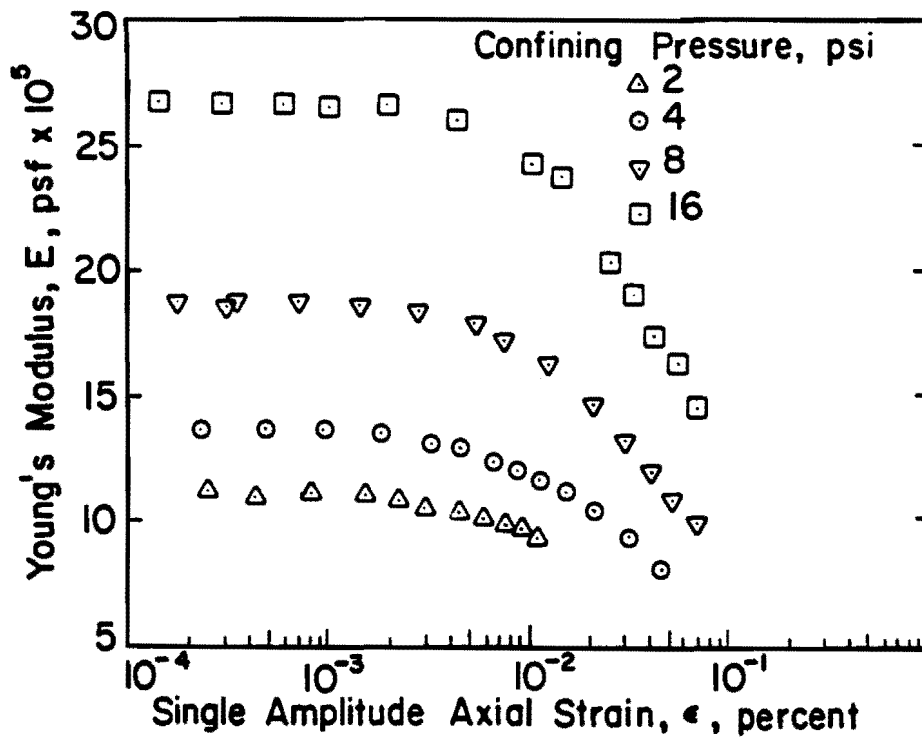


Figure 2.1 - Variation in Young's Modulus with Strain Amplitude at Different Confining Pressures of an Unsaturated Clay Subgrade.

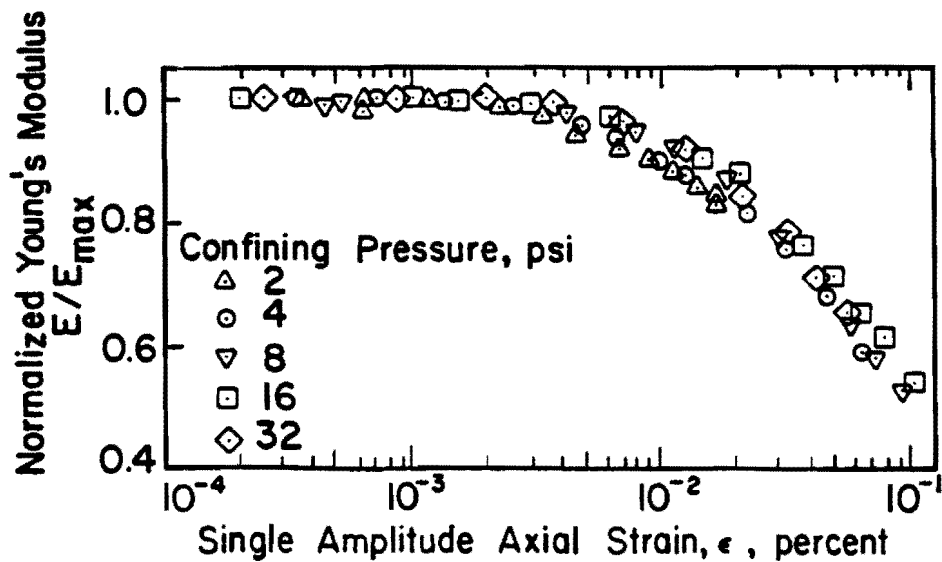


Figure 2.2 - Variation in Normalized Young's Modulus with Strain Amplitude of an Unsaturated Clay Subgrade.

to 14000 MPa), respectively. Poisson's ratio of these materials are on the order of 0.20 to 0.45 (Yoder and Witczak, 1975).

### 2.3.3 Asphalt-Cement Concrete

The main factor that affects the moduli of asphaltic materials, besides the mixture properties, is temperature. Typical variation of elastic moduli with temperature is shown in Fig. 2.3 for a bitumenous sample. As the temperature increases the material behaves less viscously resulting in a decrease in the modulus (Van der Poel, 1954). The age of the material affects the modulus; with time, asphaltic materials become stiffer. The other factor that has some effect on the asphaltic material is the level of strain (or stress). The variation of modulus with strain level is similar to the effect of temperature; that is, the modulus decreases with increase in strain level. Unfortunately, no figure indicating the trend of this variation could be found in the literature, but it seems that the asphaltic material should behave somewhat like the soil samples shown in Fig. 2.1 and 2.2. Typical values of Young's modulus and Poisson's ratio of asphaltic material are in the range of 200 to 1100 ksi (1400 to 7700 MPa) and 0.25 to 0.40, respectively. Total unit weight of this material is on the order of 125 to 145 pcf (19 to 23 kN/m<sup>3</sup>). The shear wave velocity of asphaltic material is in the range of 1700 to 4200 fps (500 to 1200 m/sec).

### 2.3.4 Concrete Material

The factors that affect the modulus of concrete, ignoring the method of preparation, consolidation and curing, are type of aggregate and water-cement ratio. The concrete used in overlay of roads and runways are of high quality and are very stiff, and it is expected to behave elastically under most of the loads imposed by vehicular traffic. The elastic modulus of concrete as reported by Yoder and Witczak (1975) ranges from 3000 to 6000 ksi (21 to 42 GPa) and Poisson's ratio varies from 0.10 to 0.25. The unit weight of concrete is typically 140 to 150 pcf (21 to 23 kN/m<sup>3</sup>). Values of compression wave velocity for concrete range from 10,000 to 14,000 fps (3000 to 4300 m/sec).

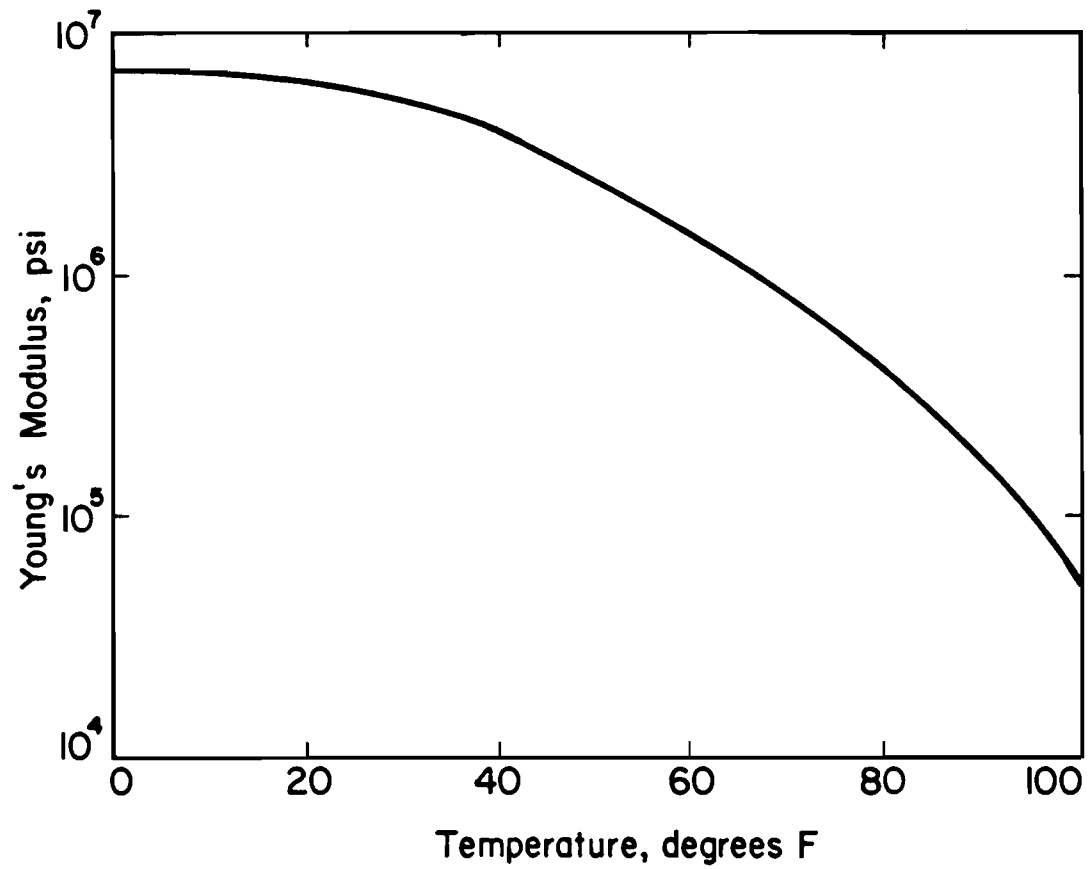


Figure 2.3 - Effect of Temperature on Young's Modulus of Asphaltic Concrete Material (inferred from Van der Poel, 1954).

## 2.4 IN SITU METHODS

Properties of materials are either measured in the laboratory or in situ, or are determined by empirical methods. Normally, values from laboratory tests underestimate the in situ results by anywhere from 10 to several hundred percent. The major reasons for this discrepancy can be due to sampling disturbance, differences in the state-of-stress between the sample and actual deposits, nonrepresentative samples, long-term time effect, and inherent errors in in situ tests (Anderson and Woods, 1975). Laboratory tests are essential to study the parameters that affect the properties of the material. In situ tests are more suitable for determining accurate values of low-amplitude dynamic properties in the field. However, in situ methods are under-utilized as they are expensive and highly specialized personnel are often required to perform them.

### 2.4.1 Nondestructive Testing of Pavements

Nondestructive testing of pavements is done by making surface measurements of the response of a pavement structure to an external force. The response is generally in terms of measurement of surface deflection at several points. Elastic theory in a layered medium is then employed to back-calculate the elastic properties of different layers.

Lytton et al (1975) studied different nondestructive methods in some detail. The major differences between different methods is the way the load is imparted to the pavement and the number and position of points at which deflections are measured. The characteristics of some deflection measuring devices are presented in Table 2.2. The methods that are based upon application of static loads consist of the Plate loading test, Benkelman beam, traveling deflectometer, Lacroix deflectograph, and curvature meter (see Haas and Hudson, 1978). Vibratory nondestructive methods apply a steady-state load to the pavement surface after applying some static seating load. The main devices in this category are Dynaflect, road rator, Waterways Experiment Station (WES) vibrator, and Federal Highway Administration (FHWA) thumper.

Table 2.2. Characteristics of Common Nondestructive Testing Devices Used on Pavement (from Eagleson, 1981).

Device	Static Load lbf	Dynamic Load lbf	Loading Concept	Load Frequency, Hz	Number of Deflection Sensors*	Spacing,+ in.
(1)	(2)	(3)	(4)	(5)	(6)	(7)
Benkelman Beam	Variable Single Axle Load	—	Static	—	1	—
Dynalect	1000	1000	Counter- rotating Weights	8	5	12
Road Rator	1500-7000	1000-8000	Electro- hydraulic Vibrator	10-80	4	12
Falling Weight Deflectometer	Variable	1500 to 24000	Drop Weight	Wide Range**	5 to 7	12

\* Sensors are velocity transducers except for Benkelman Beam where a dial gauge is used.

\*\* Duration of about 25 msec.

+ Between adjacent receivers.

Devices that use an impact as the source are the falling weight deflectometer, California (CAL) impulse testing, and Washington State University impulse testing, although the WES vibrator, FHWA thumper and road rator can also be used as impact (or static) devices.

Two devices which are widely used today to nondestructively test pavements are the Dynaflect and falling weight deflectometer. In the Dynaflect device, a peak dynamic force of 1000 lb (4500 N) is generated by two counter-rotating eccentric masses at a frequency of 8 Hz. This force is transmitted to the pavement by two, 4-in. (10-cm) wide wheels. Five equally spaced geophones are used to measure deflections of the pavement system due to the load.

The falling weight deflectometer (FWD) is different from the dynaflect device in terms of field testing procedure. The differences are basically in the number of receivers, as seven geophones are used, and the load. The load is developed by dropping a weight on a plate set on the pavement surface. The energy of the impact can be varied by changing the drop height or drop weight. The peak loading force varies from 1.5 to 24 kips (6.6 to 106 kN). The duration of impulse is around 25 to 30 msec, which simulates the duration of a load imposed by a moving wheel at 40 mph (64 km/h).

In the analysis of the load-deflection measurements, both the Dynaflect and FWD are similar. The pavement is modelled as a multi-layered linear elastic system, and each layer is characterized by Young's modulus and Poisson's ratio. A computer program based upon linear elastic theory with static loading is then used to predict the deflections at the measurement points. Computed and measured deflections are compared, and necessary adjustments in the value of the elastic modulus of each layer are made until measured and computed deflections compare well. This process is called "deflection-basin fitting."

The major assumptions in the deflection-basin fitting approach are:

1. the layers are assumed to be elastic,
2. the dynamic load can be replaced by an equal static load,

3. measured dynamic deflections are assumed equal to theoretical static deflections, and
4. the pavement layers extend horizontally to infinity, and
5. the subgrade has constant stiffness and is extended to infinity or to a rigid layer underlying the subgrade at some depth.

The main advantages of these two methods are mobility and rapid testing in the field. However, these methods do not yield a unique solution as several combinations of moduli can be determined to produce a theoretical basin which matches the experimental deflection basin. This nonuniqueness becomes more pronounced as the number of layers assumed in the theoretical profiles is increased. As such, the number of layers are normally limited to three or four and the thickness of each layer must be assumed.

#### **2.4.2 Seismic Methods**

Seismic methods are normally performed at low-strain levels. Low-strain moduli are presently the most important dynamic property of soils measured in the field. Once this parameter is combined with laboratory tests, values of moduli in the field at different strain levels can be obtained. Several different procedures to predict the in situ shear modulus-strain relationship based upon field and laboratory tests have been proposed (Stokoe and Richart, 1973; Anderson and Woods, 1975; and Stokoe and Chen, 1980). A detailed discussion on the sources of differences between in situ and laboratory results; methods of estimating the in situ shear moduli from laboratory tests; and other in situ tests such as the standard penetration tests (SPT) and cone penetration test (CPT) which have also been used to estimate modulus-strain relationships can be found in Hoar (1982).

Common methods used for in situ measurement of propagation velocities and moduli at low strains are discussed in Nazarian (1984). The state-of-practice in field seismic measurements for engineering purposes have been reviewed by Richart (1978), Woods (1978), Geophysical Exploration by U.S. Corps of Engineers (1979), Stokoe (1980), and Hoar (1982).

## 2.5 SUMMARY

In this chapter, the different types of waves that propagate in a layered medium are presented. Waves of most importance to this study are compression, shear and Rayleigh waves. The propagation velocities of these waves are defined, and the relationship of material stiffness to propagation velocities are presented. Also factors that affect the stiffness of different types of materials such as soil, asphalt-cement concrete, and portland-cement concrete are discussed. In soils, strain amplitude has the most effect on elastic moduli, but it can be neglected in this study as testing is being performed in the low-strain range where moduli are independent of strain. Therefore, the major parameters that affect moduli of soils are void ratio and state of stress. Temperature and age are parameters that affect moduli the most for asphalt concrete, while for portland-cement concrete type of aggregates, water-cement ratio and curing are the significant factors.

## CHAPTER THREE HISTORICAL DEVELOPMENTS

### 3.1 PAST INVESTIGATIONS

The first known use of surface waves to determine soil properties for engineering purposes was credited to the German Society of Soil Mechanics before World War II (DEGEB0, 1938). The primary interest of that study was to investigate the response of a foundation to steady-state vibration. A rotating-mass oscillator was used as a source to excite foundations in the range of frequencies between 10 and 60 Hz. Due to the lack of sensitive receivers in that period, excessive loads had to be imposed on the soil to generate adequate signals. As a result, nonlinear behavior was generated in the soil and somewhat unsuccessful application of the method occurred.

Bergstrom and Linderholm carried out similar tests in Sweden in 1946. This work was done on a fairly uniform soil which resulted in the surface waves exhibiting little dispersion in the study range of 14 to 32 Hz. They compared Young's moduli determined from surface wave and plate bearing tests in an attempt to correlate the modulus of subgrade reaction with Young's modulus. Plates with different diameters were used in the plate bearing tests. They found that the moduli of subgrade reaction from the large-diameter plates correlated well with the dynamic moduli from the surface wave tests. However, results from the smaller-diameter plates did not yield any appreciable relationship between the subgrade and dynamic moduli.

Van der Poel (1951) and Nijboer and Van der Poel (1953) investigated a flexible pavement system in Holland using surface waves. The range of frequencies in their tests was 10 to 60 Hz which corresponded to waves predominantly propagating in the subgrade soil.

Henkelom and Klomp (1962) used steady-state vibrators to perform surface wave tests on pavements. Mechanical and electrodynamic vibrators were used to generate low frequency (4 to 60 Hz) and high frequency (greater than 60 Hz) waves in their tests. The effect of drainage of the subgrade after a flood was investigated. The S-wave velocity pro-

files from their investigation are shown in Fig. 3.1. The material profile of the site, which was located on a runway, was not described; however, the layering in the profile is shown graphically in the figure. The ordinate which is titled as the approximate depth in Fig 3.1, corresponds to one-half of the wavelength at each frequency. The abscissa is equal to the phase velocity determined at each frequency. In other words, they assumed an effective depth of sampling equal to  $1/2$  of the wavelength and a shear wave velocity equal to the phase velocity at each frequency. The curve denoted as I in the figure is the  $V_s$  profile from a test performed when the base course was "half-way finished". The second and third curves (marked as II and III) respectively, are from tests carried out after the finishing of the base and after the wearing course had been placed. Apparently, due to the seasonal precipitation, the site was flooded, and the near-surface material became substantially softer (curve II, in Fig. 3.1). From the third test (curve III) they concluded that as the water content of the material decreased the stiffness increased. Unfortunately, they could not excite high enough frequencies to sample the pavement layers under investigation.

The U.S. Army Engineer Waterways Experiment Station (WES) has used steady-state vibrations to determine elastic properties of in situ soils over the past 20 to 25 years. Ballard (1964), Fry (1965), Maxwell and Fry (1967), Ballard and Casagrande (1967), Cunny and Fry (1973), and Ballard and Chang (1973), among others, investigated numerous sites with the surface wave technique. The tests were carried out according to specifications set by WES which are described in detail by Maxwell and Fry (1965). The sources were either electromagnetic vibrators (for generating high frequencies) or mechanical vibrators using counter-rotating eccentric masses to generate low frequencies (up to 60 Hz). The WES procedure for obtaining the shear wave velocity profile from phase-velocity/wavelength data is identical to that of Henkelom and Klomp (1962), just discussed. As an example, the shear wave velocity profile from a site located in Buckboard Mesa, Nevada investigated by Fry (1965) is shown in Fig. 3.2. The site consists of a layer of residual soil that gradually turns into dense basalt. The approximate

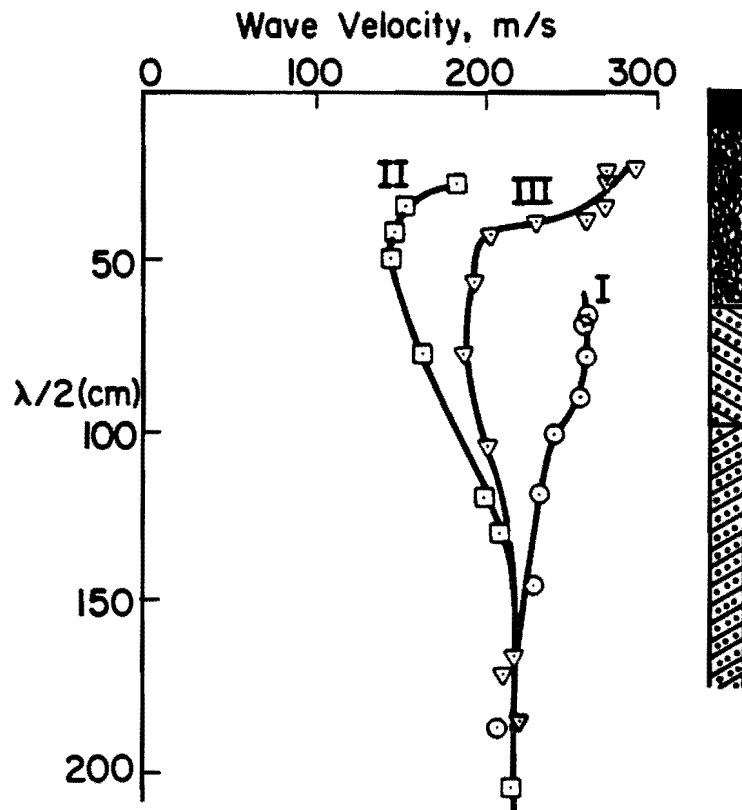


Figure 3.1 - Wave Velocity as a Function of Approximate Depth, Showing the Softening of a Base Course by Water (II) and its Gradual Recovery on Draining (III), (from Henkelom and Klomp, 1962).

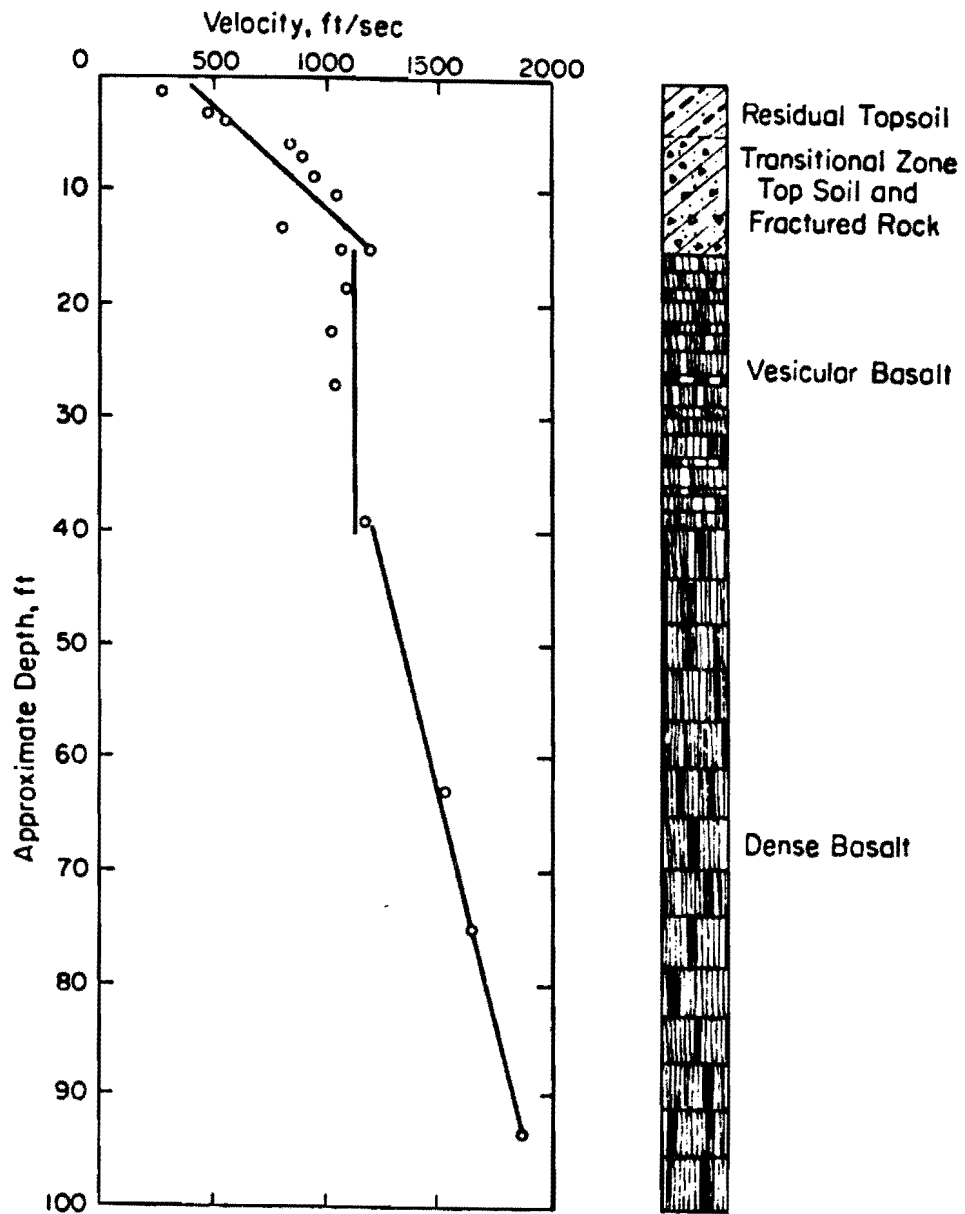


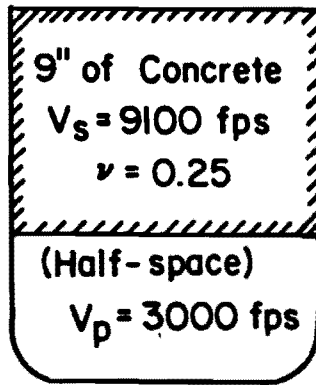
Fig. 3.2 - Shear Wave Velocity versus Depth Profile in Rock (after Fry, 1965).

depths correspond to one-half of the wavelengths, and the shear wave velocities are assumed to be identical to propagation velocities measured in situ. Cunney and Fry (1973) compared in situ elastic moduli from surface waves tests with moduli obtained by resonant column tests at 14 sites. Cunney and Fry concluded that the laboratory-determined shear and Young's moduli were generally within  $\pm 50$  percent of the in situ moduli. Woods and Richart (1967) performed a series of surface wave tests in conjunction with a testing program set up to study the effect of trenches in screening elastic waves. They followed the procedure proposed by WES.

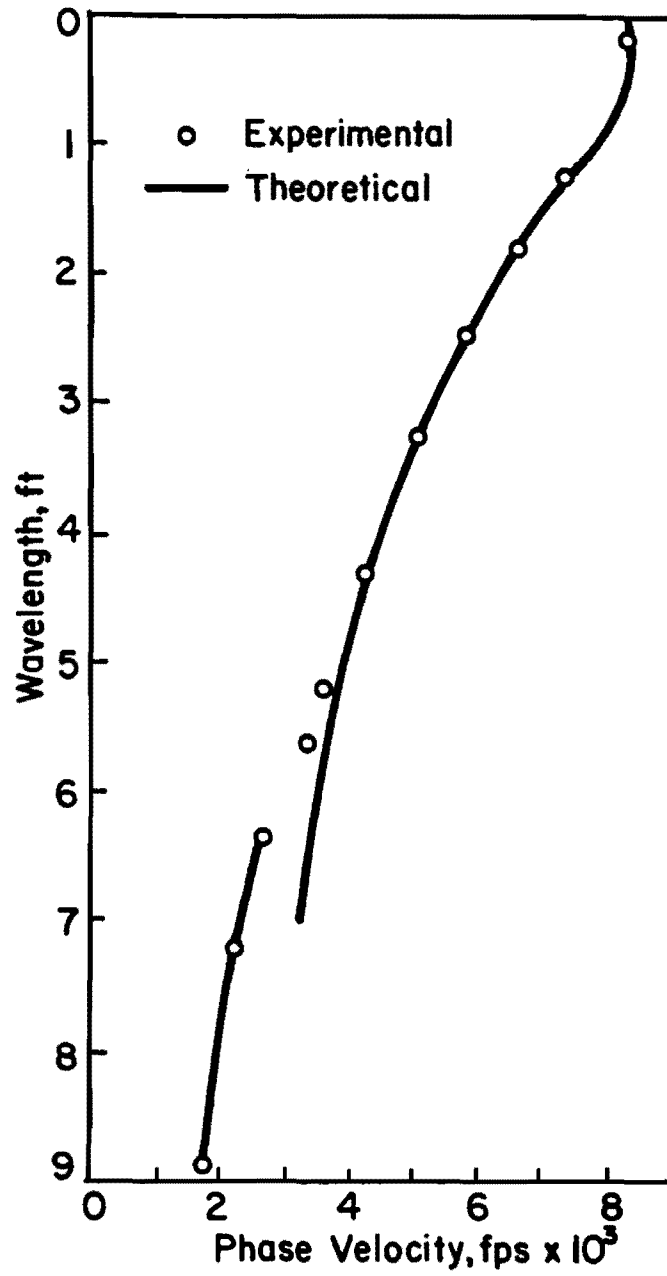
The greatest recent contribution in theoretical and practical aspects of surface wave testing on pavements was by Jones (1958). He proposed an analytical procedure to compute the moduli of different layers in a pavement system. An example of his investigation on a pavement section consisting of a 9-in. (23-cm) thick (nominally) concrete layer over subgrade is shown in Fig. 3.3. He assumed that the subgrade was a liquid layer and treated the concrete slab as a plate. From his study he reported the thickness of the concrete as 9.5 in. (24 cm). Upon coring, the concrete thickness was found to be quite close to 9.5 in. (24 cm).

Four groups of investigators have employed the spectral analysis of surface waves principles to collect data in situ. Williams (1981) used a vibrator connected to broad-band noise-generator (as opposed to a sine wave-generator) and a hammer as sources. These two sources, and sources similar to them, have the ability to generate waves over a wide range of frequencies. If the waves generated by these sources are captured on an appropriate recording device, Fourier transformed, and spectral analysis performed on them, the testing time can be reduced quite significantly (see Chapter Four). Williams' interest was solely limited to constructing the experimental dispersion curves, and he did not report any shear wave velocity profile.

Heisey (1981) used hammer blows to generate transient signals to construct the dispersion curves. He used a spectral analyzer as the recording device which accelerated the in-house data reduction several



a. Material Profile



b. Dispersion Curves

Figure 3.3 - Comparison of Theoretical and Experimental Dispersion Curves for a Concrete Layer over Soil (from Jones, 1958).

folds over Williams' approach (a tape recorder). Based upon tests on several soil and pavement sites, Heisey suggested an effective depth of sampling equal to  $1/3$  of the wavelength for each frequency. He also divided the surface wave velocities measured in the field by a factor approximately equal to 0.90 to obtain shear wave velocities.

Neilson and Baird (1975, and 1977) and Baird (1982) from the New Mexico Engineering Research Institute constructed a van to collect surface wave data conveniently. This van consists of a system operators area and a support equipment area. A data acquisition system along with a system to control the deployment of an impact system are located in the system operators area. The support equipment area houses a 215-lb (950-N) programmable drop weight and two generators. The height of the drop and the weight of the loading system can be changed. The drop weight impacts a 12-in. (30-cm) diameter plate. The impulses are simultaneously monitored with as many as eight accelerometers. The data reduction is arbitrary and requires empirical correction factors to obtain moduli of the different layers.

### 3.2 SUMMARY

In summary, in all the investigations reported above, in situ testing procedures may differ; however, invariably the goal is to determine the relationship between the propagation velocity of surface waves and wavelengths, called a dispersion curve. The next step is then to obtain a shear wave velocity-depth relationship based upon the dispersion information. In all the studies [except Jones (1958)], the dispersive characteristic of surface waves was neglected which caused an inaccuracy in the values of shear wave velocities. The reason for this inaccuracy and an alternative process for determining the shear wave velocity profile from a given dispersion curve are presented in Chapter Six.

This page replaces an intentionally blank page in the original.

-- CTR Library Digitization Team

## CHAPTER FOUR FIELD PROCEDURE

### 4.1 INTRODUCTION

With the SASW method, both the source and receivers are located on the surface of a site. Surface waves at low-strain levels are then generated and detected with this equipment. A complete investigation of each site consists of the following phases:

1. field testing,
2. determination of the dispersion curve, and
3. inversion of the dispersion curve.

The first phase, the experimental procedure used in collecting in situ data, is discussed herein. In addition different factors affecting the tests are discussed. The equipment required to perform the test is presented in Appendix A.

### 4.2 FIELD TESTING

The testing configuration used in the field is shown in Fig. 4.1. To perform a test, the steps are as follows:

1. An imaginary centerline for the receiver array is selected.
2. Two receivers are then placed on the ground surface an equal distance from the centerline (Section A.2).
3. A vertical impulse is applied to the ground by means of a hammer (Section A.1). A major portion of the various types of stress waves generated by the impulse propagates as surface waves of various frequencies.
4. Impulses are delivered several times, and the signals are averaged together (Section 4.2.1).
5. After testing in one direction is completed, the receivers are kept in their original positions, but the source is moved to the opposite side of the imaginary centerline. The test is then repeated (Section 4.2.2).
6. The same procedure (steps 2 through 5) is repeated for other receiver spacings (Section 4.2.3).

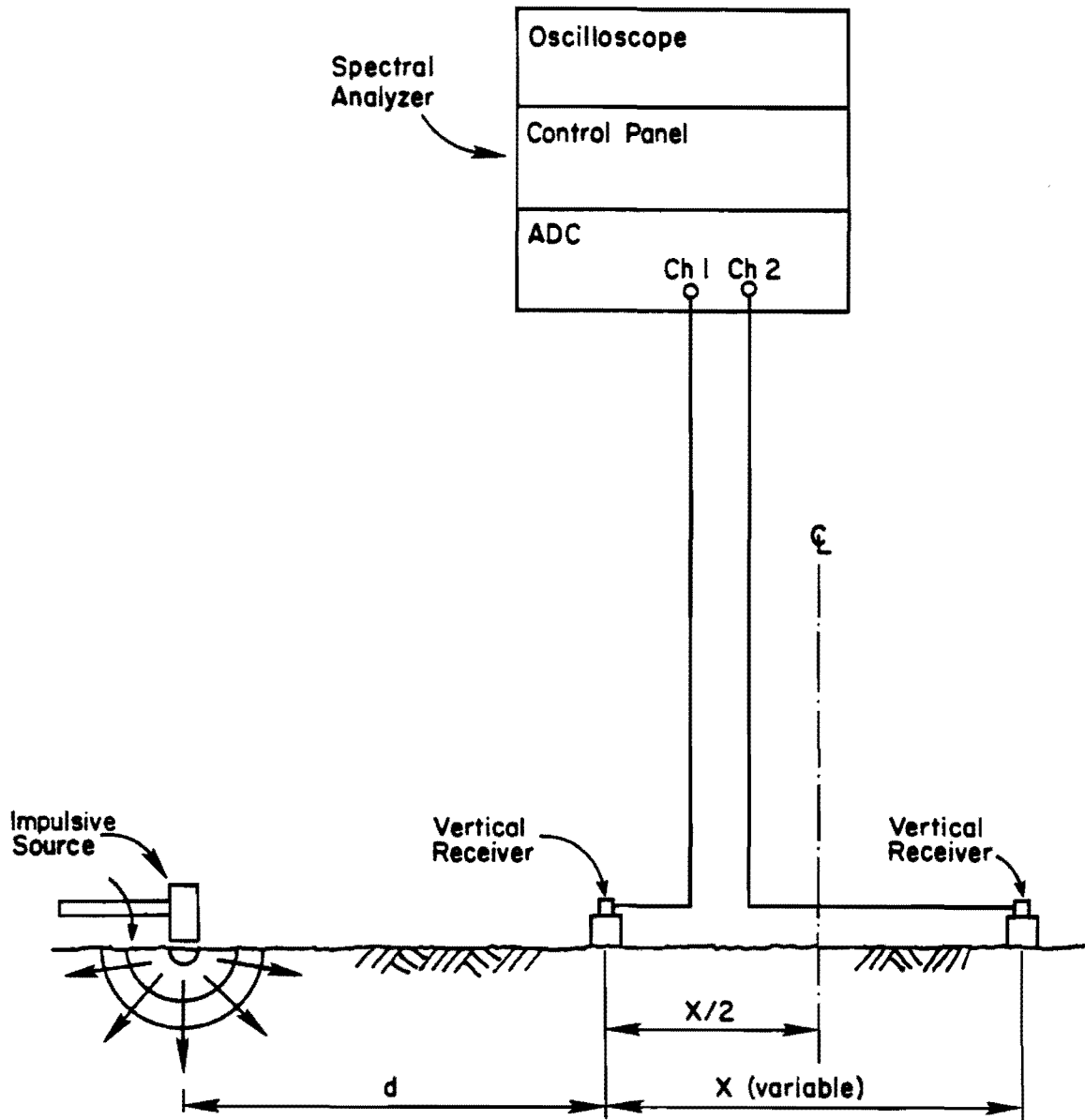


Figure 4.1 - Schematic Diagram of Spectral-Analysis-of-Surface-Waves (SASW) Method.

7. The records are monitored by a spectral analyzer and saved on magnetic tape for further reference and data reduction after the spectral functions are obtained and inspected (Section A.3).

#### 4.2.1 Advantages of Signal Averaging

Most spectral-analysis functions do not require synchronized triggering (Nazarian and Stokoe, 1985a). This point is true for the functions required in SASW testing. Therefore, it is quite simple and beneficial to enhance signals by averaging.

If one assumes that background noise is random in nature, upon averaging the sum of the background noise in the records will tend to zero. However, as the actual signals due to an impact are fairly repeatable, the average of these signals will be close to their so-called "real" value. The repeatability of the signals can be more or less assured by inspecting visually the signal on the viewing screen of the recording device during the test.

Another direct advantage of averaging is that, in the frequency domain, the coherence function can be determined. The coherence function cannot be determined from a single blow but requires two or more hits. The value of the coherence function is that it is an indication of the quality of the recorded signal, with a value of one being excellent and zero being worthless. By examining the coherence function in the field, the quality of the signals can be checked as they are recorded, and, if necessary, the test can then be immediately repeated and proper adjustments can be made.

Theoretically, the higher the number of signals averaged, the more enhanced the final results will be. Practically, the number of averages should be optimized. According to laws of statistics, the reliability of getting a value closer to the "real" value by averaging the signals is inversely proportional to the square root of the number of experiments. The Law of Diminishing Returns (Miller and Freund, 1977) suggests that it is not appropriate to take excessively large samples since the extra labor is not accompanied by a proportional gain in reliabil-

ity. Based on experimental investigations at several soil sites, Heisey (1981) recommended the average of five runs as being adequate. An example of representative cross power spectra and coherence functions after for averages of 5 and 25 runs are shown in Fig. 4.2. No appreciable difference can be detected and, therefore averaging five signals is adequate and recommended.

#### 4.2.2 Advantages of Reversing the Source

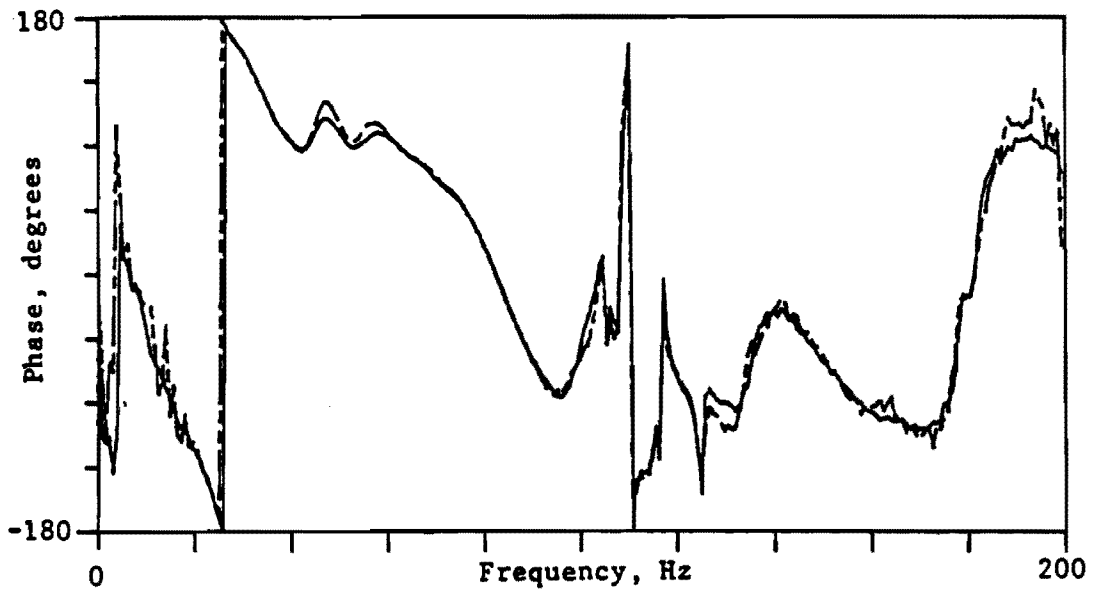
Reversing the source is the process of performing a test from two opposite sides of the receiver array as shown in Fig. 4.3. In this process the test is first performed in one direction (which is termed the forward profile, hereafter). Then, without moving the receivers from their original position, the source is moved to the opposite side of the array. The input channels of the recording device are switched so that the far receiver in the forward profile is now the near receiver for the ongoing test. The test is performed again with this configuration (reverse profile). By averaging the forward and reverse profiles, the effect of any (undesirable) internal phase shifts associated with the receivers or the recording device are minimized or eliminated. In Fig. 4.4 the cross power spectra of typical forward and reverse profiles are compared.

A point of interest is that if layers in the substructure are dipping, by running forward and reverse profiles the average can be interpreted as the average properties of equivalent horizontal layers.

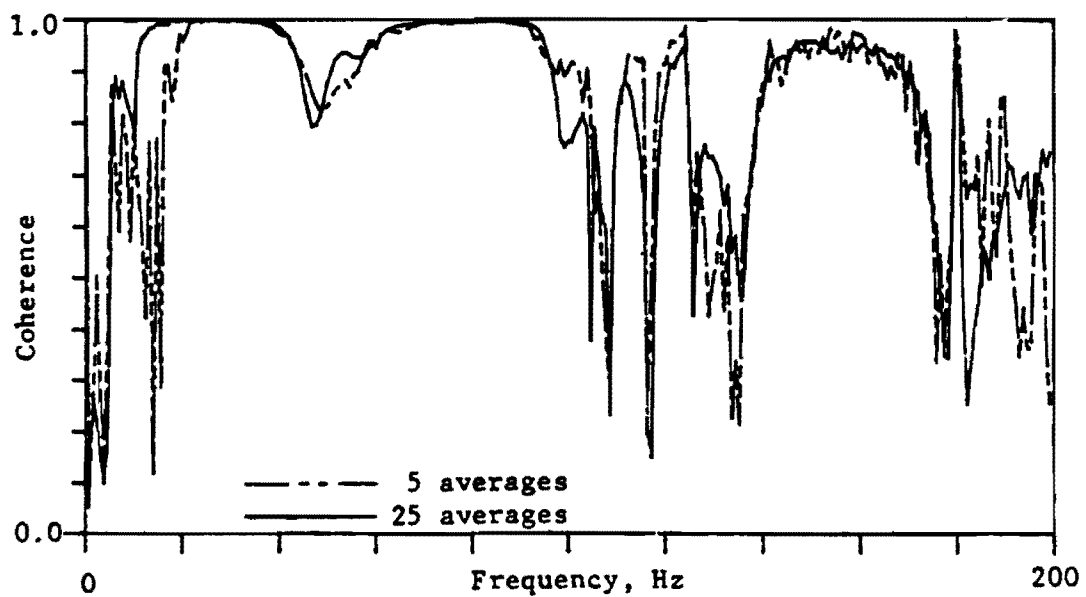
#### 4.2.3 Source-Receiver Arrays

The factors that affect appropriate spacing of receivers have been studied by Heisey (1981). These factors include: velocity of material; depth of investigation; range of frequencies; attenuation properties of substructure; and sensitivity of the instrumentation (receivers and recording device).

On the basis of studies at several soil sites, Heisey (1981) suggested that the distance between the receivers,  $X$ , should be less than

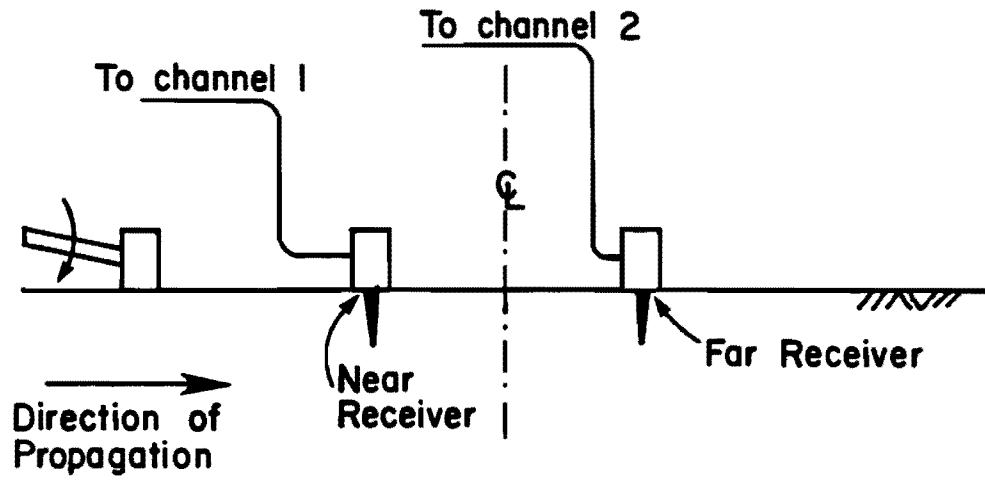


(a) Phase of the cross spectrum

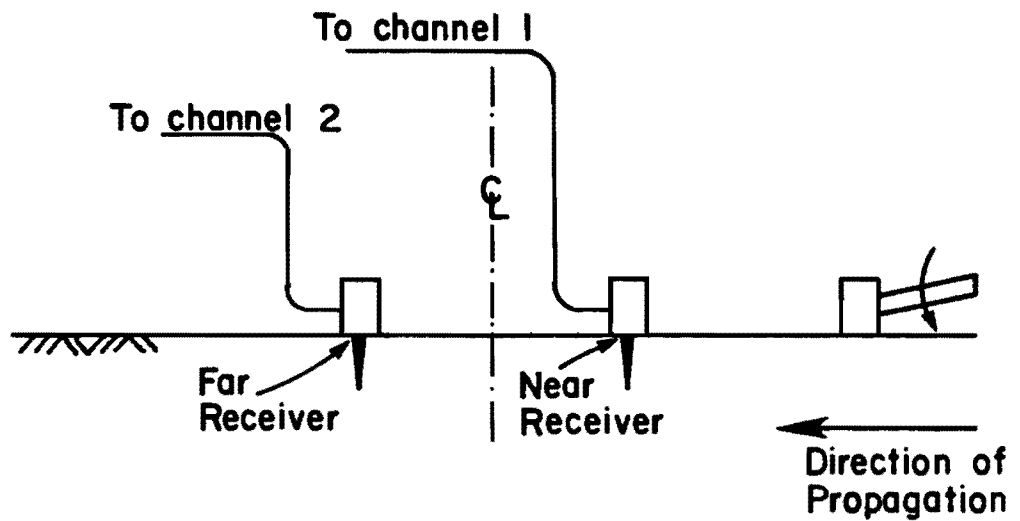


(b) Coherence function

Figure 4.2 - Comparison of Using 5 and 25 Averages to Obtain Representative Spectral Measurements (from Heisey, 1981).



(a) Forward Profile



(b) Reverse Profile

Figure 4.3 - Schematic of Forward and Reverse Profiles.

two wavelengths and greater than one-third of a wavelength. This relationship can be expressed as:

$$L_{ph}/3 < X < 2L_{ph} \quad (4.1)$$

As the velocities of different layers are unknown before testing, it is difficult to know if these limits are satisfied. Practically speaking, it is more appropriate to test with various distances between the receivers in the field and then evaluate the range of wavelengths over which reliable measurements were made. The relationship between receiver spacing and wavelength is then better expressed as:

$$X/2 < L_{ph} < 3X \quad (4.2)$$

The procedure is to select a spacing between receivers, perform the test, and reduce the data to determine the wavelengths and velocities. The next step is to eliminate the points that do not satisfy Eq. 4.2.

Theoretically, one experiment in seismic testing is enough to evaluate the properties of the medium. For a more precise measurement, several tests are generally required. Various geometries of the source-receiver set-up can be used in testing. The two most common types of geometrical arrangements for the source and receivers are the common source/receiver and the common midpoint geometries.

In the common source/receiver (CSR) geometry, either the source or receivers are fixed in one location and the other is moved during testing. In the common midpoint (CMP) geometry, both the source and receivers are moved the same distance about an imaginary centerline. For a medium consisting of a stack of horizontal layers with lateral homogeneity, the results of the tests performed with both methods should theoretically be identical. If the layers are not horizontal or the elastic properties of any layer varies laterally, the CMP geometry is preferred. In the CMP arrangement, the velocities are averaged over the testing range. There is a trade-off, however; in a single CMP test there is no way to determine the dip of the layers.

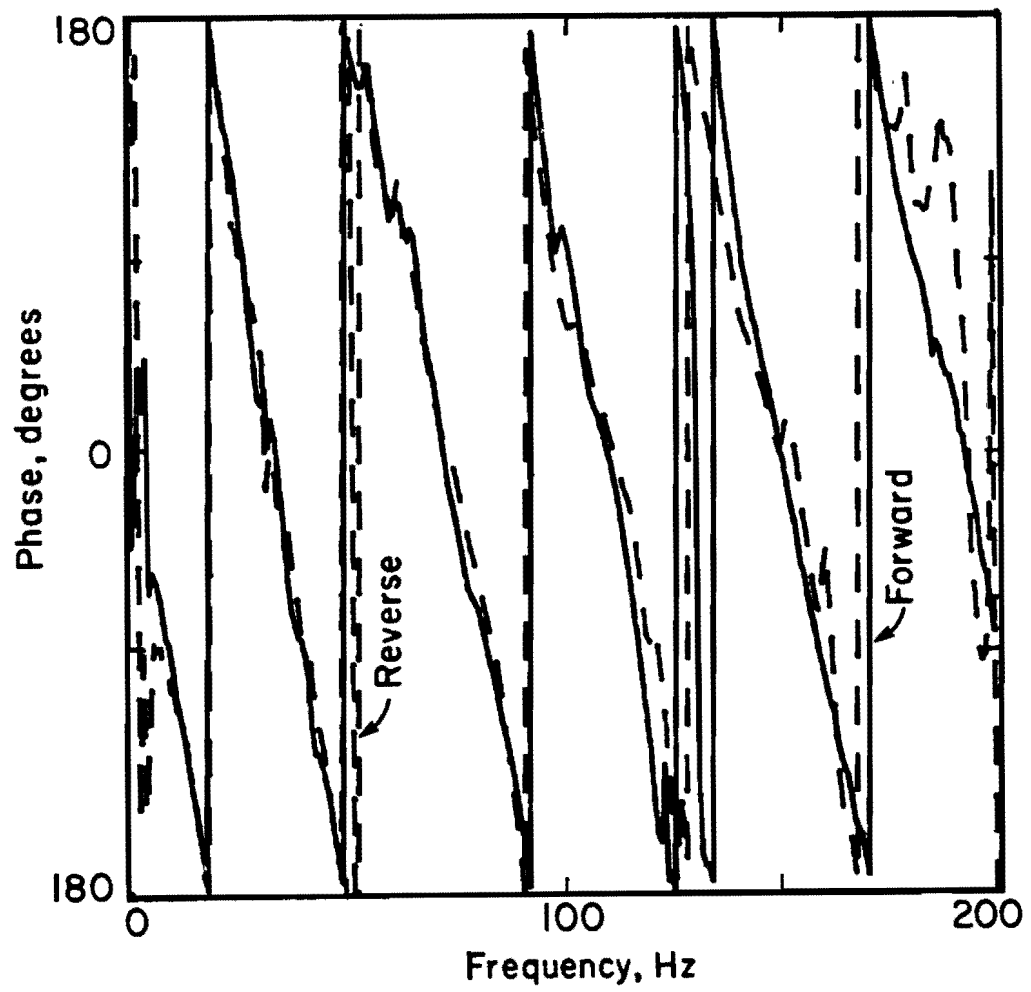


Figure 4.4 - Comparison of Phase Information of Cross Power Spectrum from Forward and Reverse Profiles.

In the SASW method, the area between the two receivers is important, and the properties of the materials between the source and the near receiver have little effect on the test. Thus, the imaginary centerline in the CMP method is selected between the receivers. The two receivers are moved away from the imaginary centerline at an equal pace, and the source is moved such that the distance between the source and near receiver is equal to the distance between the two receivers. This geometry of source and receivers is called Common Receivers Midpoint (CRMP) geometry, hereafter.

To study the effect of set-up configuration during SASW testing, a series of tests was performed at a soil site located at the Walnut Creek Treatment Plant in Austin, Texas. This site has been used extensively as a pilot site. Heisey (1981), Patel (1981), and Hoar (1982), among others have performed studies at this site and the properties of the materials are known quite well. Thus, both the CSR and CRMP were studied at Walnut Creek. Schematics of the two geometries are shown in Figs. 4.5 and 4.6.

The dispersion curves obtained from these two set-ups are shown in Figs. 4.7 and 4.8. Also shown on each figure is the range in velocities from the other figure. The scatter in the dispersion curves is much less in the CRMP approach. As such, the average dispersion curve obtained from the CRMP geometry is more reliable and more representative of the subsurface material.

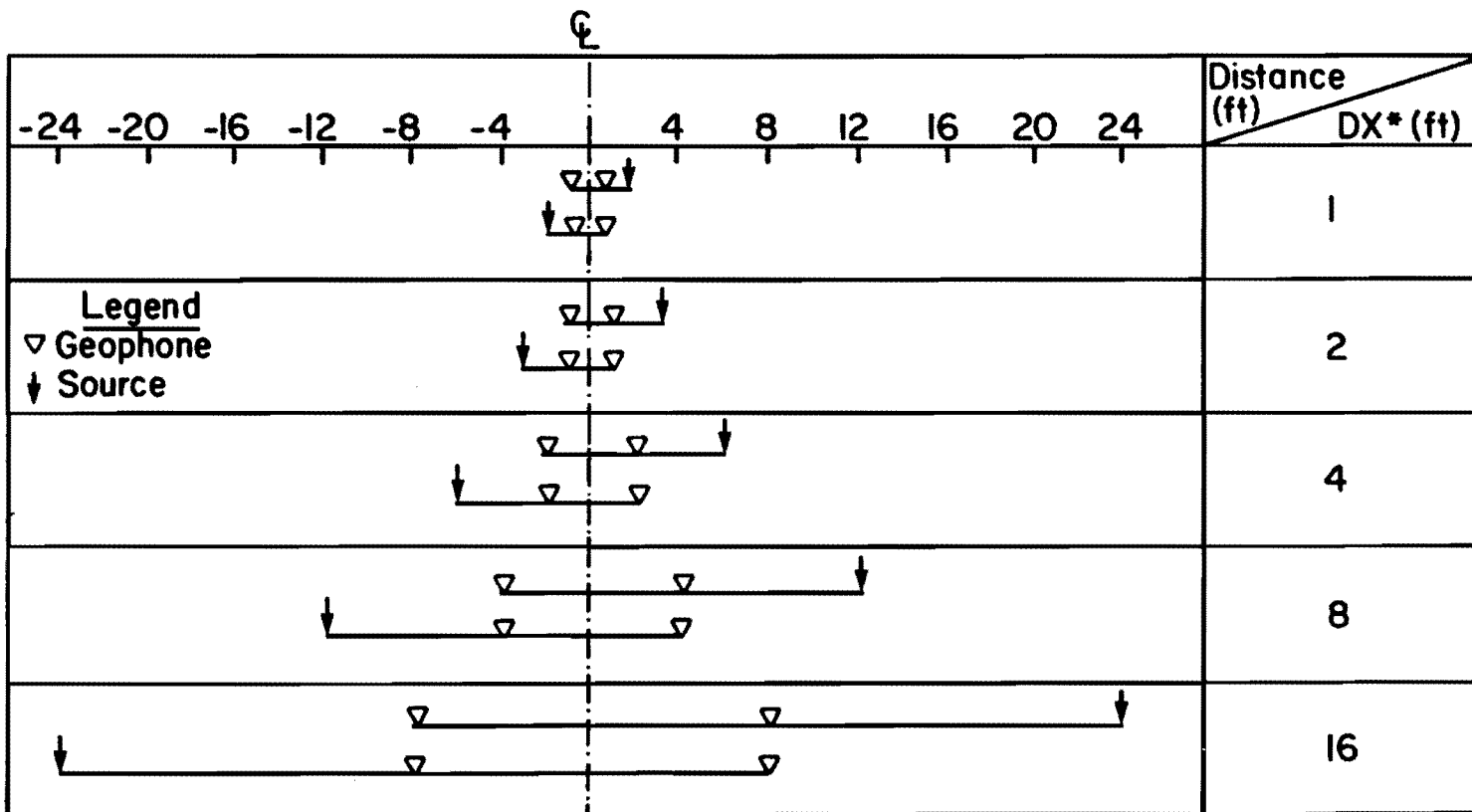
The distances between the receivers used in one series of tests depend mainly on the depth of investigation and properties of the substructure. In soil sites the receivers are placed 2 ft (0.6 m) apart for the first test and the distance is, generally, doubled for each subsequent test. The maximum spacing is normally 64 ft (19 m) and distances of up to 128 ft (38 m) have been used successfully. On pavements the same pattern is employed except that the receivers are placed one ft (0.3 m) apart for the initial test and generally spacings no larger than 24 ft (7 m) are used.

The other factor of importance in the experimental set-up is the distance between the source and the near receiver. Lysmer (1968), based

32   28   24   20   16   12   8   4   0	Distance (ft) / DX*(ft)
	1
	2
<p><b>Legend</b>            ▽ Geophone            ↓ Source</p>	4
	8
	16

\*DX = Receiver Spacing

Figure 4.5 - Common Source Geometr. .



**Legend**  
 ▽ Geophone  
 ↓ Source

\*DX = Receiver Spacing

Figure 4.6 - Common Receivers Midpoint Geometry.

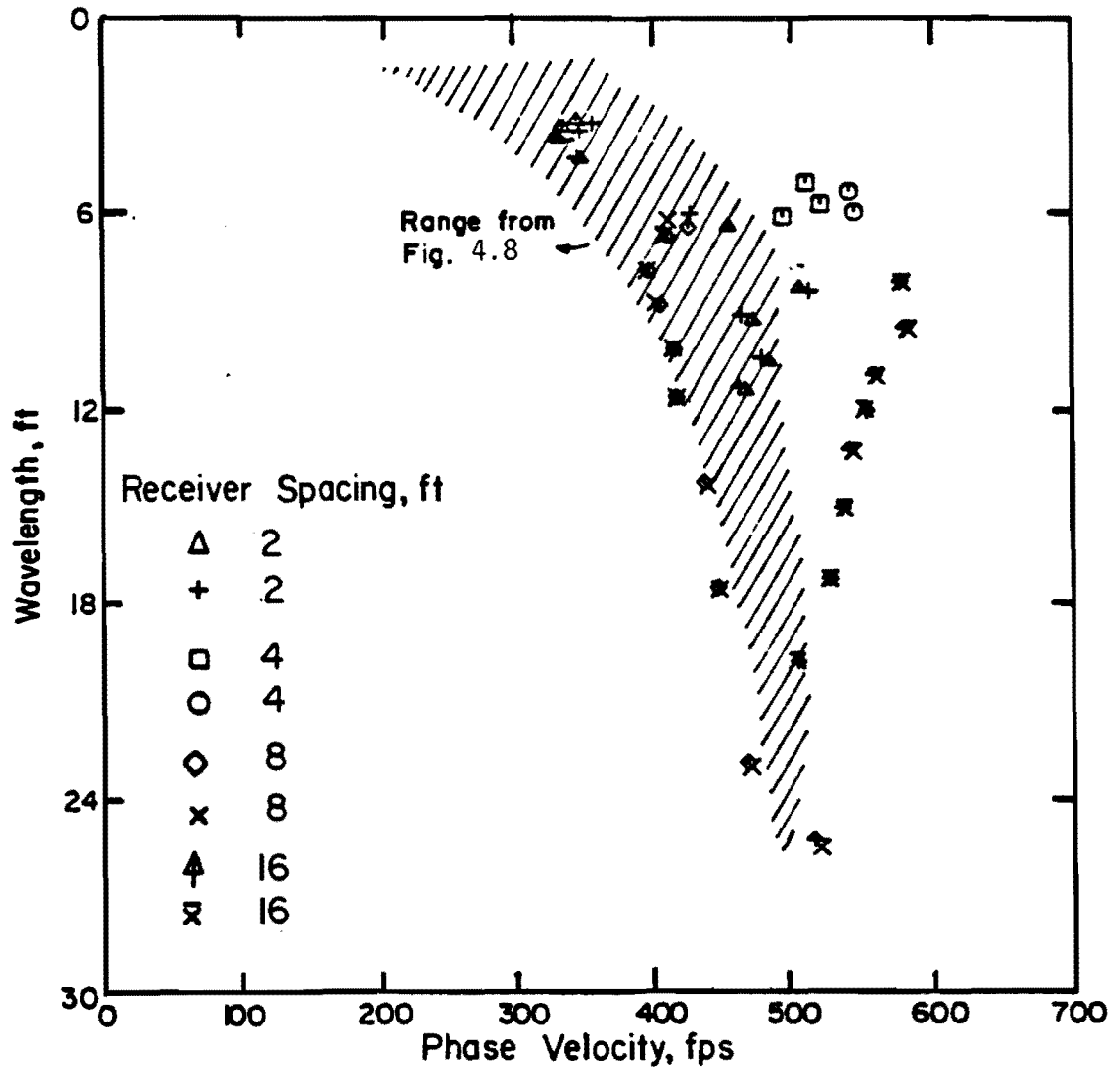


Figure 4.7 - Dispersion Curves from SASW Tests Performed Using Common Source Geometry at Walnut Creek Site.

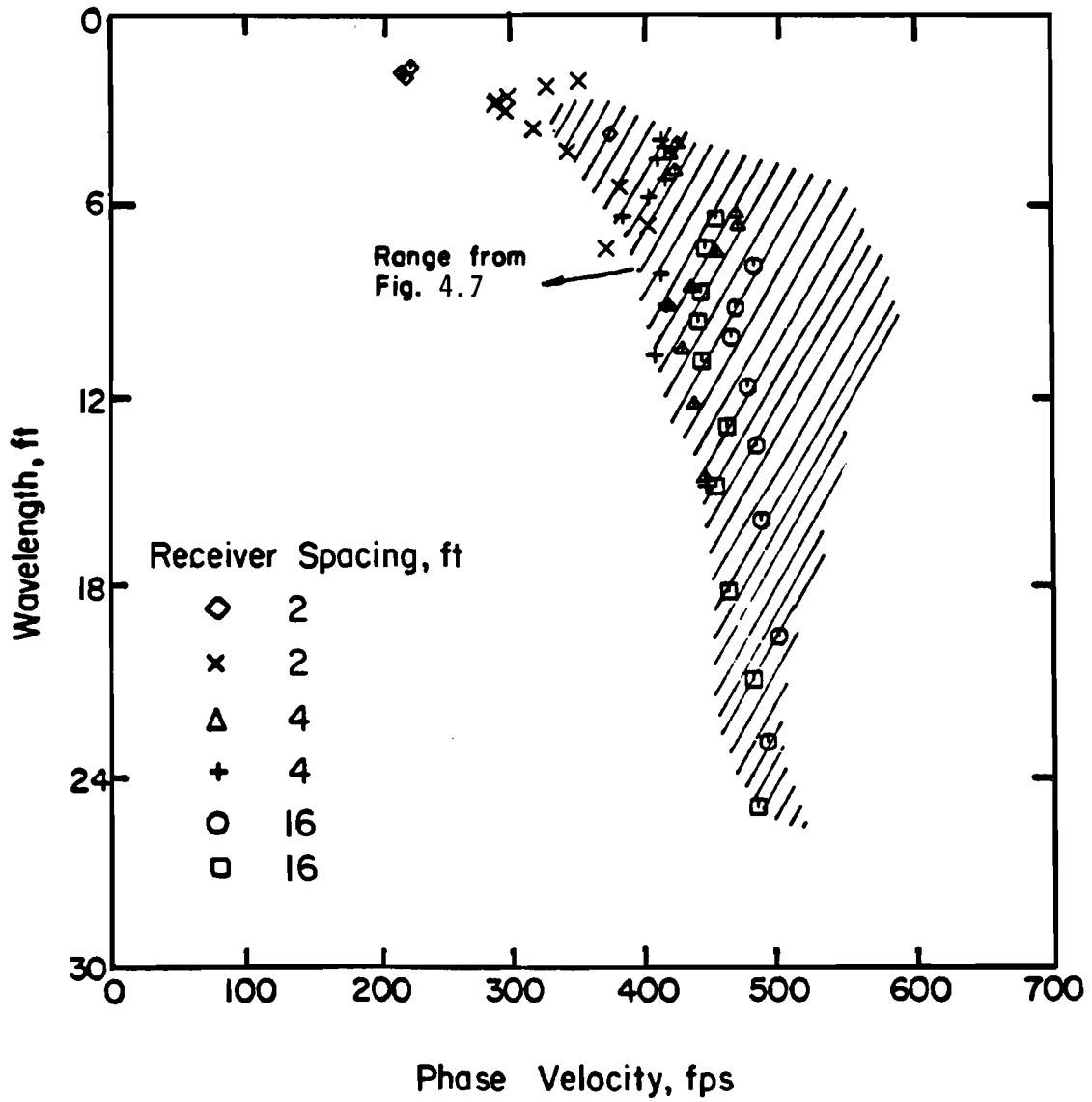


Figure 4.8 - Dispersion Curves from SASW Tests Performed Using Common Receivers Midpoint Geometry at Walnut Creek Site.

on theoretical studies, suggested that, at a distance of 2.5 wavelengths from the source, the wave field for the surface waves is fully developed. Heisey (1981) based on several experimental studies suggested that a distance equal to the distance between the receivers is adequate, provided the criteria expressed in Eq. 4.1 are met during data reduction. Although in most of the experiments carried out in this study Heisey's suggestion was employed, it seems that this matter should be studied more thoroughly. Recently, the distance between the source and near receiver was increased to several times the distance between the receivers. Preliminary studies at one site indicate that the effect of this was small on the experimental dispersion curve. As an example, the phase information of cross power spectra for a receiver spacing of two ft (0.6 m) for source-to-near-receiver distances of two, four and six ft (0.3, 0.6 and 1.2 m) are shown in Fig. 4.9. The curves follow each other closely except in the range of 2000 to 3000 Hz where the coherence values for the spacing of four ft (1.2 m) was not high.

### 4.3 FIELD EQUIPMENT

The necessary elements for performing a SASW test are a source, receivers, and recording device. Each of these items are discussed in Appendix A.

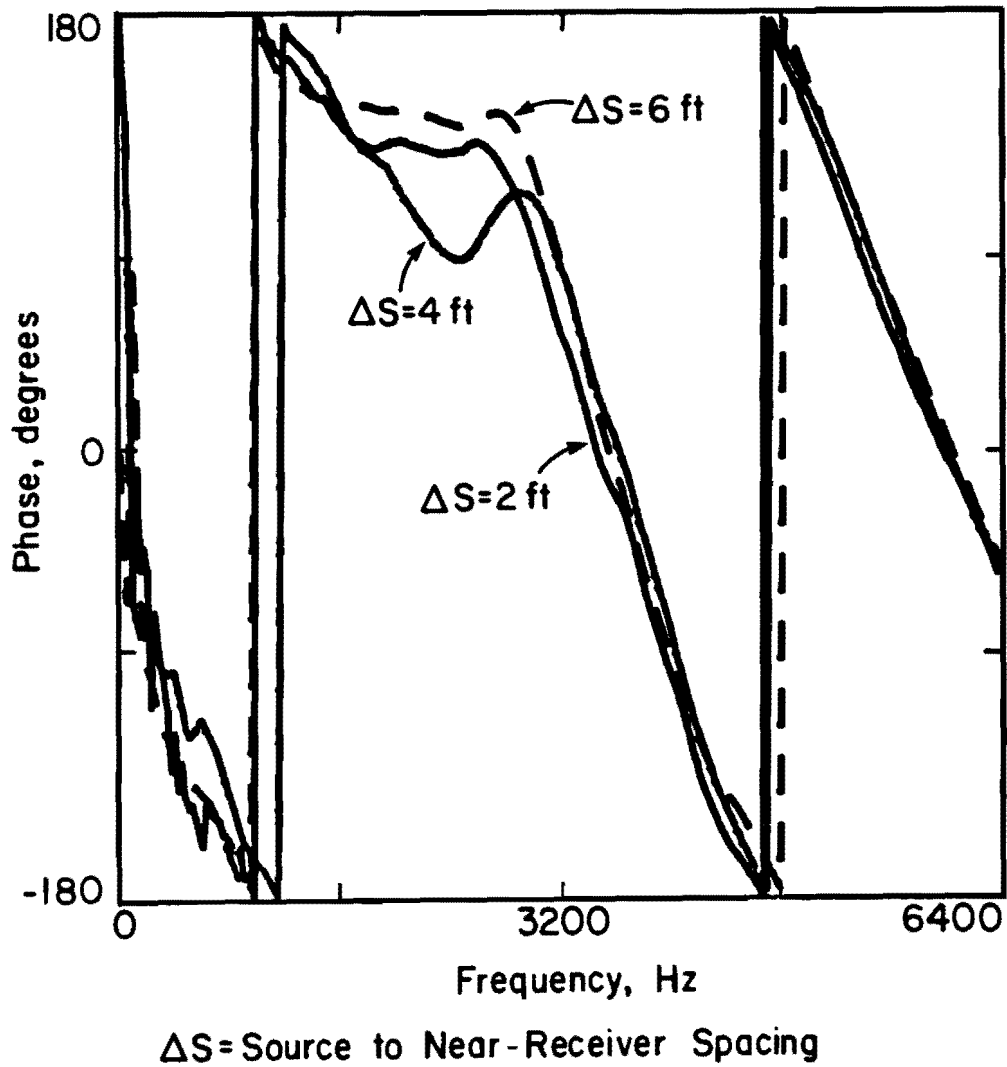


Figure 4.9 - Comparison of Phase Information of Cross Power Spectrum for Different Source-to-Near-Receiver Spacings.

This page replaces an intentionally blank page in the original.

-- CTR Library Digitization Team

## CHAPTER FIVE IN-HOUSE DATA REDUCTION

### 5.1 INTRODUCTION

Once data have been collected in the field as discussed in Chapter Four, they must be manipulated in a fashion appropriate for data reduction. Field data are in the form of phase information of cross power spectra and coherence functions from forward and reverse profiles at different receiver spacings. From the coherence function of each test, the range of frequencies with high quality data are selected. In the selected frequency ranges, phase information of the cross power spectrum is used to calculate phase velocities and associated wavelengths for each frequency. The wavelength/phase velocity relationships from all records are determined and combined with the outcome being a dispersion curve (see Nazarian and Stokoe, 1985a). This dispersion curve can be considered as the raw data from SASW testing. The procedure used in this study for construction of dispersion curves is discussed in the next sections.

### 5.2 CONSTRUCTION OF A DISPERSION CURVE

#### 5.2.1 Theoretical Considerations

Assume that for a given frequency,  $f$ , the phase difference is equal to  $\phi$ . By using the principle of a rotating vector, a phase shift of 360 degrees is equivalent to a travel time of one period. For a harmonic wave, the period,  $T$ , is the reciprocal of the frequency of that wave (i.e.,  $T = 1/f$ ). Therefore, the travel time,  $t$ , can be obtained by:

$$t = (\phi/360) \cdot T \quad (5.1)$$

or alternatively:

$$t = \phi/(360 \cdot f) \quad (5.2)$$

Now, if the distance between receivers,  $X$ , is known, phase velocity of propagation,  $V_{ph}$  is equal to:

$$V_{ph} = X/t \quad (5.3)$$

For a wave propagating in an elastic medium, the product of frequency and wavelength is constant, with this constant value equal to the velocity of propagation associated with that frequency. Therefore, wavelength for each phase velocity,  $L_{ph}$ , can be determined by:

$$L_{ph} = V_{ph}/f \quad (5.4)$$

It can be seen then that if phase and frequency are known, phase velocity and wavelength can be easily determined utilizing Eqs. 5.2 through 5.4.

### 5.3 Automated Data Reduction

Practically speaking, the process described in Section 5.2 is carried out for each record through an automated process. A schematic of this process is shown in Fig. 5.1. The spectral analyzer is connected to a micro-computer (Hewlett Packard 9836S). The HP 9836S is connected to a terminal which enables the operator to communicate with the CDC dual Cyber system of The University of Texas. Three computer programs are coded to facilitate this process.

The first one, called TRANS1 is used with the micro-computer so that phase information of the cross power spectrum (or transfer function) can be transferred from the analyzer through the HP 9836S to the CDC computer. In the next step, the data are consolidated and arranged in a manner usable with the CDC system by program TRANS11. Program TRANS12 is then used to utilize Eqs. 5.2 through 5.4 to calculate the dispersion curves. Finally, Program EXPER1 is used for statistical evaluation of the data at each frequency and to obtain the final dispersion curve. This statistical procedure is discussed later in this section.

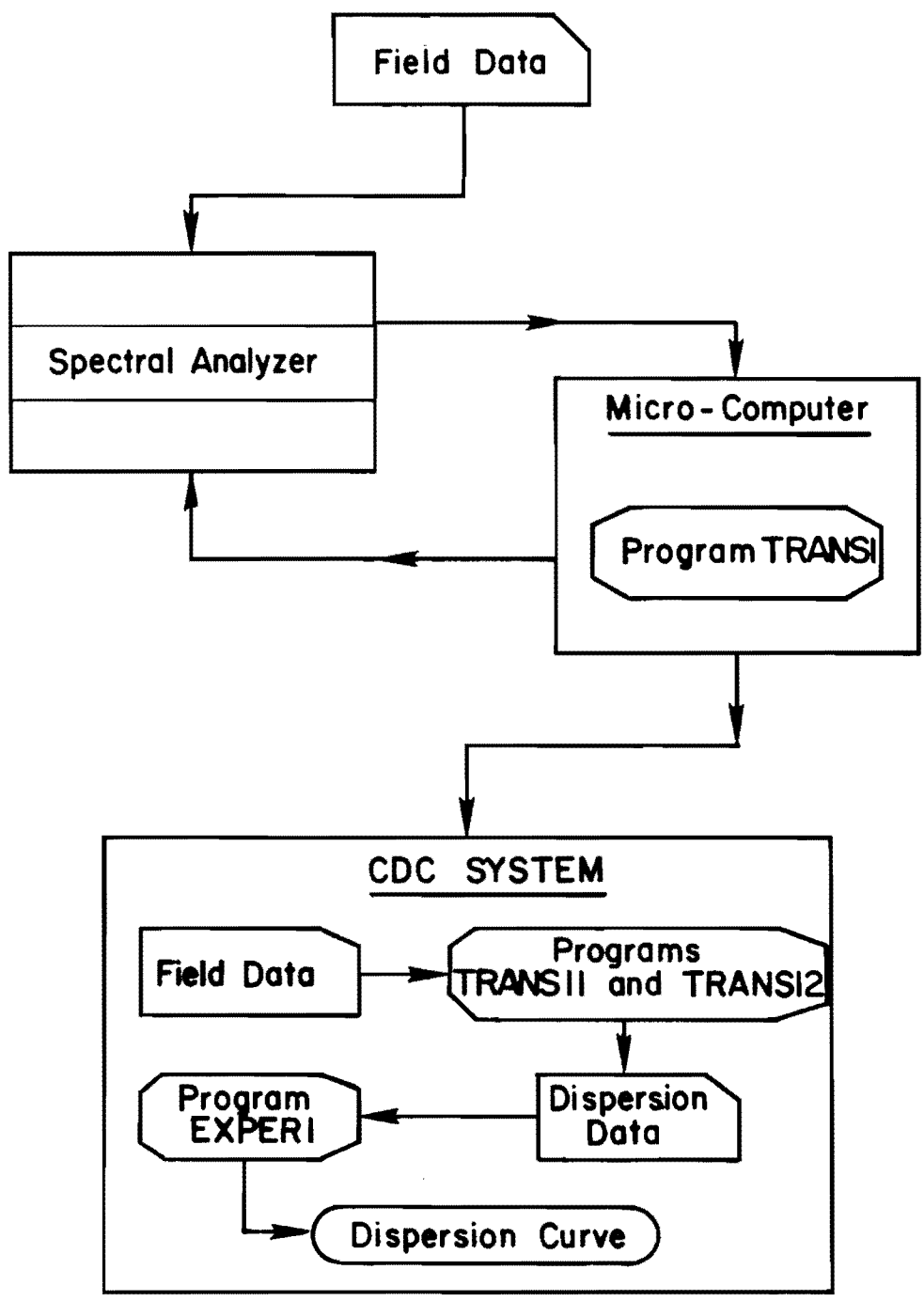
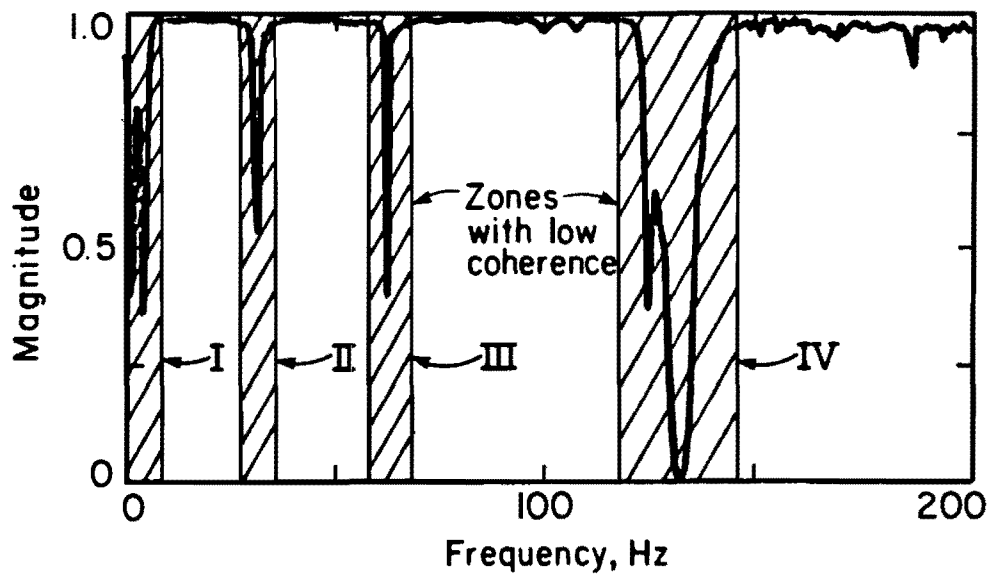


Figure 5.1 - Schematic of Automated Data Transfer.

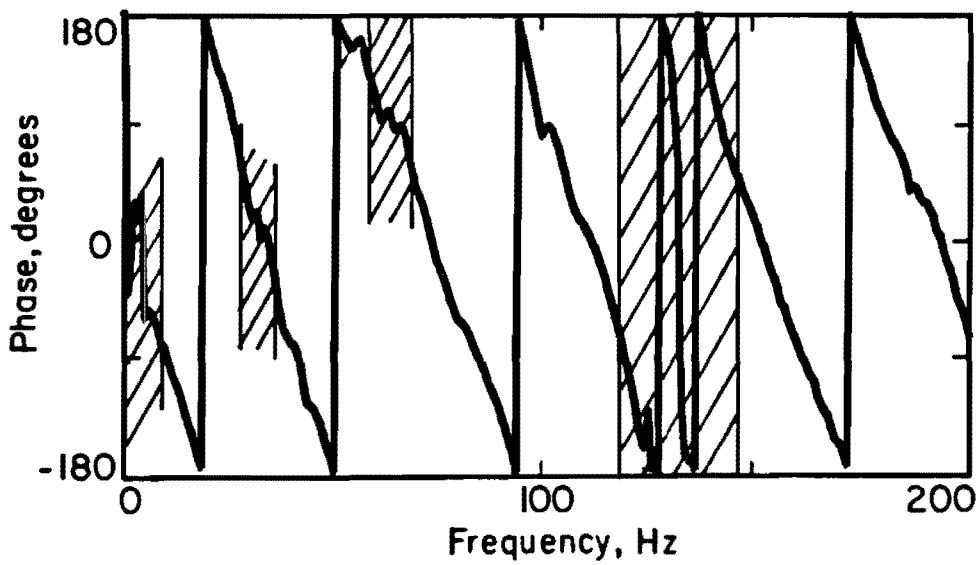
To clarify the process, typical phase information from one cross power spectrum and an associated coherence function are selected, and the different steps described above are illustrated.

The cross power spectrum and coherence function for one source/receiver set-up at a soil site is shown in Fig. 5.2. The site is called the Wildlife site hereafter, as the actual testing was performed in a wildlife preserve in southern California. The receiver spacing is equal to 8 ft (2.4 m), and the source/near-receiver distance is also 8 ft (2.4 m). To conserve space and to maintain good resolution, the phase plot shown in Fig. 5.2b oscillates between -180 and 180 degrees. (This is a typical display technique used by waveform-analysis equipment.) The first step is to find the actual phase for each frequency by counting the number of 360-degree cycles preceding each frequency and adding that to the fraction of the remaining cycle to obtain the actual phase. This process is called unfolding of the phase.

Figure 5.3 shows the same phase plot as in Fig. 5.2b after the appropriate number of cycles is added to each value of phase read off Fig. 5.2b. Four regions with low coherence values exist in Fig. 5.2a. A low value of coherence at a certain frequency corresponds to poor quality of data at that frequency. There are several reasons for low coherence value which are discussed in Nazarian and Stokoe (1985a). The four regions which are marked as I, II, III and IV in Fig. 5.2a are four typical reasons for low coherence. The first zone (I), which covers from 0 to 5 Hz, exhibits low coherence because of the nonlinear behavior of the geophones around and below their natural frequency, and, more importantly, because no energy is generated in this region. Zone II is in the vicinity of 30 Hz, which corresponds to the frequency of rotation of the mechanical parts of the power generator. The third zone of low coherence is due to 60-cycle electrical noise. In the range of 120 to 140 Hz, the last zone of low coherence occurs. In this region the energy coupled to the ground does not contain appreciable energy, especially at the far receiver.



a. Coherence Function



b. Cross Power Spectrum

Figure 5.2 - Typical Coherence Function and Cross Power Spectrum from Wildlife Site.

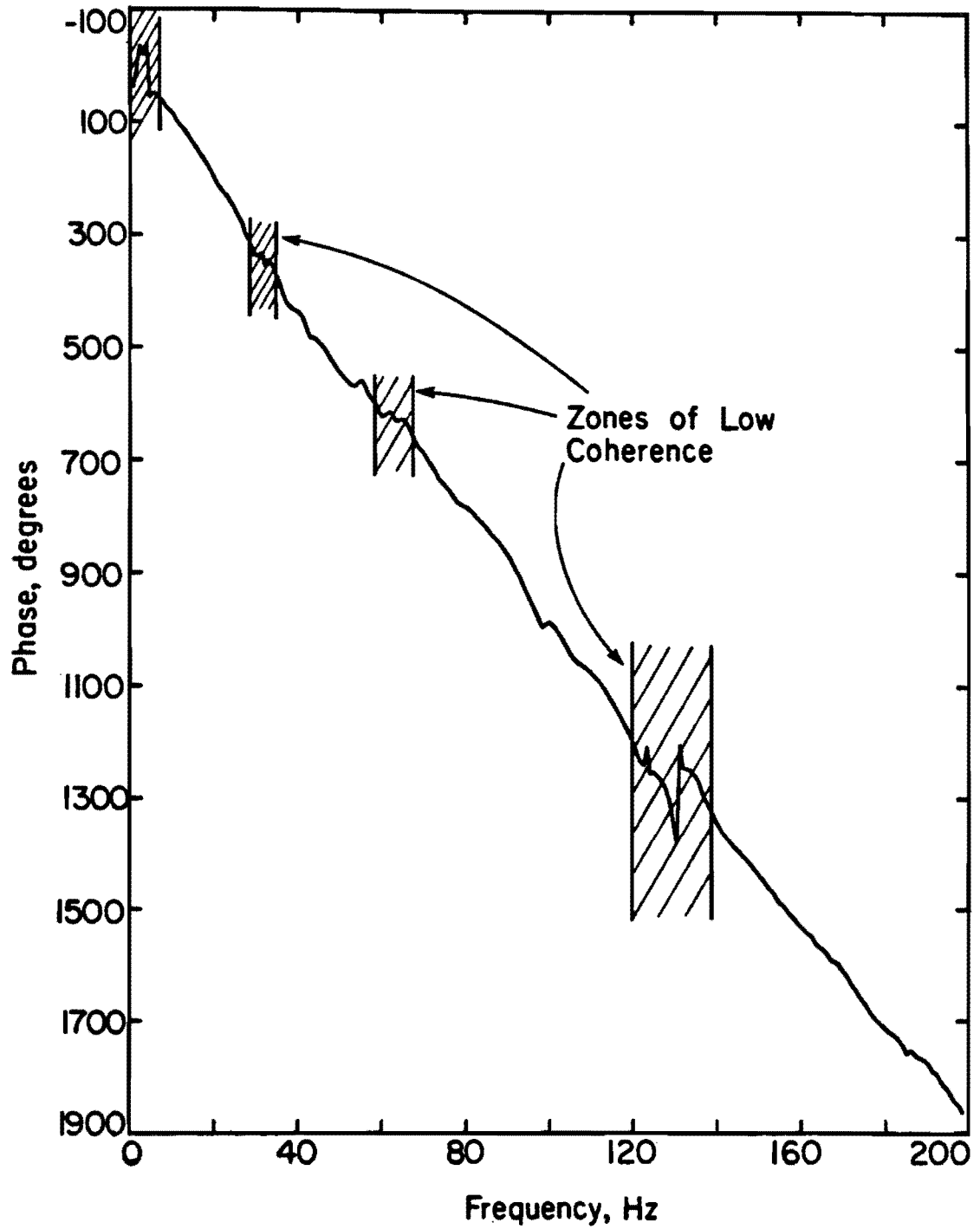


Figure 5.3 - Unfolded Phase Information of Cross Power Spectrum (Obtained from Figure 7.2b).

Figure 5.4 represents a portion of Fig. 5.2b with an expanded scale. Five points, 1 through 5, are marked in this figure at frequencies of 15, 25, 35, 45 and 70 Hz, respectively. The process of determining phase velocity versus wavelength from the phase and frequency of point 3 ( frequency of 35 Hz) is shown in Table 5.1. For all points in Fig. 5.2b, the same procedure was followed. The outcome, which is a dispersion curve, is shown in Fig. 5.5. It should be mentioned that frequencies in the range of zero to 5 Hz, 28 to 32 Hz, 57 to 63 Hz, and 120 to 140 Hz were not included in the figure as the coherence function indicated a lack of quality in these ranges. These low-coherence ranges which were deleted are marked as shaded regions in Figs. 5.2a and 5.3.

The symbols shown with open circles in Fig. 5.5 do not meet Heisey's criteria (Eq. 4.2) and are discarded from construction of the final dispersion curve. A close-up of the dispersion curve for all points that meet these criteria is shown in Fig. 5.6. The range of the frequencies that satisfy Heisey's criteria for this receiver spacing is roughly from 14 to 72 Hz (approximate range of frequencies in Fig. 5.4). The five points marked in Fig. 5.3 are shown in this figure as well. It is interesting to note that as the frequency increases (i.e., at shorter wavelengths) the data points are much closer to one another. The range of frequencies of 15 to 25 Hz covers a range of wavelengths of approximately 9 ft (2.7 m); but for the same increment of frequencies, say from 35 to 45 Hz, only a 2.5-ft (0.75-m) range in wavelengths in the dispersion curve is obtained. As there are equal number of data points in both regions, the dispersion curve is better defined at higher frequencies than at lower ones. To overcome this problem the frequency bandwidth is decreased (in the field during data collection) as distance between the receivers is increased. However, it would be preferable to use a recording device that could digitize more than 256 points as used herein.

Figure 5.7 shows the coherence function and the cross power spectrum from the reverse profile at the same location. The phases of the cross power spectra from the forward and reverse profiles are compared

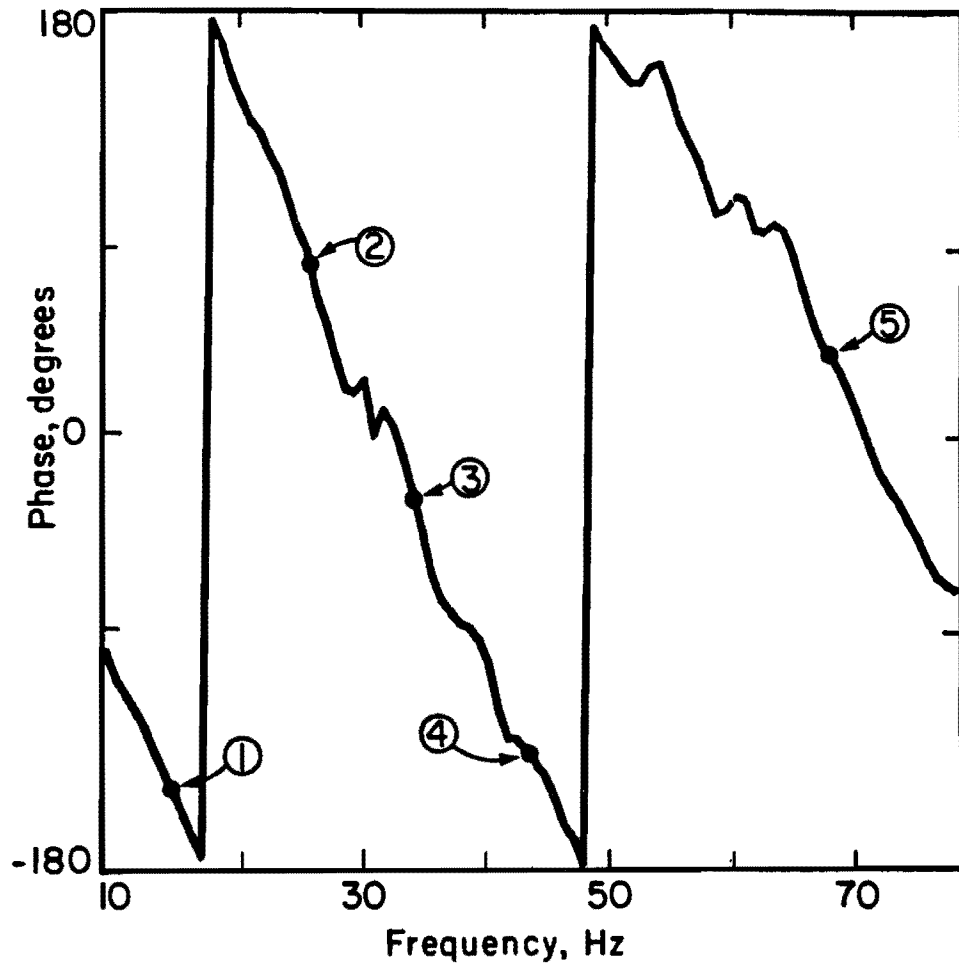


Figure 5.4 - Phase Information of Cross Power Spectrum in Range of Frequencies of 10 to 80 Hz (Expanded Version of Figure 7.2b)

Table 5.1. Example of Determination of Dispersion Data from Phase Information of Cross Power Spectrum.

GIVEN:

$$\text{Frequency, } f = 35 \text{ Hz}$$

$$\text{Raw Phase, } \phi_R = 19.2 \text{ degrees}$$

$$\text{Receiver Spacing, } X = 8 \text{ ft}$$

SOLUTION:

1. Find Actual Phase,  $\phi$

$$\phi = 180 + 180 + 19.2 = 379.2 \text{ degrees}$$

2. Find Travel Time,  $t$

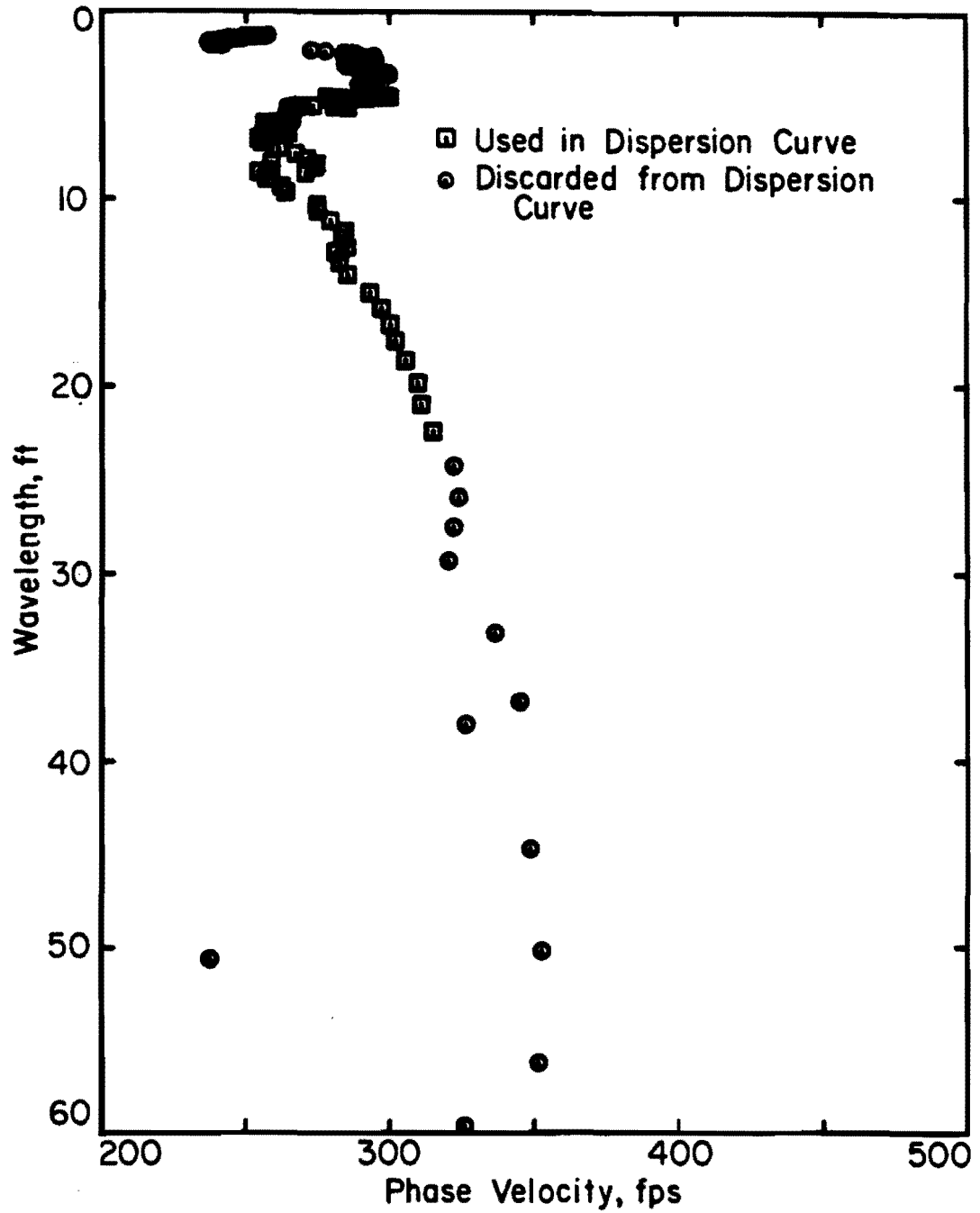
$$t = \frac{379.2}{360} \times \frac{1}{35} = 30.1 \times 10^{-3} \text{ sec}$$

3. Find Phase Velocity,  $V_{ph}$

$$V_{ph} = \frac{8}{30.1 \times 10^{-3}} = 266 \text{ ft/sec}$$

4. Find Wavelength,  $L_{ph}$

$$L_{ph} = 266/35 = 7.6 \text{ ft}$$



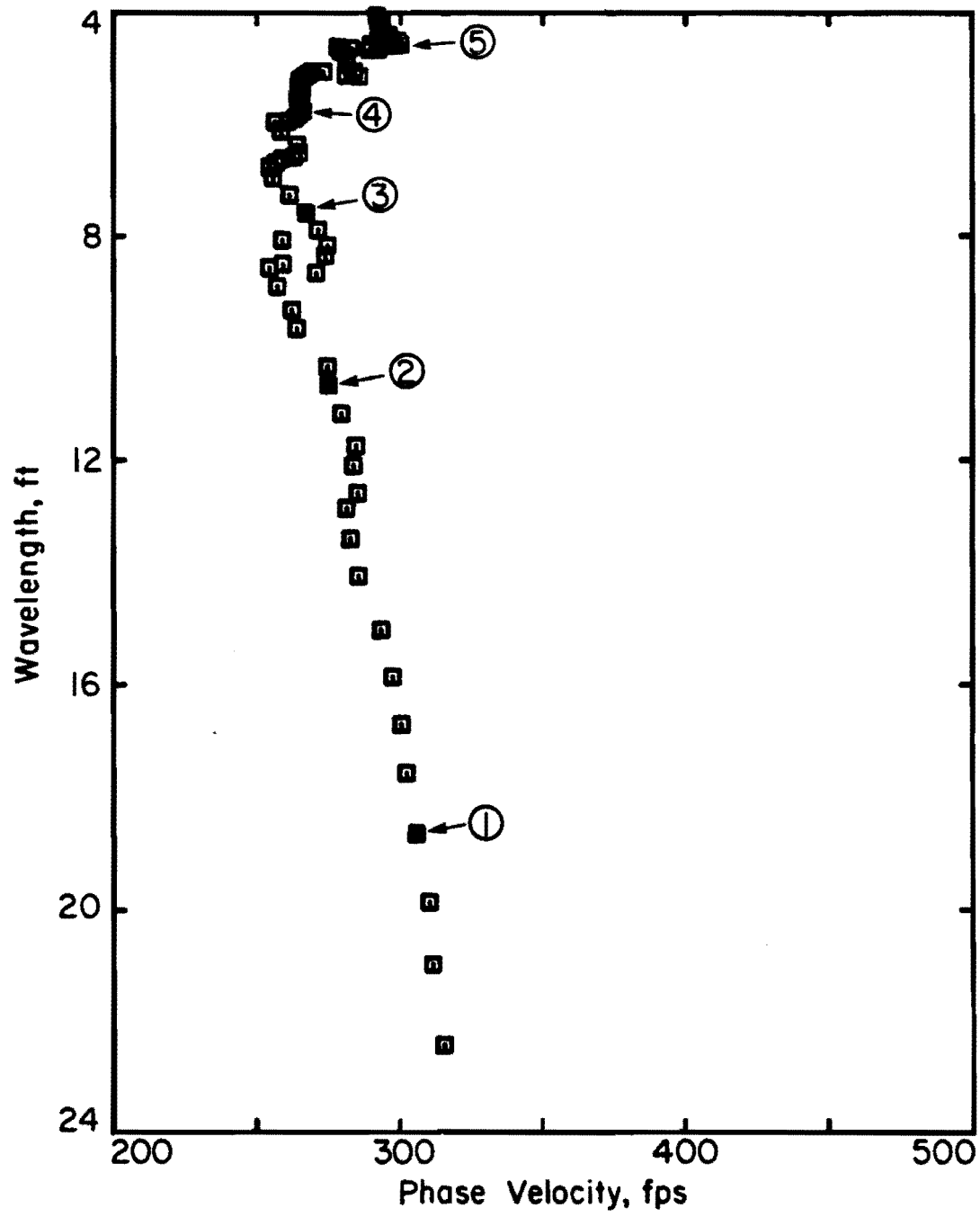


Figure 5.6 - Dispersion Curve Data After Filtering.

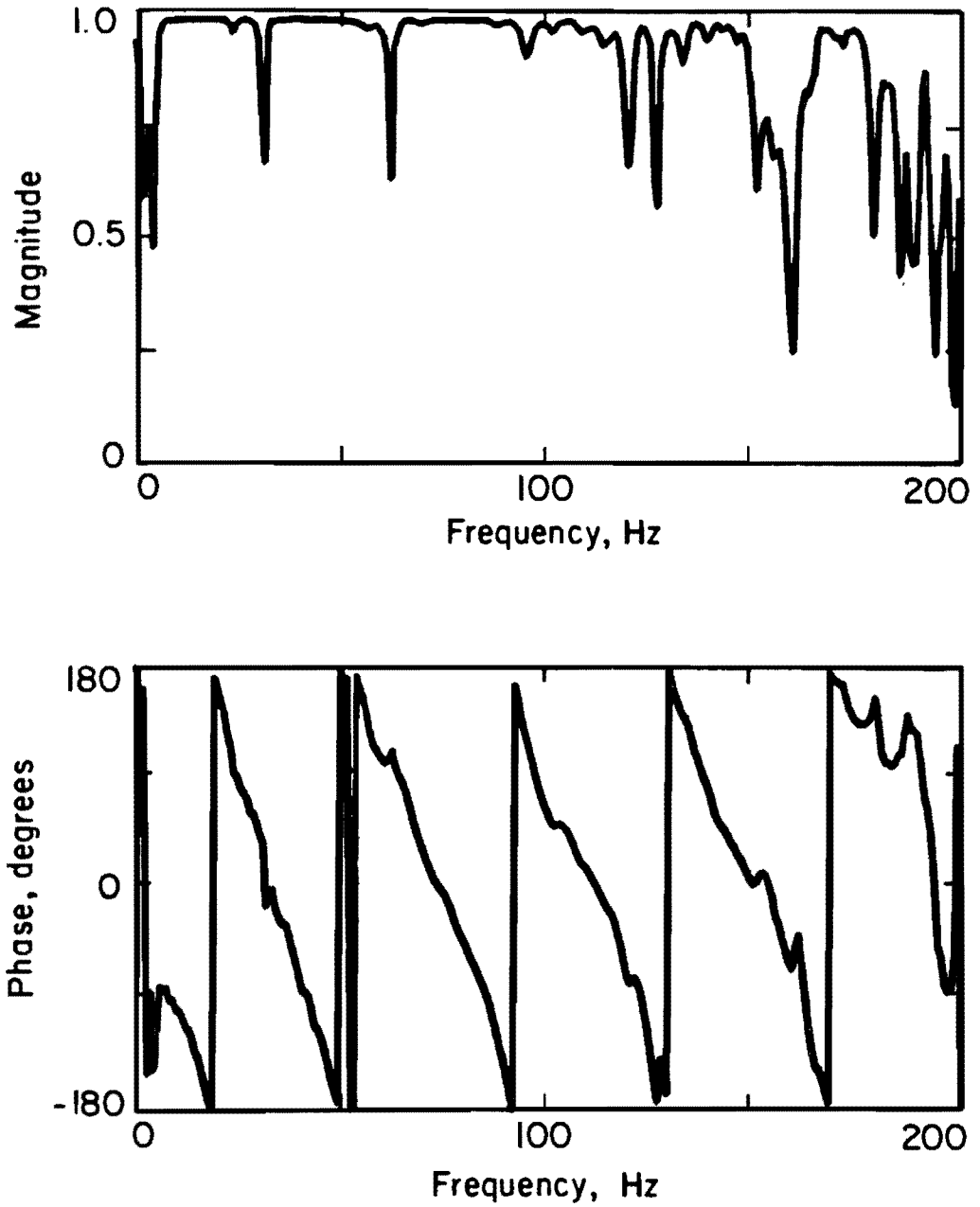


Figure 5.7 - Coherence Function and Phase Information of Cross Power Spectrum Measured from Reverse Profile.

in Fig. 5.8. The two curves follow each other quite closely in the range of usable frequencies. The dispersion curves constructed from the two profiles (forward and reverse profiles) are compared in Fig. 5.9 to demonstrate typical variations in the two dispersion curves. The deviation between the two curves is quite small, and at no point is there more than about a five percent difference.

The same process shown for one receiver spacing is repeated for other spacings as well. If the pattern of testing shown in Fig. 4.6 is followed, the dispersion curves from different spacings will overlap over a wide range in wavelengths. Therefore, for each frequency several dispersion data are available. To combine these data, statistical criteria were defined primarily for the purpose of identifying and eliminating the outliers from the actual data. These criteria are incorporated in Program EXPER1. At each frequency the mean, standard deviation and coefficient of variation of the phase velocities at that frequency are computed. For coefficients of variation of less than 7.5 percent, the mean is considered as the average value. If the coefficient of variation is greater than 7.5 percent, the points lying outside two-thirds of one standard deviation are disregarded, and the process mentioned above is repeated on the remaining points. At very high and very low frequencies, usually only two data points are available. In these cases the mean and the coefficients of variation are calculated, and, if the latter are higher than five percent, these points are omitted.

The final dispersion curve considering all receiver spacings at this site is shown in Fig. 5.10.

To study the repeatability of data collected in the field, a series of tests was carried out on the same day at an angle to the one just discussed. The same centerline was maintained, and the same receiver spacings were employed. The lateral homogeneity of the site was assured by comparing the profiles obtained with several cone penetration tests (CPT) at this site. The results of the two experiments are compared in Fig. 5.11 in the form of dispersion curves. The two dispersion

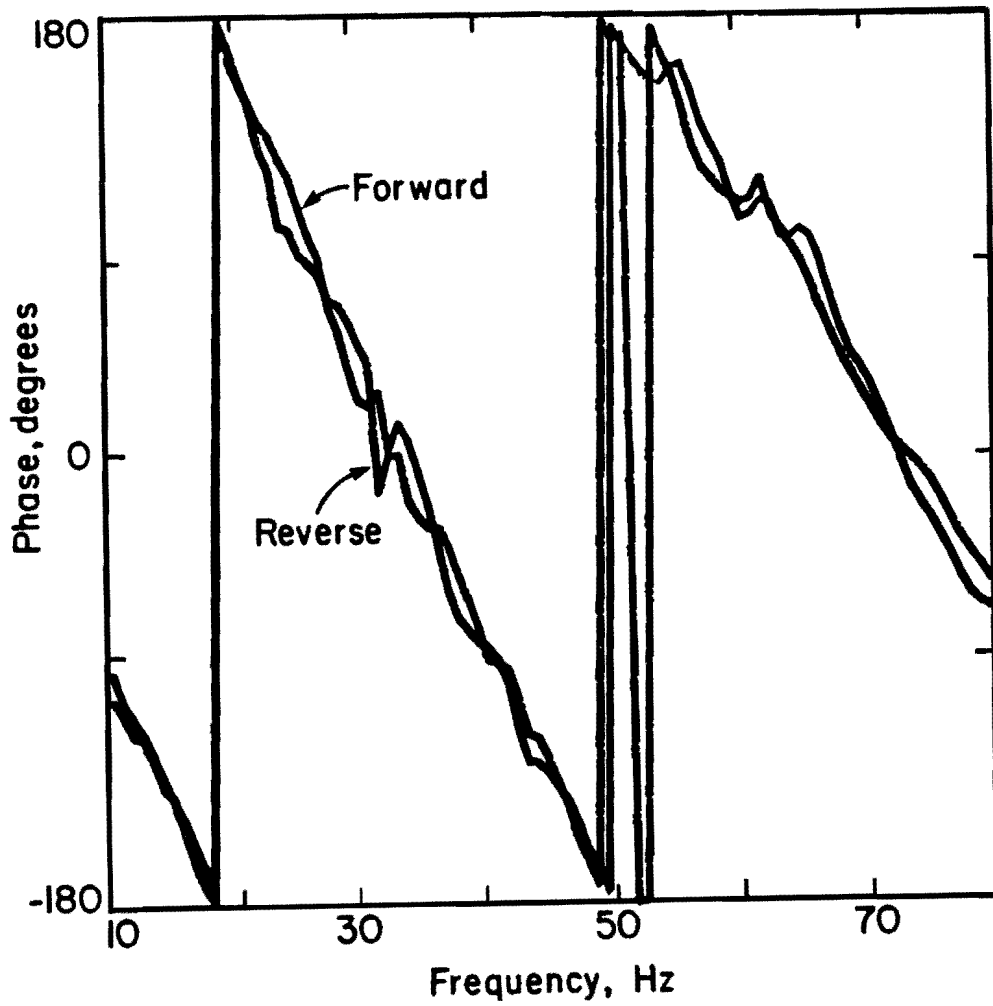


Figure 5.8 - Comparison of Cross Power Spectra from Forward and Reverse Profiles.

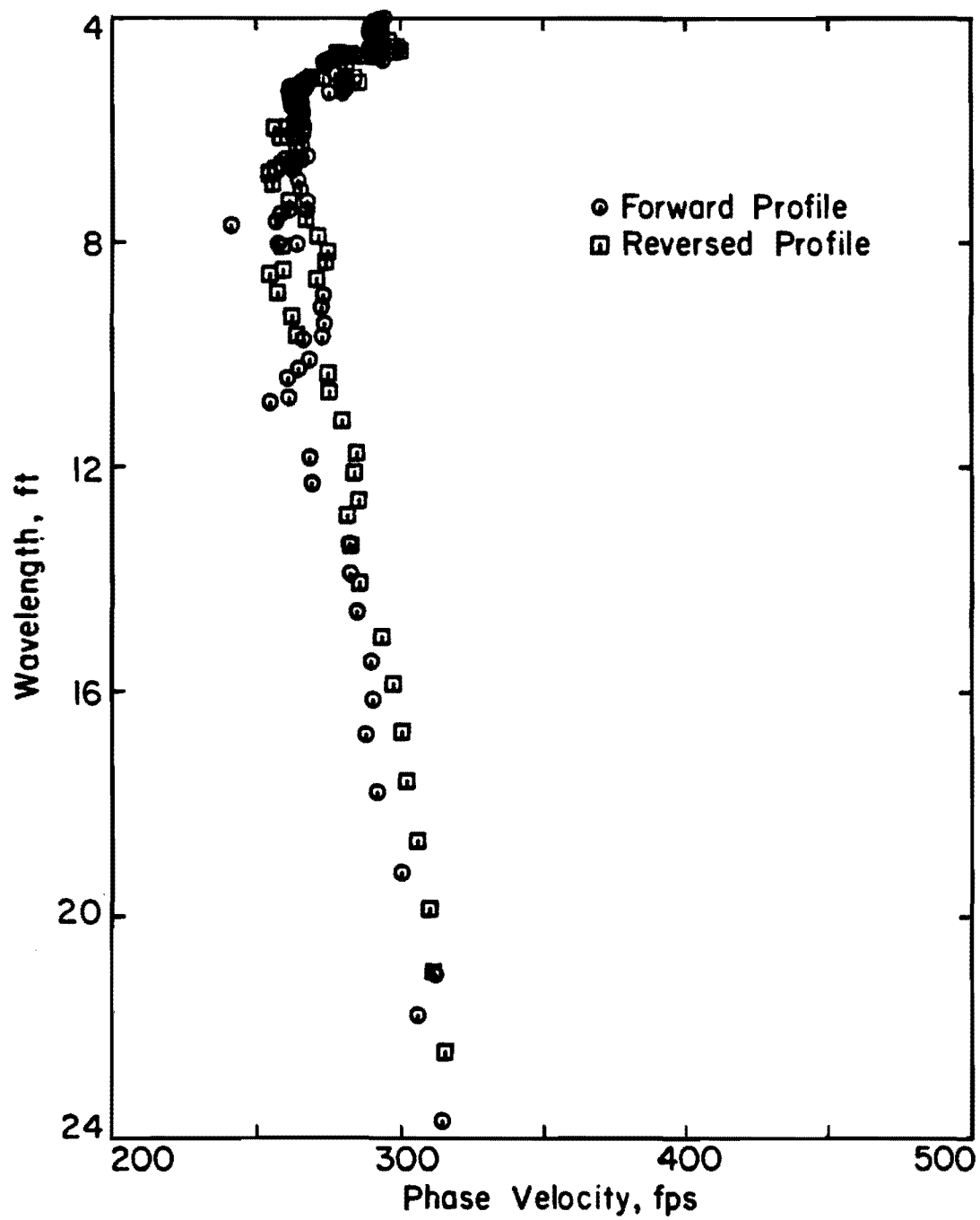


Figure 5.9 - Comparison of Dispersion Curves from Forward and Reverse Profiles.

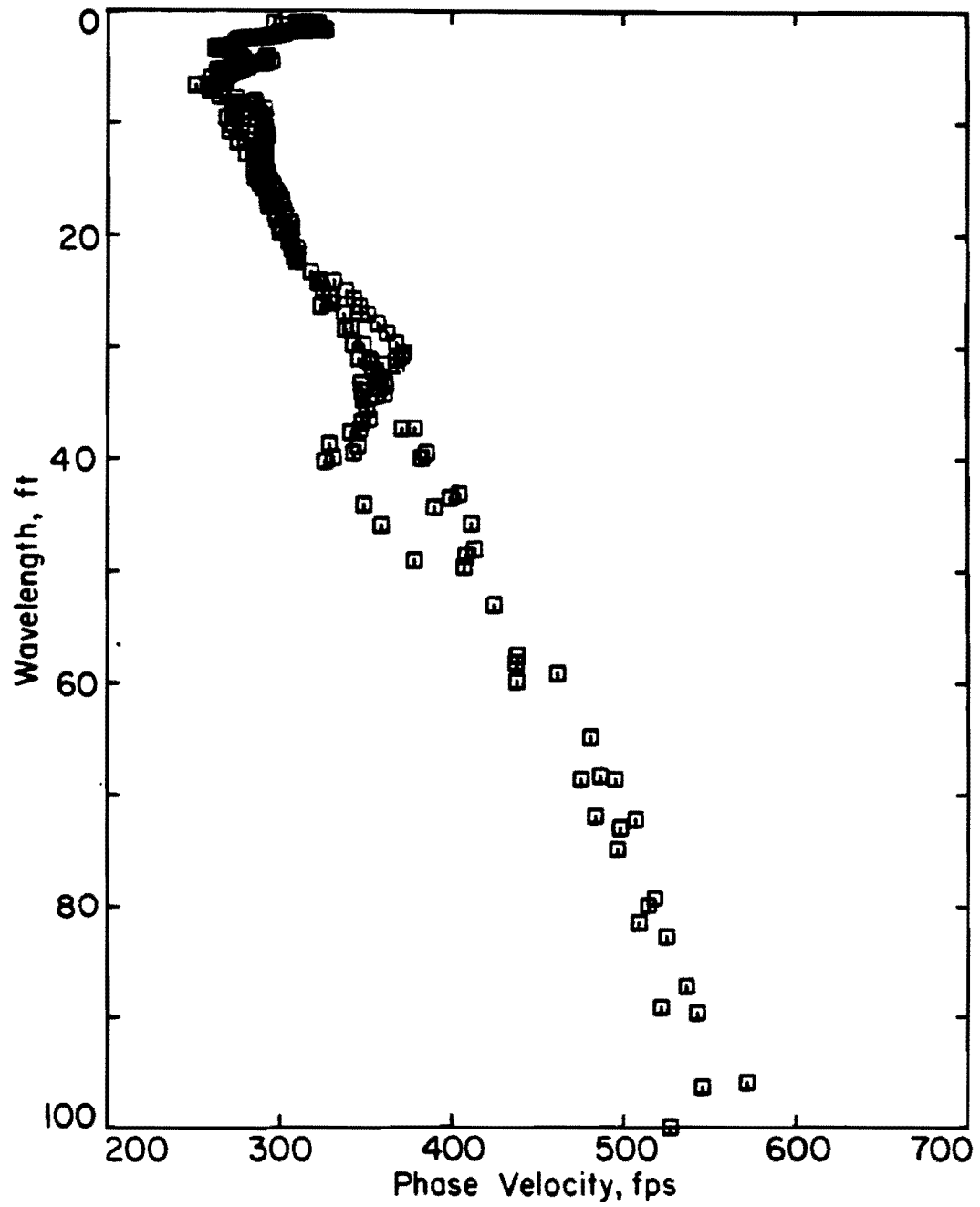


Figure 5.10 - Dispersion Curve from All Receiver Spacings for Wildlife Site.

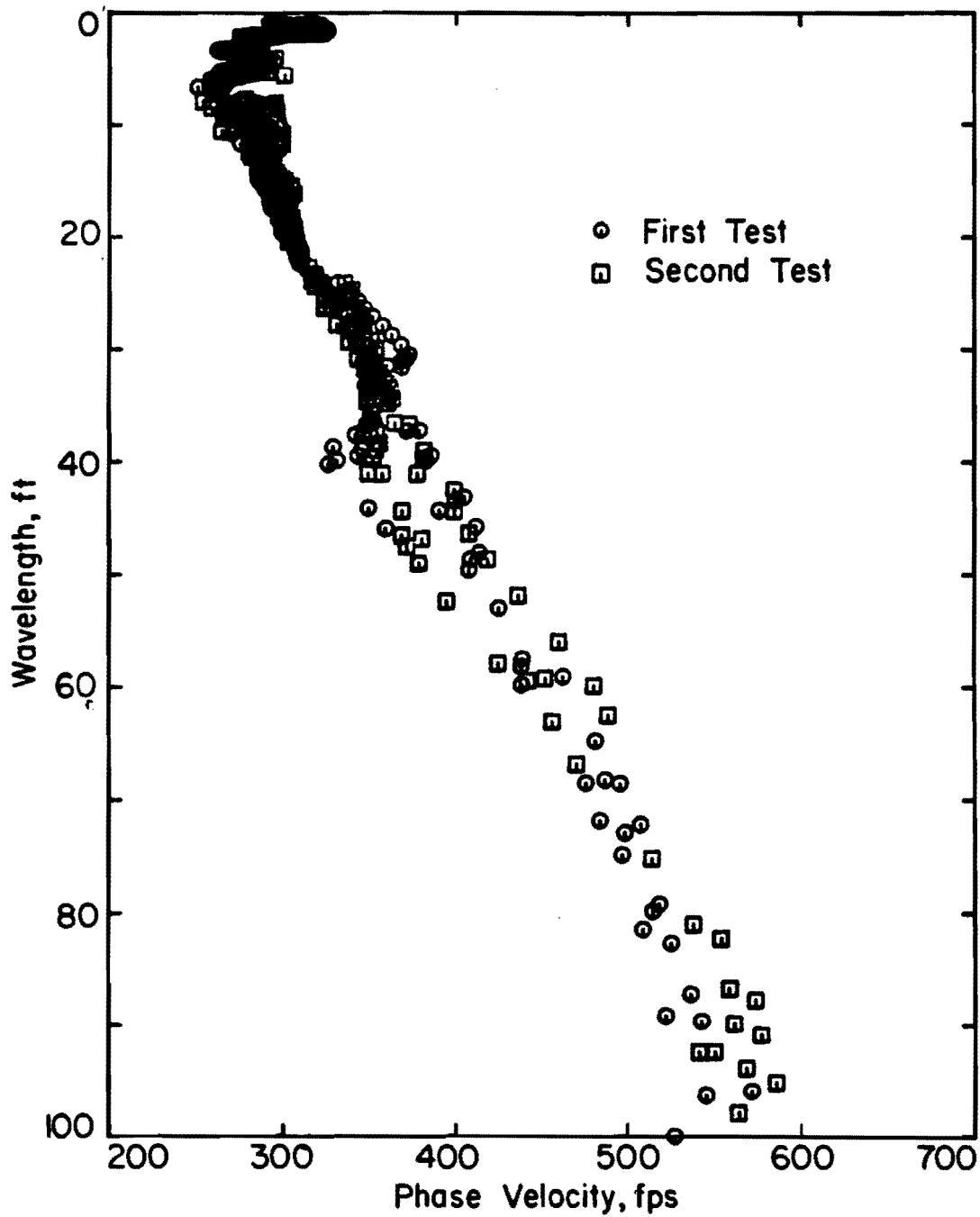


Figure 5.11 - Comparison of Dispersion Curves from Two Directions.

curves are in excellent agreement. Thus, it can be concluded that the tests are quite repeatable.

A similar data reduction process is followed for pavement sites and is presented in Appendix B.

#### 5.4 SUMMARY

In this chapter, the practical details of data reduction in SASW testing are presented (once data have been collected in the field). Construction of the dispersion curve from in situ data in the form of phase information from cross power spectra is discussed. During the course of this study, full-automation of the process of construction of dispersion curves was achieved. In this process, a desk-top computer has been utilized to transfer data to the more efficient CDC computer (more efficient for use in the inversion process) in a matter of minutes.

## CHAPTER SIX

### INVERSION PROCESS

#### 6.1 INTRODUCTION

The final task in SASW testing is to determine the shear wave velocity profile. This step is called inversion of the dispersion curve or simply inversion. (Sometimes this step is called forward modelling in geophysics or system identification in structural dynamics). Inversion is an iterative process in which a theoretical dispersion curve is calculated for an assumed shear wave velocity profile. The theoretical and experimental dispersion curves are compared, and the assumed profile is modified to improve the match. This process is continued until the two curves closely match. The inversion process is described in the next sections.

#### 6.2 INVERSION PROCESS

Three generations of inversion evolved during the course of this study. In the first generation the following steps were used:

1. the thicknesses of the layers were determined by dividing the dispersion curve into several sections and by assuming that  $1/3$  of the wavelength was equal to the effective sampling depth,
2. the shear wave velocity of the top layer was then assumed to be approximately equal to 110 percent of the phase velocity of the top layer,
3. the second layer was assumed to be a half-space, and the shear wave velocity of this layer was changed until the theoretical and experimental dispersion curves compared well up to approximately three times the sum of thicknesses of layers one and two (although the second layer was assumed to extend to infinity for the inversion process, the thickness of this layer was determined in Step 1),

4. the next layer was then added and assumed to be the new half-space and the thickness of the second layer was changed to its assumed value (from Step 1), and the matching process identical to Step 3 but for a three-layered system was performed, and
5. sequentially all the other layers were included by repeating the process described in Steps 3 and 4.

This process was quite tedious and time consuming. In addition, when the profile consisted of layers with large contrasts in stiffnesses (such as pavements), the intermediate layers had unrealistically high velocities. An example of this effect is included in Section 7.4. This first-generation inversion process was abandoned (improved upon) in the early stages of this study.

In the second-generation inversion, the velocities of the layers in the profile were estimated at the beginning and input into the computer program based upon Dunkin's (1965) approach (see Nazarian and Stokoe, 1985a). The process was quite similar to the procedure of the third level described below. In the case of soil sites, the ordinary construction of the determinant based upon discussion in Nazarian and Stokoe (1985a) was used. For pavement sites, layers with shear wave velocities greater than the phase velocity under consideration were included in construction of the determinant so that the real roots of the dispersion equation were always calculated.

In the third generation, the inversion program was modified by adding Thrower's (1965) recommendations, as presented below. The approach used herein is based upon construction of a theoretical dispersion curve from an assumed shear wave velocity profile and comparison of this curve with the experimental dispersion curve.

The dispersive characteristic of surface waves is discussed in Nazarian and Stokoe (1985a). The theory discussed in that report was incorporated into a computer algorithm. The main feature of the algorithm is to generate a theoretical dispersion curve once the thicknesses, stiffnesses (S- and P-wave velocities), and densities of

different layers are input. The program is interactive for ease of use and a user's manual is provided in a separate report (Nazarian, 1985b). Ranges of frequencies and velocities are selected for each search. These ranges are divided into several increments (on the order of 10 to 25 increments). The dispersion equation is only a function of frequency and phase velocity for a given stiffness profile. Therefore, the dispersion equation can be written as:

$$g(f, V_{ph}) = 0 \quad (6.5)$$

To solve this equation, either the value of frequency or phase velocity should be assumed.

Equation 6.5 is solved numerically by the computer as an explicit solution is not available, except for simple one- or two- layered systems. Schwab and Knopoff (1970) have shown that, to solve the dispersion equation numerically, it is more desirable to assume the frequency and to determine the value of  $V_{ph}$  at that frequency. At very high and very low frequencies, phase velocities do not vary by much, and they are quite close to the R-wave velocities of the top and bottom layers, respectively. If the frequency is assumed as the dependent variable in Eq. 6.5, and if the assumed phase velocity is close to the R-wave velocity of the first or last layer, the solution to the equation will have many roots that may cause numerical difficulties. Therefore, in program INVERT, frequency is assumed as the independent variable. At each increment of frequency, the program computes the determinant for each increment of velocity in the range of velocities selected. Roots of the dispersion equation, for that increment of frequency, are located between two phase velocities whose determinants have opposite signs.

An example of output from program INVERT is shown in Fig. 6.1. The location of the roots are marked by dashed lines. A more detailed description of the program is presented in Nazarian (1985) and Nazarian and Stokoe (1985b).

## \*\*\*\*\* LAYER PROPERTIES \*\*\*\*\*

LAYER	THICKNESS (ft)	SHEAR WAVE VELOCITY (fps)	COMP. WAVE VELOCITY (fps)	DENSITY (slug)
1	1.0	1000.	2000.	3.4
2	1.0	1500.	3000.	3.4
3	1.0	1500.	3000.	3.4

## \*\*\*\*\* DISPERSION CURVE DATA \*\*\*\*\*

NUMBER OF POINTS=	14
VELOCITY	WAVELENGTH
1342.	13.42
1298.	6.49
1228.	4.09
1120.	2.80
1028.	2.06
980.	1.63
957.	1.37
948.	1.18
1373.	1.53
938.	1.04
1340.	1.34
933.	.93
1298.	1.18
930.	.85

$V_{ph} \begin{matrix} \diagup \\ f^* \end{matrix}$	100.00	200.00	300.00	400.00
1400	.12E+01	.72E+00	.11E+01	.88E+00
1350	.11E+00	.25E+00	.53E+00	.11E+01
1300	-.55E+00	.84E-02	.24E+00	.30E+01
1250	-.10E+01	-.18E+00	.55E-01	.13E+01
1200	-.14E+01	-.34E+00	-.73E-01	.29E+00
1150	-.17E+01	-.47E+00	-.10E+00	.62E-01
1100	-.19E+01	-.57E+00	-.23E+00	-.39E-01
1050	-.22E+01	-.66E+00	-.28E+00	-.96E-01
1000	-.24E+01	-.74E+00	-.32E+00	-.13E+00
950	-.26E+01	-.81E+00	-.35E+00	-.16E+00
900	-.28E+01	-.87E+00	-.37E+00	-.18E+00

800.00	900.00	1000.00	1100.00
.33E-02	-.16E-01	-.59E-01	-.16E+00
.30E-01	.14E-01	-.51E-02	-.16E+00
.50E-01	.33E-01	.20E-01	-.94E-03
.67E-01	.49E-01	.36E-01	.24E-01
.86E-01	.64E-01	.49E-01	.37E-01
.12E+00	.84E-01	.64E-01	.49E-01
.19E+00	.13E+00	.92E-01	.69E-01
.24E+01	.60E+00	.26E+00	.16E+00
.65E-01	.74E-01	.79E-01	.82E-01
.11E-02	.49E-02	.63E-02	.65E-02
-.22E-01	-.16E-01	-.13E-01	-.10E-01

\*f = frequency in Hz  
+V<sub>ph</sub> = phase velocity in fps  
--- = location of fundamental root  
=== = location of higher-mode root

number in each box represents value of det (R<sub>11</sub>)

dashed line represents one solution to Eq. 25

Figure 6.1 - Example of Output from Computer Program INVERT.

A high number of increments is desirable for obtaining accurate results. However, the computation time increases drastically as the number of increments is increased. Practically speaking, instead of selecting a wide range of frequencies and velocities with a large number of increments, it is more economical to limit the ranges and number of increments and to perform more runs.

The first step in the inversion process is to assess a shear wave velocity profile from the dispersion curve. For more clarity, different steps discussed here are applied to the dispersion curve from the Wildlife site. To avoid confusion the dispersion curve should be divided into small sections which are plotted with an expanded scale. Several layers (on the order of 3 to 5) are selected, and a shear wave velocity is assigned to each layer. It is beneficial to use the simplified inversion method (discussed in Chapter Three) as the first assumed profile. With more experience, more realistic assumptions can be made. Any additional information available about the site can be used to accelerate significantly the inversion process. It should be mentioned that this is mainly a preliminary trial just to obtain a (reasonable) starting point for the second stage of matching process.

In the case of Wildlife, the dispersion curve is divided into four, constant-velocity layers as shown in Fig. 6.2. The  $V_s$  profile is obtained by dividing the wavelength axis by three, multiplying the velocity axis by 1.1 and "eye-balling" the velocities and thicknesses. The profile obtained is shown in Fig. 6.3. The theoretical dispersion curve from this profile is compared with the experimental one in Fig. 6.4. The velocities of different layers are changed until the two curves roughly match. The theoretical dispersion curve after some improvement in the  $V_s$  profile is shown in Fig. 6.4, and the shear wave velocity profile is compared with the initial profile in Fig. 6.3.

In the second stage, each layer in the shear wave velocity profile obtained in the first stage is divided into sublayers, and a more refined matching process is employed. When the theoretical and experimental curves match over the range of available wavelengths, the final shear wave velocity profile is obtained.

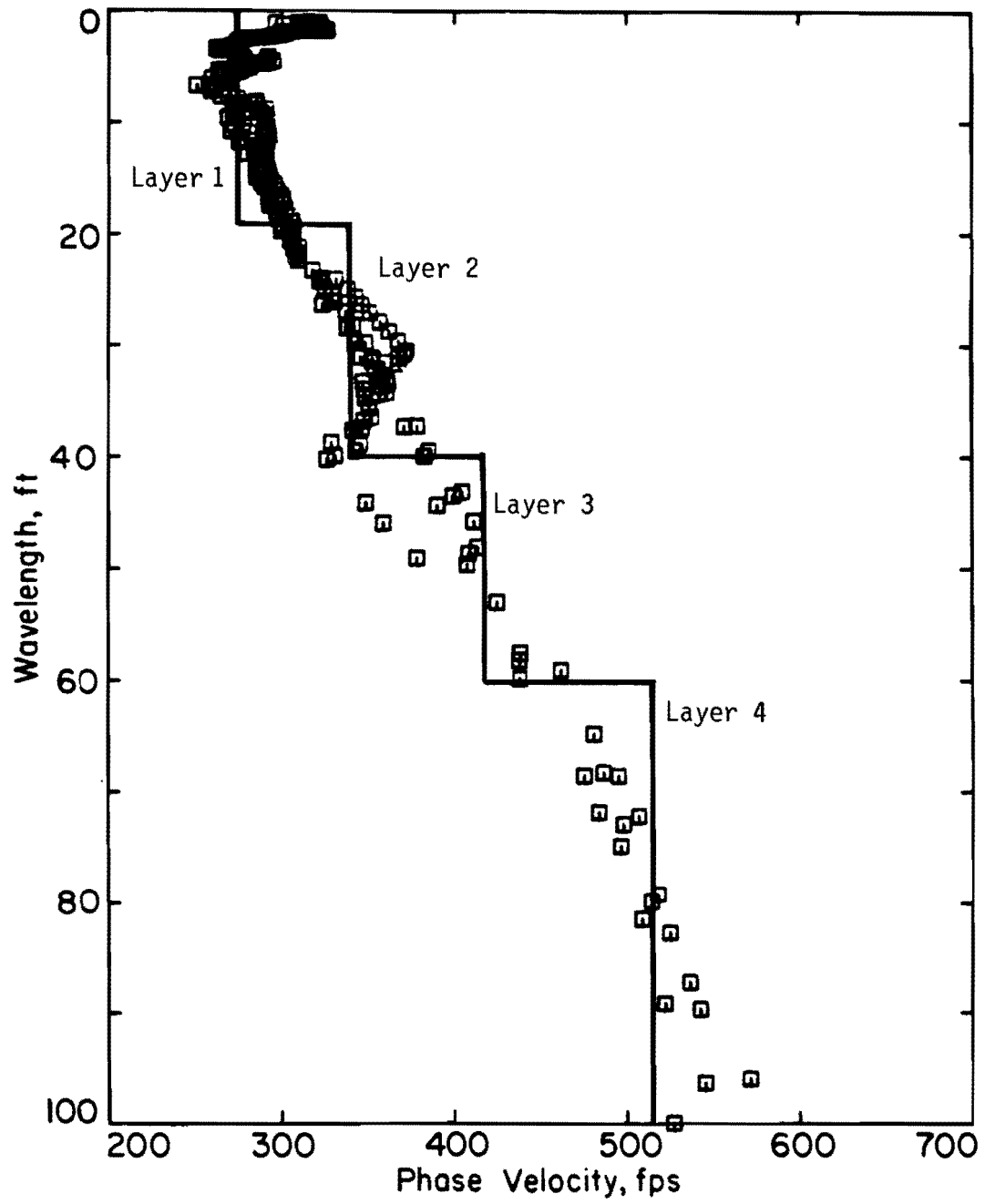


Figure 6.2 - Division of Dispersion Curves into Layers for Estimation of Initial Shear Wave Velocity Profile.

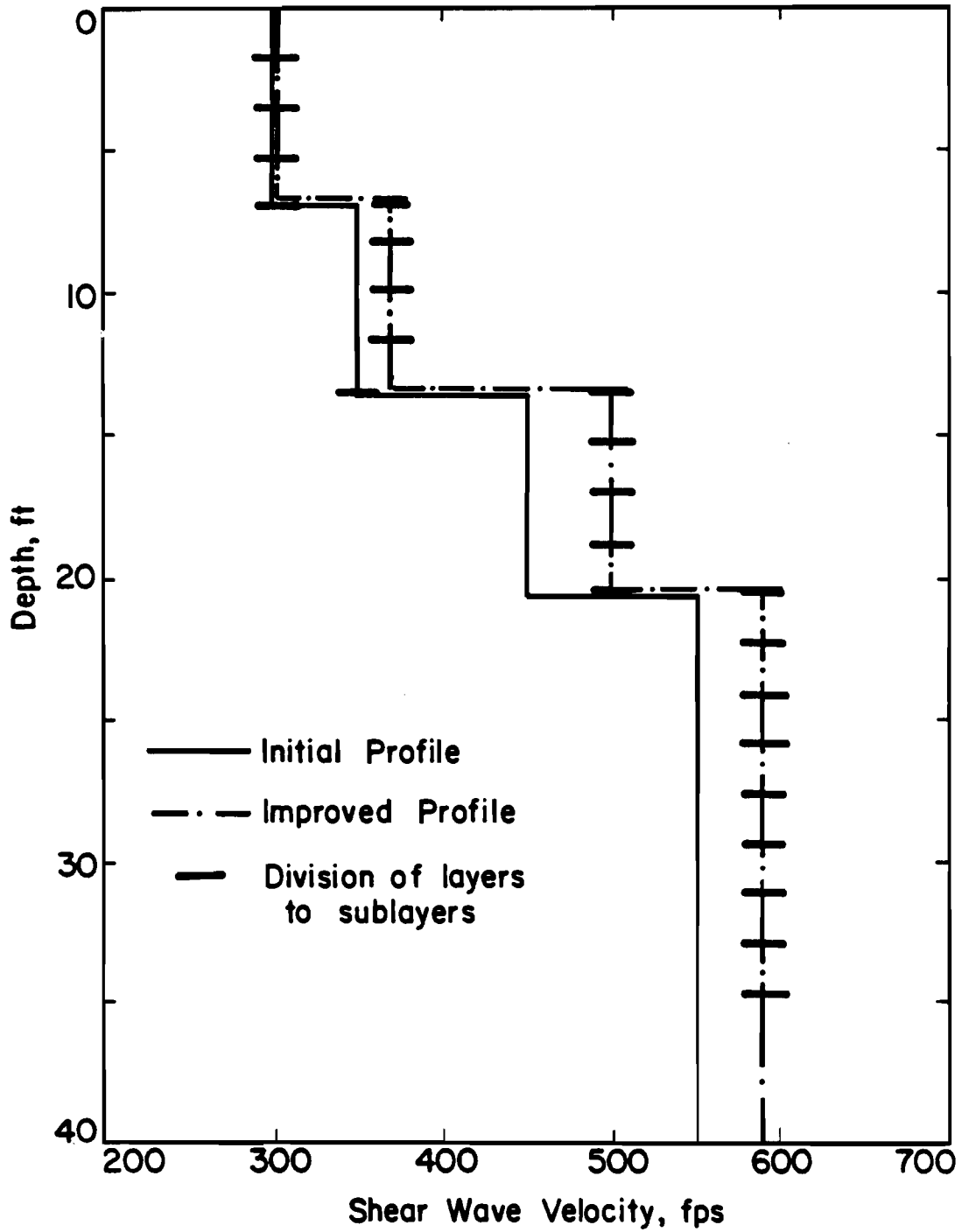


Figure 6.3 - Initial and Improved Shear Wave Velocity Profiles from First Stage of Inversion.

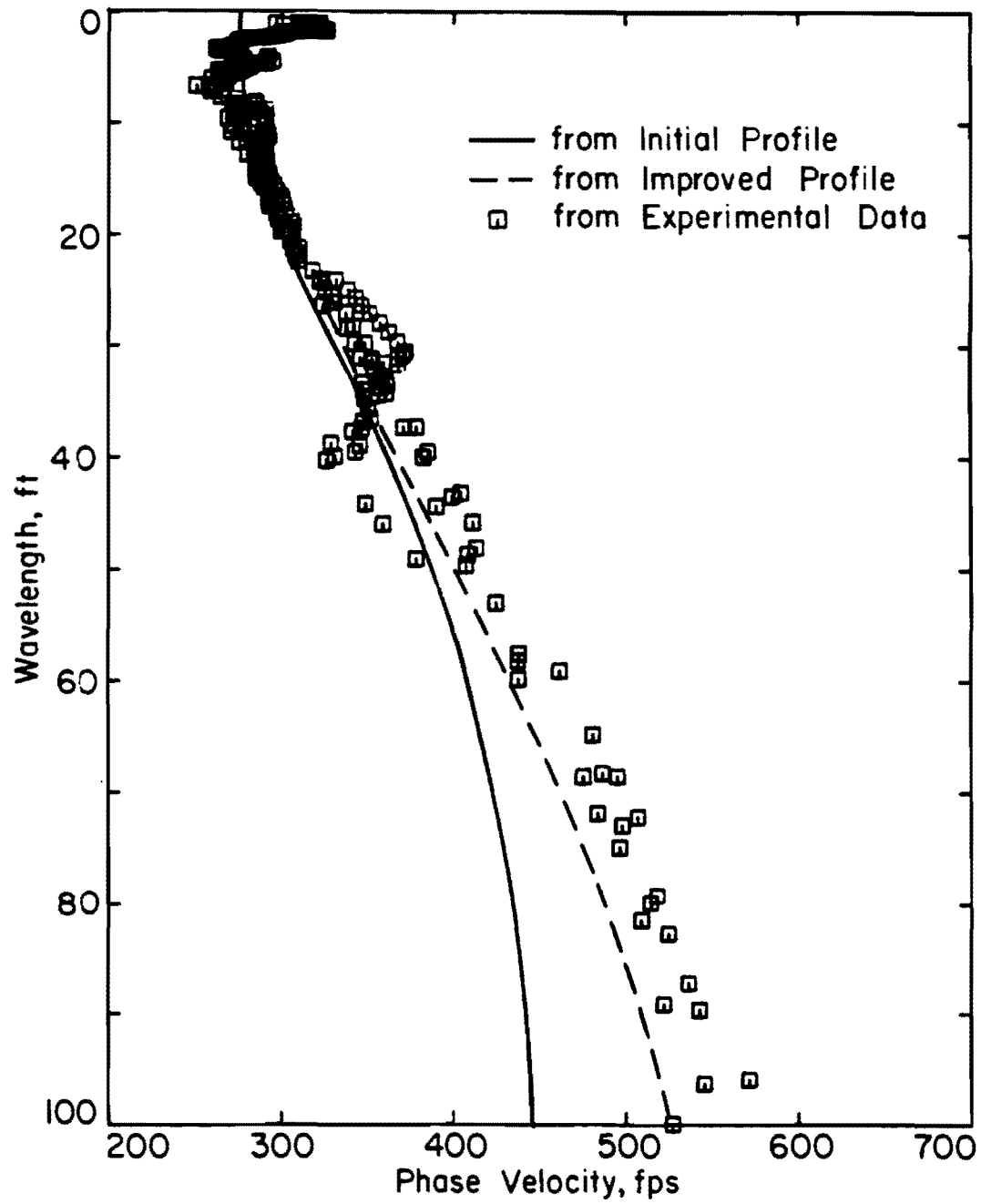


Figure 6.4 - Comparison of Theoretical and Experimental Dispersion Curves from the First Stage of the Inversion Process.

In the first stage, the dispersion curves are roughly matched as the resolution is not adequate enough for closer matching. However, in the second stage, the resolution is much greater, and the theoretical and experimental curves can be compared in a more refined manner by changing the velocities of sublayers. The other reason for this two-stage process is to avoid large variations in shear wave velocities after the initial stage. Small changes in the properties of a sublayer will have only local effects and will not cause any significant variation in the overall theoretical dispersion curves.

The question that arises is what fraction of the longest wavelength should be regarded as the depth to the top of the half-space (which is assumed as the last layer in the shear wave velocity profile). In other words, if the longest wavelength which has been measured in the field is  $L_{\max}$ , what percentage of  $L_{\max}$  should be the maximum depth of the shear wave velocity profile in the inversion process. There is no absolute or unique answer to this question as different investigators have employed different depths. First, results from this study show that the dispersion curve below wavelengths at which data points become widely spaced should be disregarded. For example, in many cases such as ones discussed in the next chapter, dispersion data were extended up to a wavelength of 200 to 300 ft (60 to 90 m); but normally below the wavelength of 100 to 150 ft (30 to 50 m) there are so few data points that they should not be considered. Second, only 1/3 of the wavelength should be chosen as the depth to the half-space. For example, if the longest wavelength is equal to 100 ft (30 m), a shear wave velocity profile to a depth of about 30 to 35 ft (9 to 11 m) should be defined and from that point on the medium should be treated as a half-space.

In the case of the Wildlife site, the layers in the  $V_s$  profile were divided into sublayers as shown in Fig. 6.3. The theoretical and experimental dispersion curves after completion of the matching process are presented in Fig. 6.5 over the range of wavelengths of 10 to 20 ft (zero to 6.7 m) and a complete set of comparison of the two curves is presented in Appendix C. The scales are greatly expanded to demonstrate

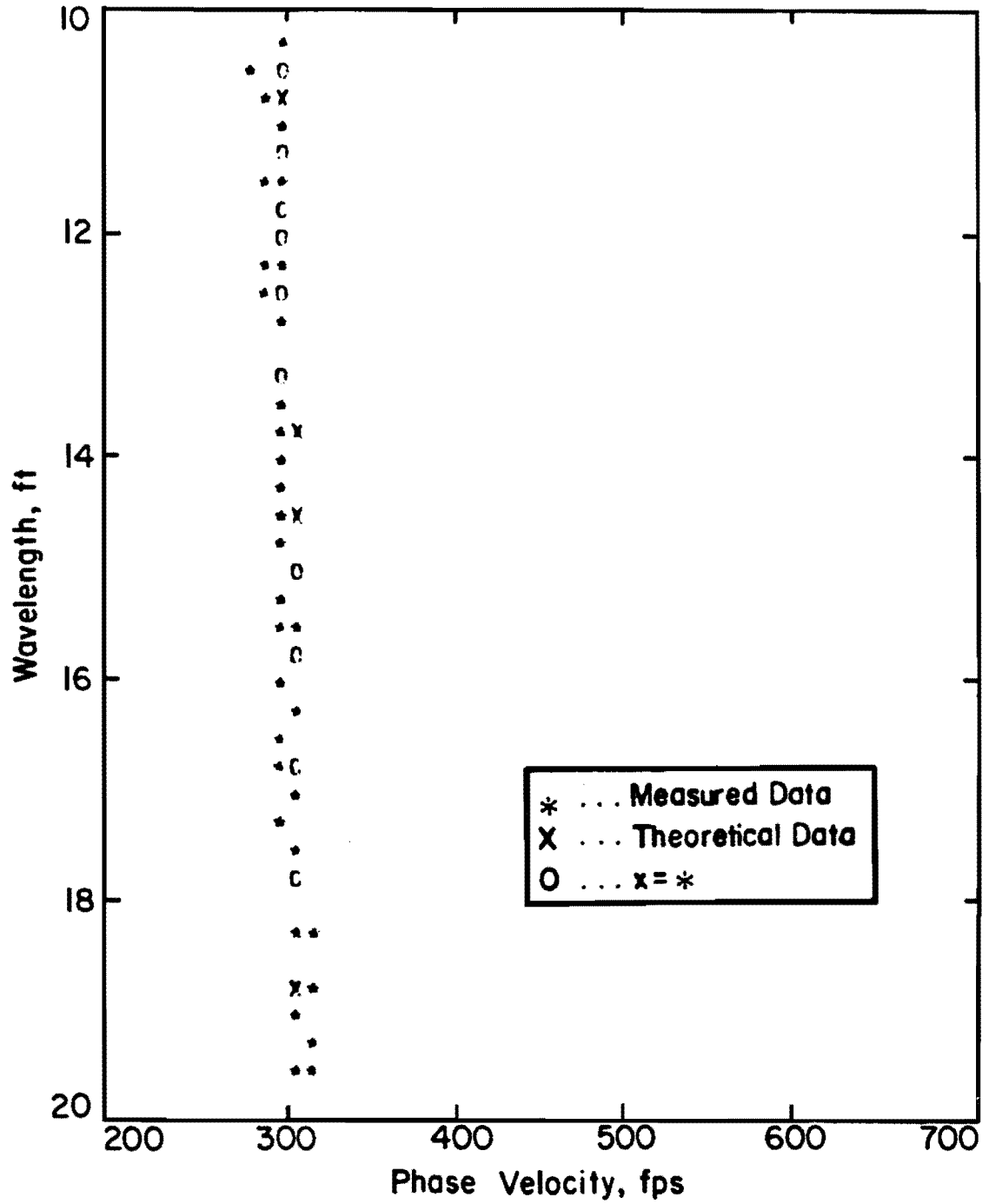


Figure 6.5 - Comparison of Theoretical and Experimental Dispersion Curves after Completion of Inversion Process at Wildlife Site (Range of Wavelengths of 10 to 20 ft).

the closeness of the match. The curves follow each other very closely. The shear wave velocity profile after inversion is shown in Fig. 6.6.

In the inversion process, the mass densities were assumed to be constant and Poisson's ratios of all layers were selected as 1/3. In Nazarian and Stokoe (1985a) it is shown that the effect of these two parameters are quite small in construction of theoretical dispersion curves. However, the effect of misjudging Poisson's ratio and mass density on determining elastic moduli is more pronounced. The values of shear and Young's moduli are proportional to mass density and the square of the shear wave velocity for a given material. Therefore, mis-estimation of the mass density has a linear effect on shear modulus. For example, if the actual mass density is 20 percent more than the estimated value, the calculated shear modulus will be 20 percent less than the actual value.

Mis-estimation of Poisson's ratio has little effect on shear modulus, but it will affect Young's modulus. Shear modulus,  $G$ , and Young's modulus,  $E$ , are interrelated by Poisson's ratio,  $\nu$ , as follows:

$$E/G = 2(1 + \nu) \quad (6.1)$$

Therefore, for Poisson's ratios of 1/4 and 1/2, the ratio of Young's to shear moduli are equal to 2.5 and 3, respectively. An error of about 20 percent is introduced to the value of Young's modulus if the Poisson's ratio of 1/2 is assumed while the actual value is 1/4.

Fortunately, mass densities and Poisson's ratios of soil deposits and pavement systems are relatively well known so that ranges of 20-percent errors mentioned in both examples are usually in excess of actual cases.

To complete the discussion, the inversion process on a flexible pavement site is presented in Appendix D.

### 6.3 COMPARISON WITH PREVIOUS INVERSION MODELS

In the simplest form, inversion has been carried out by assuming that the shear wave velocity is equal to anywhere from 1.0 to 1.1 times

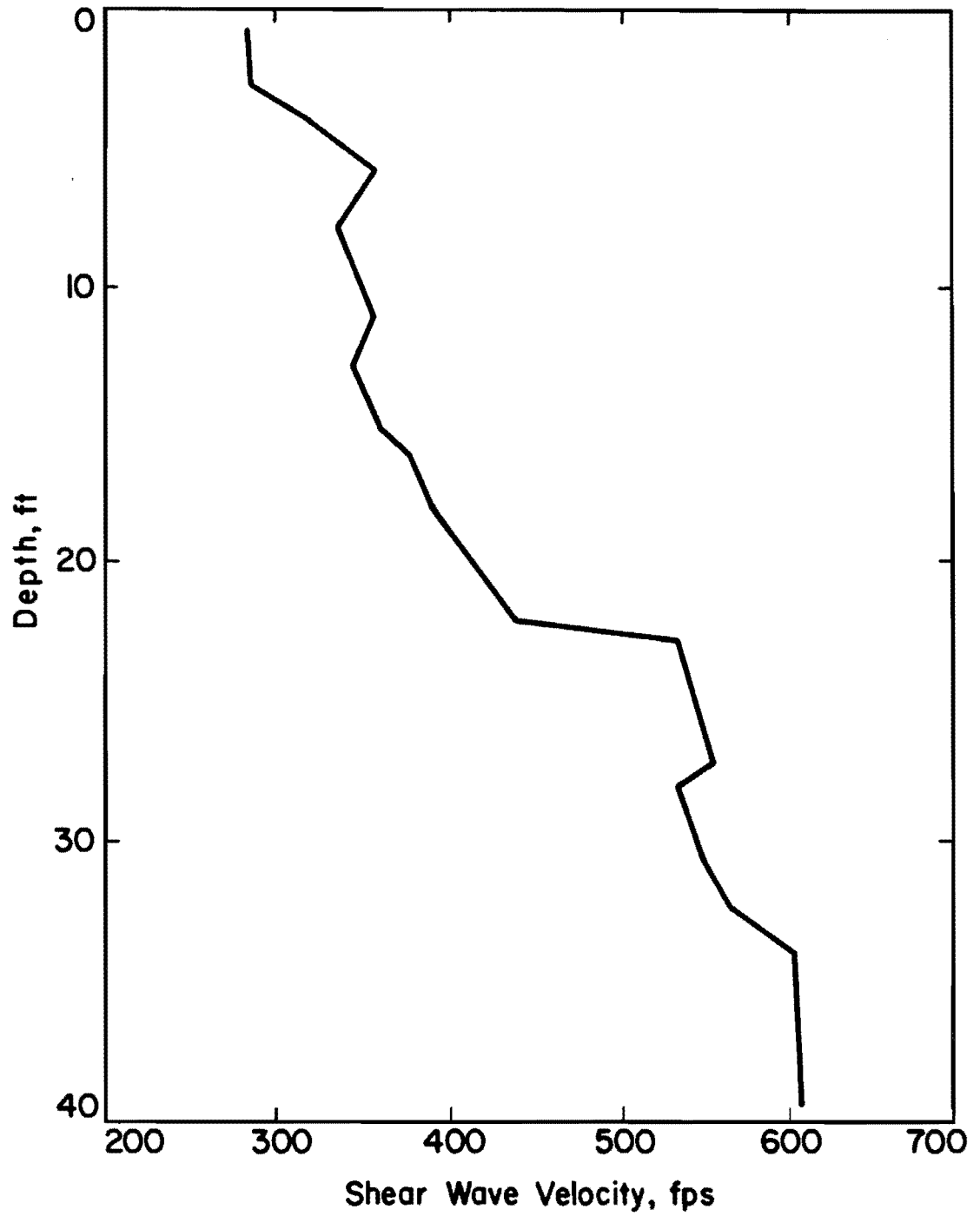


Figure 6.6 - Shear Wave Velocity Profile from Wildlife Site after Completion of Inversion Process.

the phase velocity and the depth of sampling is equal to  $1/3$  or  $1/2$  of the wavelength. For soil deposits in which the properties vary only slightly, utilization of this process may cause only a small error. However, for media in which there exists a significant variation in material properties with depth, the final shear wave velocity profile is significantly in error. For example, the dispersion curve reported by Ballard (1964) for a site in Nevada is shown by the data points in Fig. 6.7. This site was selected because the results are well documented. Frequencies measured in these tests ranged from 11 to 120 Hz. For frequencies less than 25 Hz [wavelengths greater than 40 ft (12 m)], a hydraulic vibrator with variable mass was used as the source. Above that frequency (from 35 to 120 Hz), an electromagnetic vibrator was employed to generate Rayleigh waves. A discontinuity in the dispersion curve at a wavelength of about 40 ft (12 m) exists. This discontinuity corresponds to the point where the sources were changed. Therefore, it seems that changing the sources caused some inconsistency in this region.

To perform inversion, Ballard assumed that the shear wave velocity was equal to the phase velocity and that the effective depth of sampling was equal to  $1/2$  of the wavelength. Based upon this shear wave velocity profile, a theoretical dispersion curve was generated with program INVERT. The phase velocities that should have been measured by Ballard are shown by the solid line in Fig. 6.7. It can be seen that the experimental and theoretical curves do not agree.

An attempt was made to invert correctly the dispersion curve gathered by Ballard. In this attempt, the  $V_s$  profile reported by Ballard was used as the initial profile in program INVERT, so that shear wave velocities reported by Ballard and from this attempt could be compared directly. An approximate shear wave velocity profile was determined so that the theoretical dispersion curve approximately followed the experimental curve. This profile is called an approximate one due to the fact that an accurate dispersion curve cannot be defined with so few data points over a range of wavelengths of 2 to 200 ft (0.6 to 60 m). The differences with shear wave velocity profiles are quite

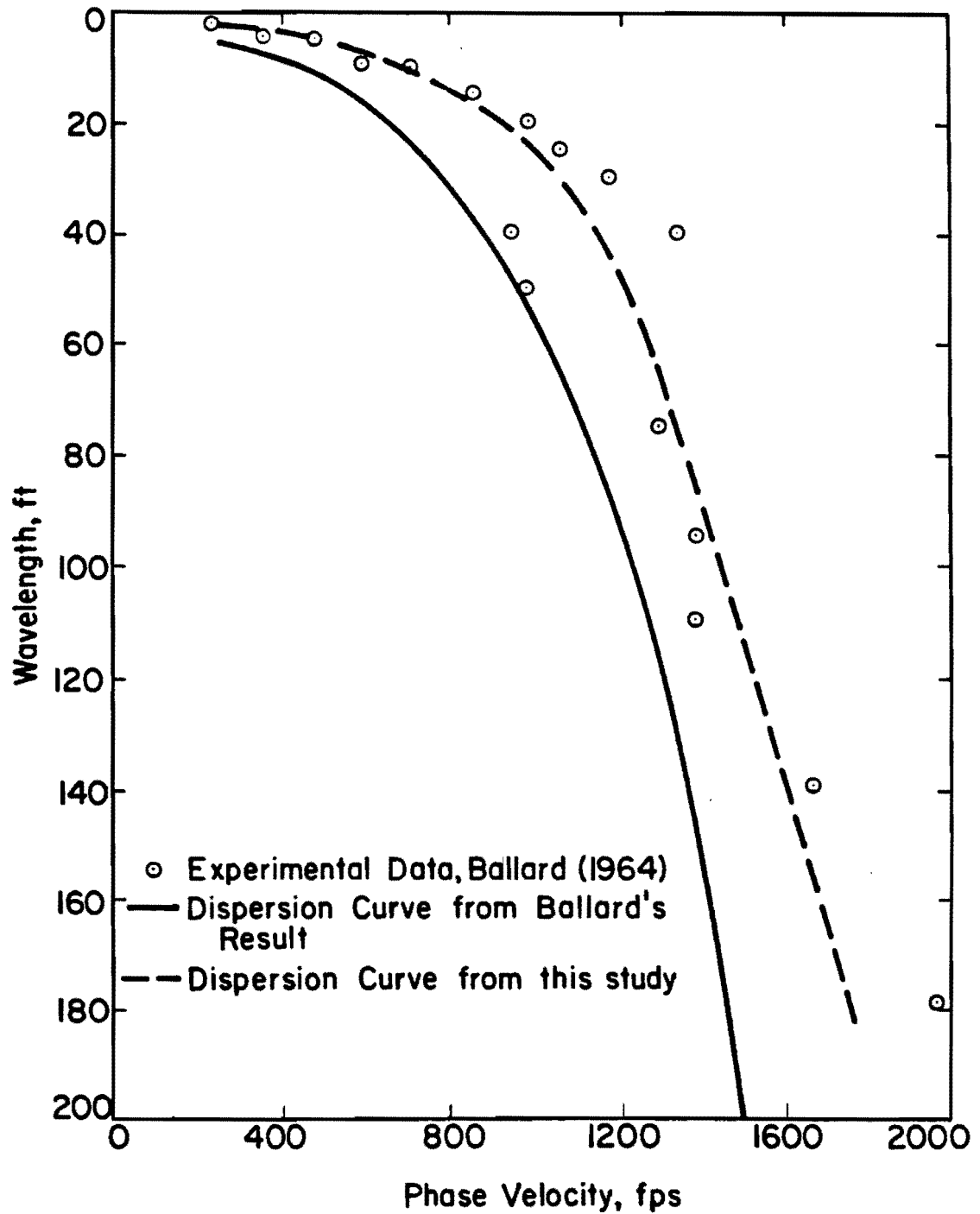


Figure 6.7 - Comparison of Theoretical and Experimental Dispersion Data from a Site in Nevada Tested by Ballard (1964).

drastic, and, therefore, the simplified inversion process employed by many investigators in the past should no longer be used.

#### **6.4 SUMMARY**

The inversion process which is the procedure for determining the shear wave velocity profile from the dispersion curve is discussed and illustrative examples are included for better understanding of this process. Finally, with an example, it is shown that the simplified inversion process, performed in the past by geotechnical and pavement engineers, of scaling dispersion curves is not appropriate and should be avoided.

This page replaces an intentionally blank page in the original.

-- CTR Library Digitization Team

## CHAPTER SEVEN

### CASE STUDIES

#### 7.1 INTRODUCTION

In this chapter several case studies are presented to demonstrate the precision and utility of the method as well as its shortcomings.

The SASW method has been employed at more than 60 sites nationwide (Nazarian and Stokoe, 1982, 1983, 1984a, 1984b, and 1984c; Nazarian et al, 1983, 1984; Stokoe and Nazarian, 1983a, 1983b, 1984a, 1984b, 1984c). Several illustrative and typical examples are selected and presented herein. The examples are divided into three categories, soil sites, flexible pavement sites, and rigid pavement sites. In all examples the SASW results are compared with other independent in situ tests performed at or in the vicinity of the SASW tests.

Development of the technique is not fully completed in terms of full automation of the technique, improvement of sources and recording device, etc. The other point which requires thorough investigation is the resolution of the method. This should be done by performing a series of tests in controlled environments using materials with well known properties so that the SASW results can be compared with those of the theory used herein. Improvements made in data collection and reduction during the course of this study are also demonstrated in some examples.

#### 7.2 SOIL SITES

The SASW method was applied to more than 30 sites at various locations in the United States during the course of this study. The most simple sites, in terms of data reduction and inversion, are soil sites, as variation in the shear wave velocities of different layers are generally small compare to pavements. In addition, major layers in the soil sites are commonly much thicker than in pavements. The results from investigation of one site are presented herein.

### 7.2.1 Effectiveness of Compaction

This site was located in a refinery in South Texas. The objective of the project was to obtain a shear wave velocity profile for dynamic machine foundation design. Crosshole tests were performed to determine the  $V_s$  profile, and SASW tests were carried out for experience and learning.

In April, 1982 a series of crosshole tests was performed at the site on the natural ground surface. Approximately a week later SASW tests were carried out at the same location. The dispersion curve from this series of tests is shown in Fig. 7.1. The shear wave velocity profile obtained from the dispersion curve is illustrated in Fig. 7.2. Twelve, 1-ft (0.3-m) thick layers were used in the inversion process. Also shown in the figure are the shear wave velocities from the cross-hole tests. The velocities determined by the two methods compare well.

About two months after SASW testing, the site was excavated to a depth of 2 ft (0.6 m) below the existing elevation and backfilled with 4 ft (1.2 m) of compacted select material. A second series of SASW tests was conducted about 10 days after the compaction was completed (May, 1982). The dispersion curve from these tests is shown in Fig. 7.3. Unfortunately the two dispersion curves (before excavation and after backfilling) cannot be directly compared due to the difference in elevations at which the tests were performed and the differences in surface materials. The second dispersion curve was inverted using 14 layers, each 1-ft (0.3-m) thick. The shear wave velocity profile for this site is presented and compared with that of the previous tests in Fig. 7.4. For depths greater than 6 ft (2 m), values of shear wave velocity from both before and after tests in the natural material agree closely. From 4 to 6 ft (1.2 to 1.8 m) the natural soil is also stiffer due to the compaction operation on the fill. In the depth range of 2 to 4 ft (0.6 to 1.2 m), the backfill has a much higher shear wave velocity than the original soil. As such, the compaction operation caused an improvement in the stiffness of this region.

Due to heavy seasonal precipitation a few days before the second set of tests, the top one ft (0.3 m) of compacted material was quite

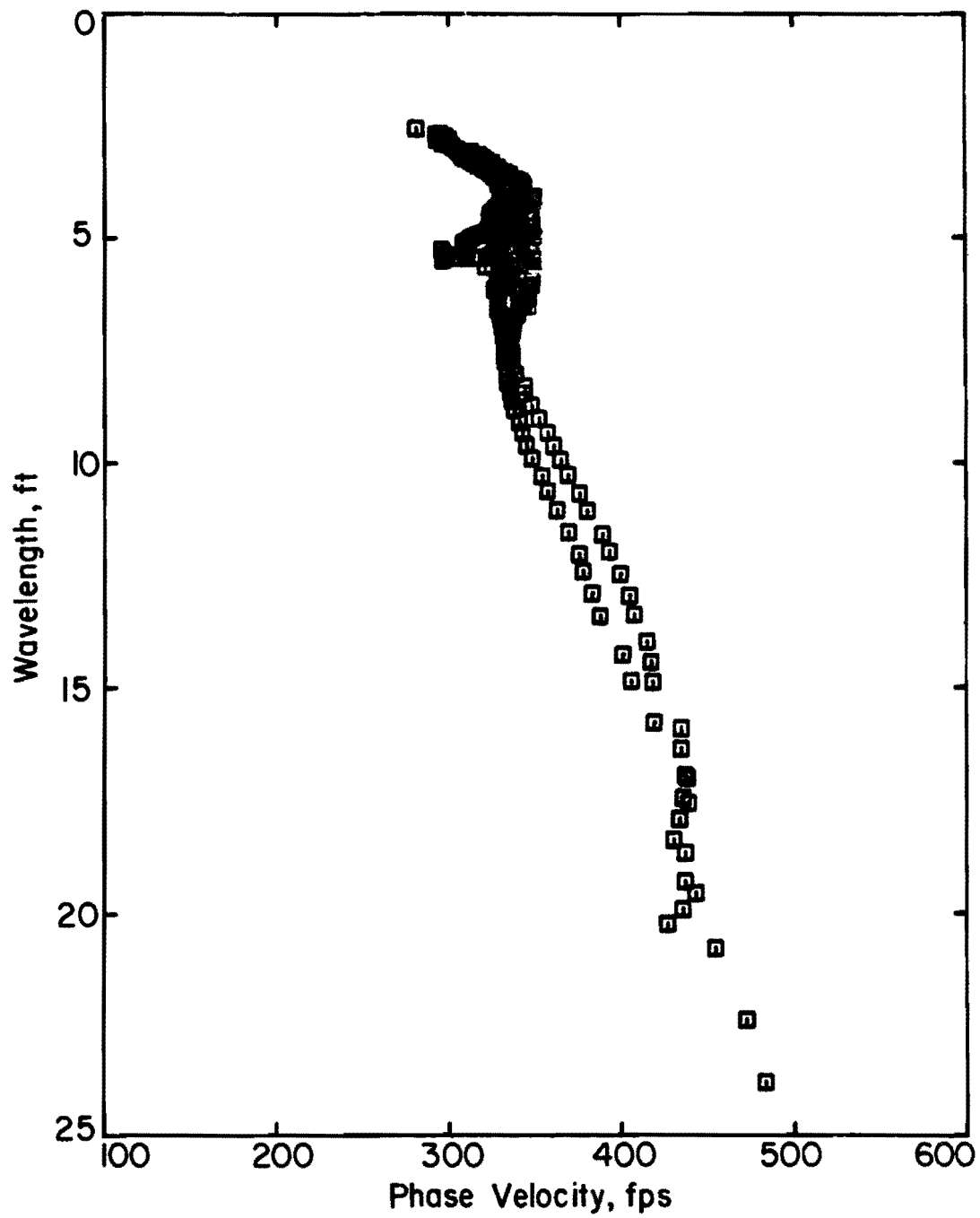


Figure 7.1 - Dispersion Curves from SASW Tests at Compaction Site before Excavation.

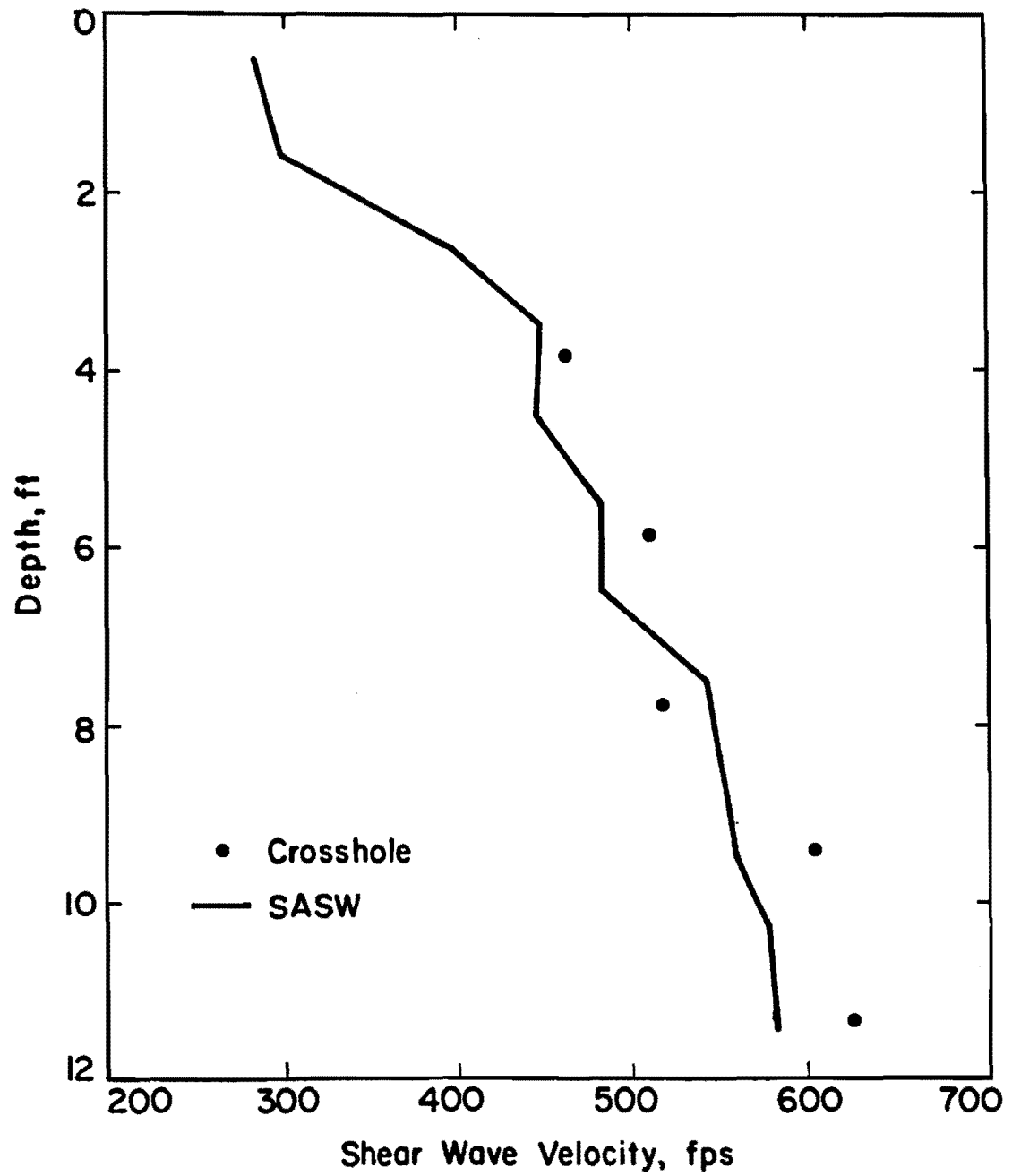


Figure 7.2 - Shear Wave Velocity Profiles from SASW and Crosshole Tests at Compaction Site before Excavation.

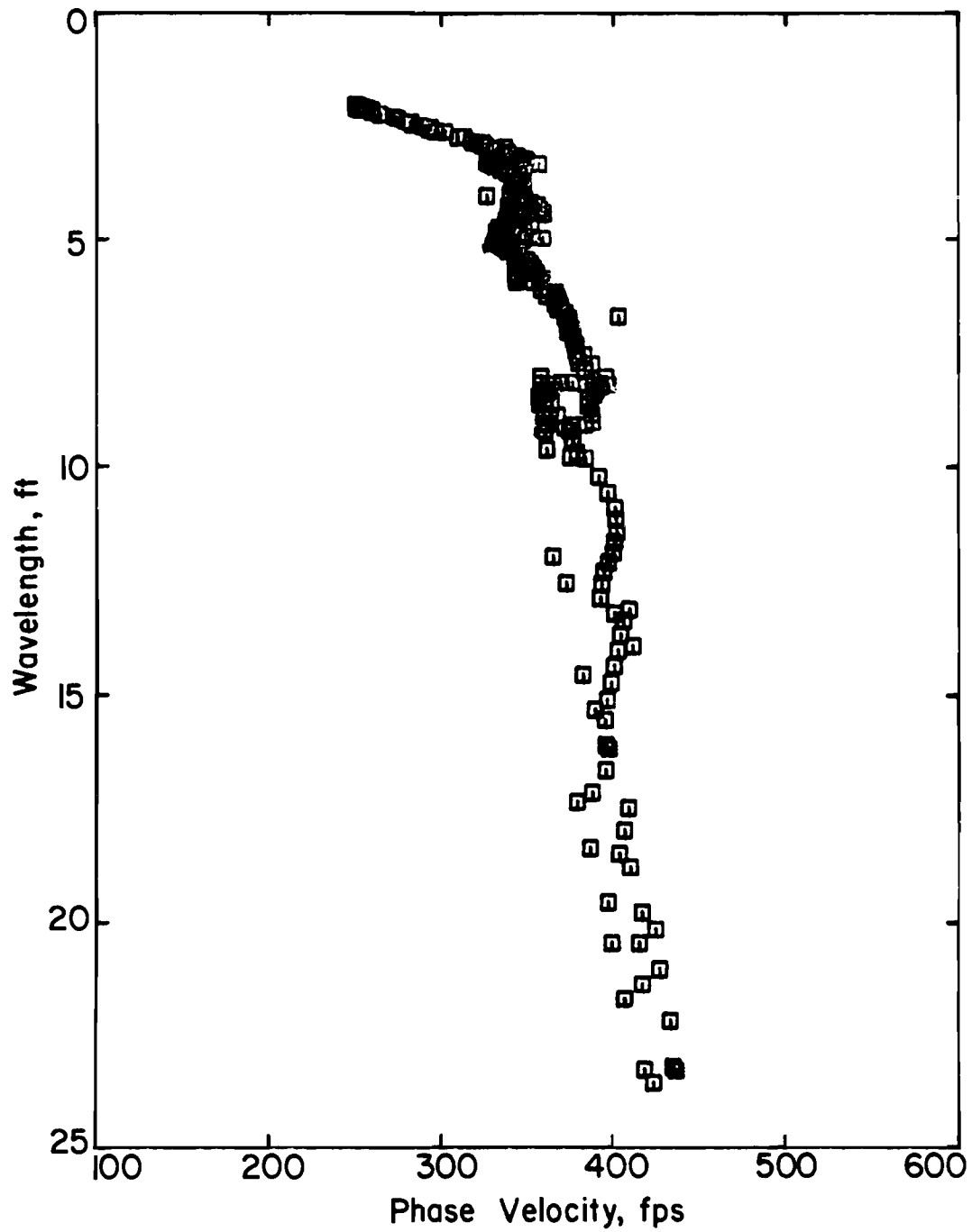


Figure 7.3 - Dispersion Curve from SASW Tests at Compaction Site after Backfilling.

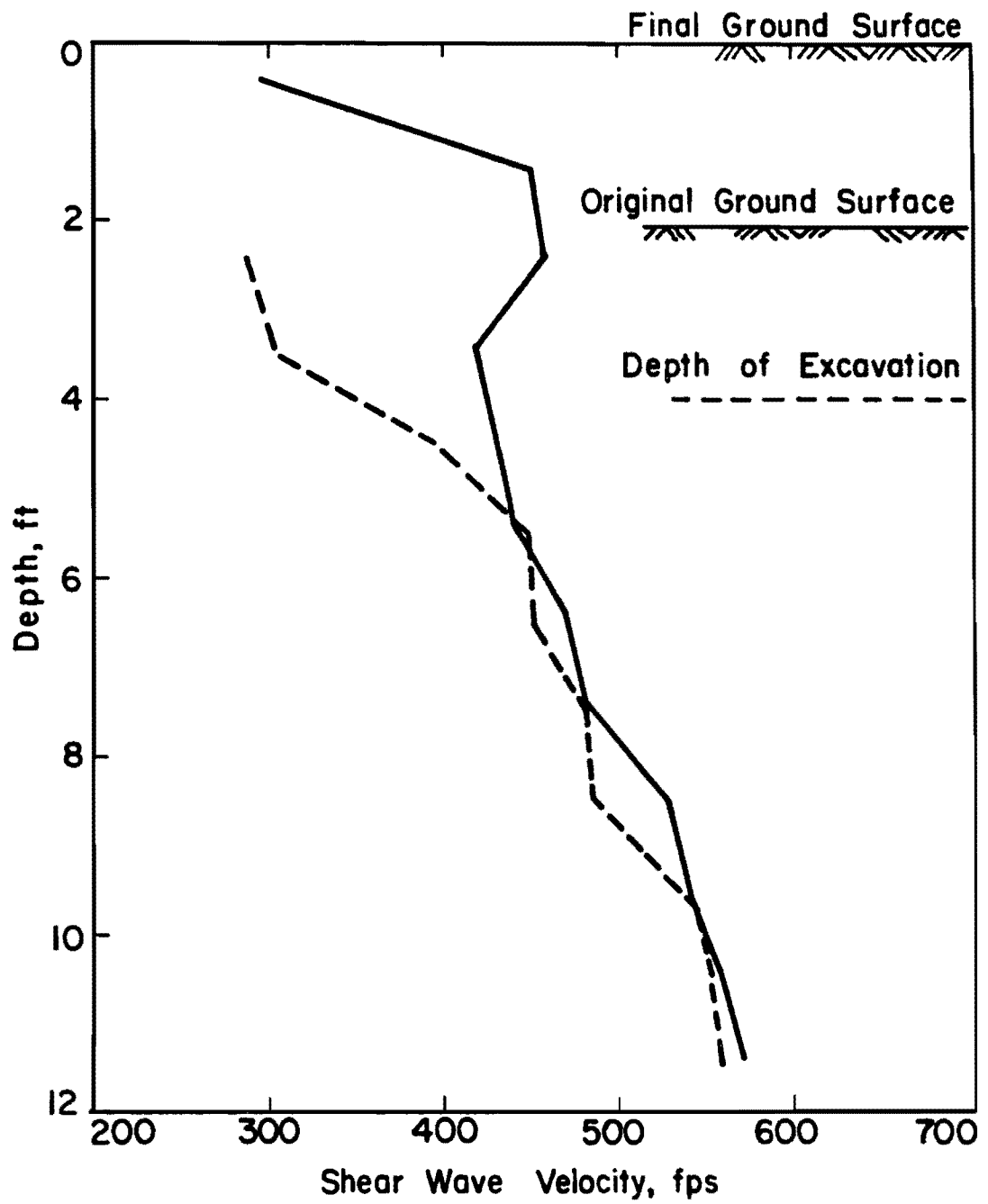


Figure 7.4 - Comparison of Shear Wave Velocity Profiles at Compaction Site before and after Compaction.

soft [ $V_s$  less than 400 fps (120 m/s)]. If the crude inversion technique presented in Section 6.3 had been used, the stiffness of the fill material would have been underestimated as the existence of a low velocity layer (as in this example) has the tendency to shift the whole dispersion curve towards lower phase velocities.

### 7.3 FLEXIBLE PAVEMENT

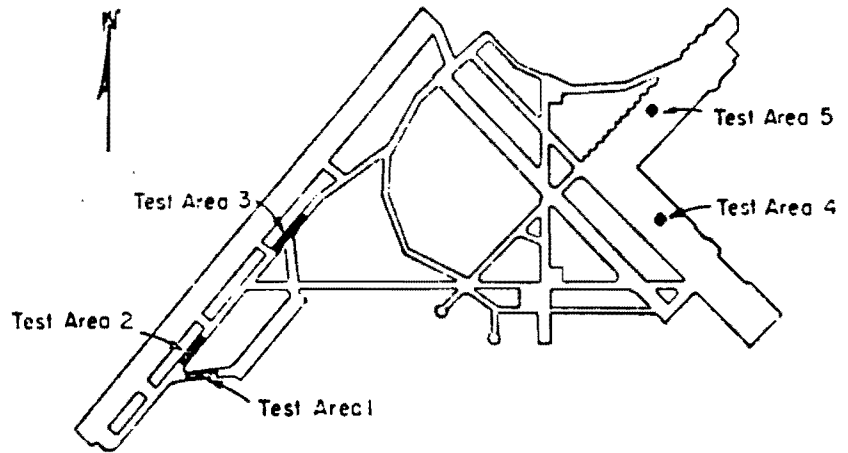
Next to soil sites, inversion of the dispersion curves from flexible sites can be performed reasonably easily. More than 15 asphaltic pavement sites have been tested, and the results from two sites are presented to demonstrate the function of the SASW method as well as some of the limitations on this type of pavement.

#### 7.3.1 McDill Air Force Base

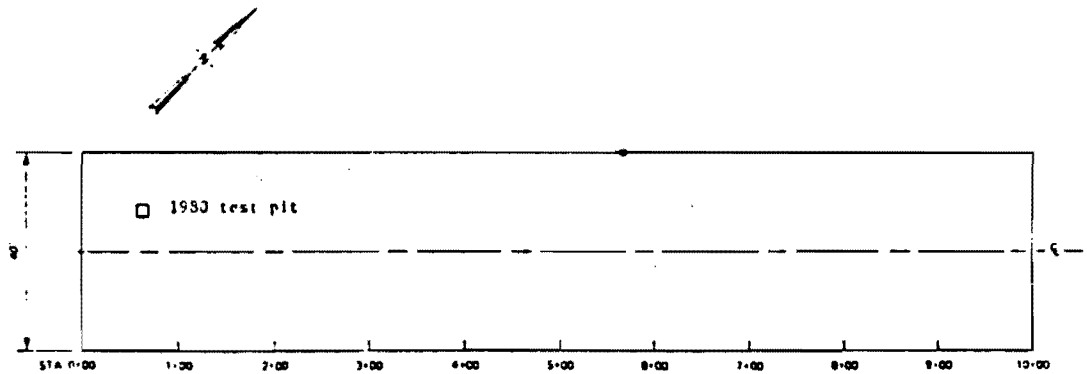
The SASW method was employed at five sites at McDill Air Force Base (AFB), in Tampa, Florida in August, 1983 (Stokoe and Nazarian, 1984b). The crosshole method was also used at three of the SASW sites for comparison. The airfield layout along with location of the test sites are shown in Fig. 7.5a. The site discussed herein is site 3, and its exact location is shown in Fig. 7.5b. Personnel of the Air Force had run California Bearing Ratio (CBR) tests at the location marked as the test pit in Figure 7.5b. The centerline of the SASW array was located close to test pit.

A composite profile of the site is shown in Fig. 7.6. The profile consists of approximately 5 in. (12.5 cm) of high quality asphaltic-concrete (AC) underlain by 8.5 in. (21 cm) of lime rock, 5.5 in. (13.5 cm) of sandy-silt and then a sandy subgrade. This material profile agrees reasonably well with that measured during the drilling operation for the crosshole seismic tests.

The dispersion curve from this site is presented in Fig. B.4, and the process of inversion is discussed in detail in Appendix D. The shear wave velocity profile along with the layering used in inversion are shown in Fig. 7.7. A total of 20 layers was used, and the thicknesses of the layers were increased gradually as the properties of

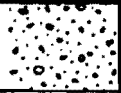
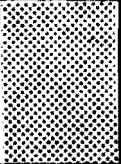
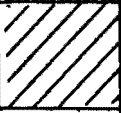
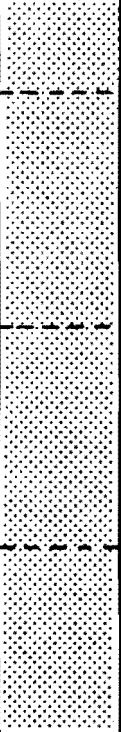


a. Airfield Layout Showing Location of Tests Areas.



b. Close-up of the Site.

Figure 7.5 - Location of Sites Tested at McDill Air Force Base.

Depth, in.	Material		Dry Unit Weight, pcf	Water Content, percent	CESS+		CBR percent
	Symbol	Classi- fication			COMP*	OMC**	
(1)	(2)	(3)	(4)	(5)	(6)	(6)	(7)
5.0		AC					
13.5		Lime Rock	114.1	10.4	97.1	11.3	10
19.0		SP-SM	107.3	9.1	96.1	11.5	25
24.0		SP	97.0	10.8 9.4	92.2	12.1	30
36.0				4.7			
48.0				14.6			

\*Percent Compaction

\*\*Optimum Water Content

+CESS = Compactive Effort on Subgrade Soil

Figure 7.6 - Composite Profile of Site 3 at McDill Air Force Base.

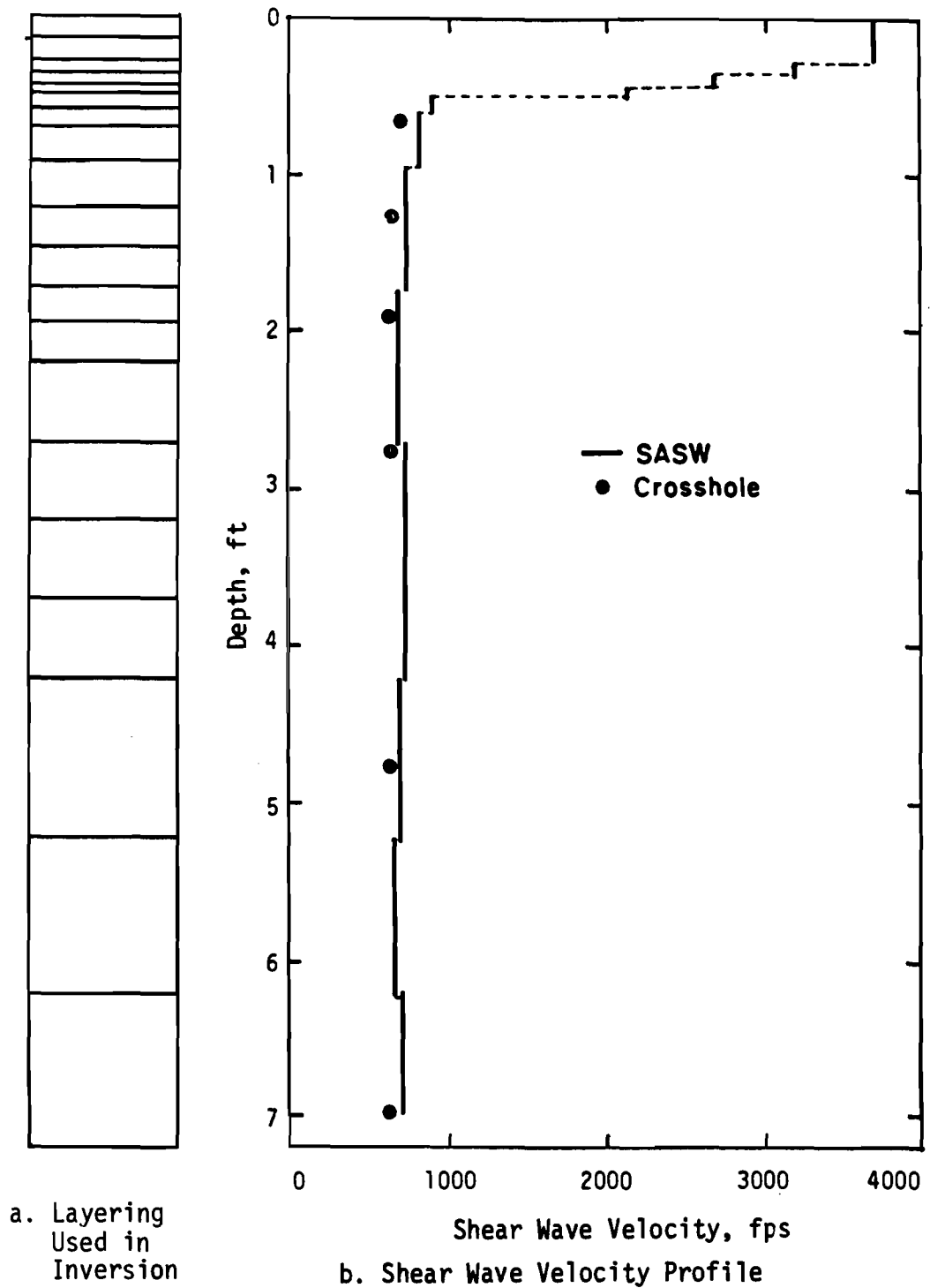


Figure 7.7 - Comparison of Shear Wave Velocity Profiles from SASW and Crosshole Tests at McDill Air Force Base.

near-surface materials are generally of most interest in a pavement system.

The results of the SASW tests are compared with S-wave velocities obtained from crosshole tests in Fig. 7.7. The velocities compare well below a depth of 1.5 ft (0.45 m). Unfortunately, S-wave velocities in the asphalt could not be measured with the crosshole test. The shear wave velocity of the lime rock is quite low as predicted by the crosshole test and as reflected in the California Bearing Ratio (CBR) results presented in Fig. 7.6.

Young's modulus profile from the crosshole and SASW tests are presented in Fig. 7.8 and Table 7.1. To obtain Young's moduli from the crosshole tests, the following procedure was followed.

1. As both P- and S-wave velocities of the layers were determined, Poisson's ratio was calculated from:

$$\nu = [0.5(V_p/V_s)^2 - 1]/[(V_p/V_s)^2 - 1] \quad (7.1)$$

2. Shear modulus was calculated for the measured S-wave velocity and an assumed unit weight using Eq. 2.1.
3. Young's modulus was then calculated utilizing Eq. 2.2 as shear modulus and Poisson's ratio were known.

Young's moduli obtained from the SASW tests were determined based on the assumed Poisson's ratios and unit weights used in the inversion process. Values of Poisson's ratio of 0.25 for the asphalt and 0.33 for the other materials were assumed. Unit weights were assumed to be equal to 135 and 110 pcf (21.2 and 17.3 kN/m<sup>3</sup>) for the asphalt and remainder of the profile, respectively. The difference in the moduli from SASW and crosshole tests is 15 percent on the average, with a maximum deviation of 26 percent as shown in column 6 of Table 7.1.

In pavement sites (such as in this case), the inversion process is not sensitive to change in the velocity of the layer immediately below because of the the large velocity contrast between the surface

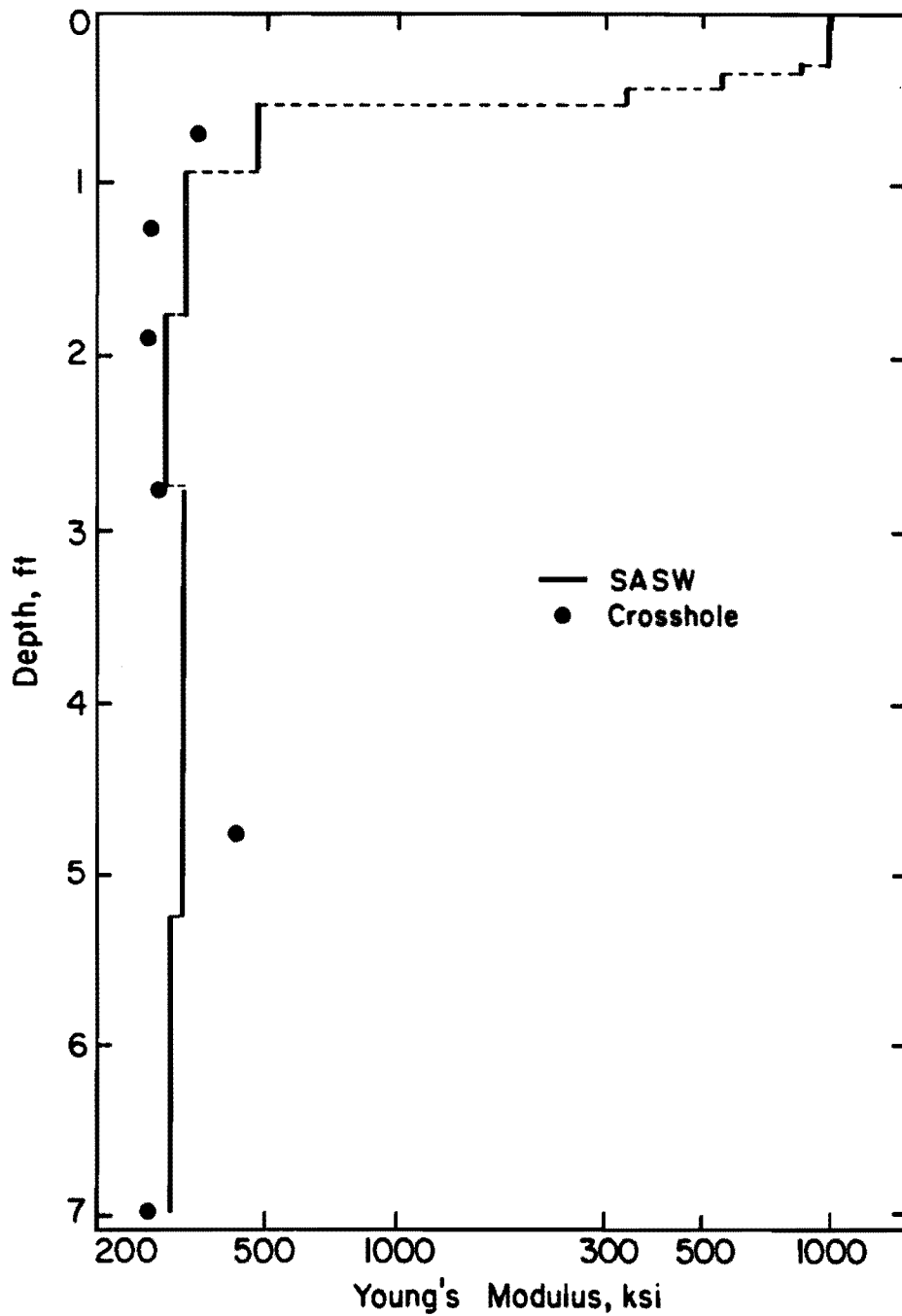


Figure 7.8 - Comparison of Young's Modulus Profiles from SASW and Crosshole Tests at McDill Air Force Base.

Table 7.1. Comparison of Young's Moduli from SASW and Crosshole Tests at McDill Air Force Base.

Depth ft	Young's Modulus, ksi			Differences	
	SASW2 <sup>+</sup>	SASW <sup>++</sup>	Crosshole	$\frac{2-3}{3}$	$\frac{4-3}{3}$
(1)	(2)	(3)	(4)	(5)	(6)
0.20	1103	1282	949*	-13.9	-26.0
0.67	292	42.6	35.5	585.4	-16.7
1.25	161	31.9	26.1	404.7	-18.2
1.92	33.9	29.7	25.6	14.1	-13.8
2.75	30.6	32.7	29.1	-6.4	-12.4
4.75	29.2	31.2	36.7	-6.4	17.6
7.00	25.3	31.1	27.1	-18.6	-12.9

+ from Second Version of Inversion Process

++ from Third Version of Inversion Process

\* from P-Wave Velocity

layer and the base. The velocity in this region may be in error which results in a nonuniqueness in the results in this region. This matter is the greatest weakness of the latest inversion process and should be studied more thoroughly in the future.

Shear wave velocities obtained by the second phase of the inversion process, discussed in Section 6.2, are shown in Fig. 7.9 along with shear wave velocities determined from program INVERT. Young's moduli from the second inversion process are also given in Table 7.1. At depths below 2 ft (0.6 m), moduli from both inversion processes compare well. Near-surface moduli from the second process are as much as five times stiffer (and incorrectly estimated). The two profiles follow each other in the subgrade soil, as expected. However, near the surface, the moduli of the lime rock is overestimated by as much as five times relative to the new process. Notice that the CBR value of the lime rock is only 10, whereas a typical base material has a CBR of nearly an order of magnitude higher. Therefore, it can be seen that the new version of inversion is more apt to predict the stiffnesses of near-surface materials.

### 7.3.2 Embankment Site

A series of tests was performed in Austin, Texas on a flexible pavement section in October, 1982. The profile consisted of 2.5 in. (6.3 cm) of asphaltic concrete over 15 in. (38 cm) of cement treated base underlain by clayey subgraded. The dispersion curve from this site is shown in Fig. 7.10. The shear wave velocity profile after inversion is shown in Fig. 7.11 along with the layering used in the inversion process. A series of crosshole tests was also performed approximately two weeks prior to the SASW tests. The results from the crosshole tests are shown in Fig. 7.11. The shear wave velocity profiles from the two tests compare well except at a depth of 1.5 ft (0.45 m) which corresponds to the base material. Deviation between the velocities at this depth is about 25 percent. It seems that this difference is due to the fact that the inversion process still overestimates somewhat the property of the material adjacent to the top layer because a stiff layer

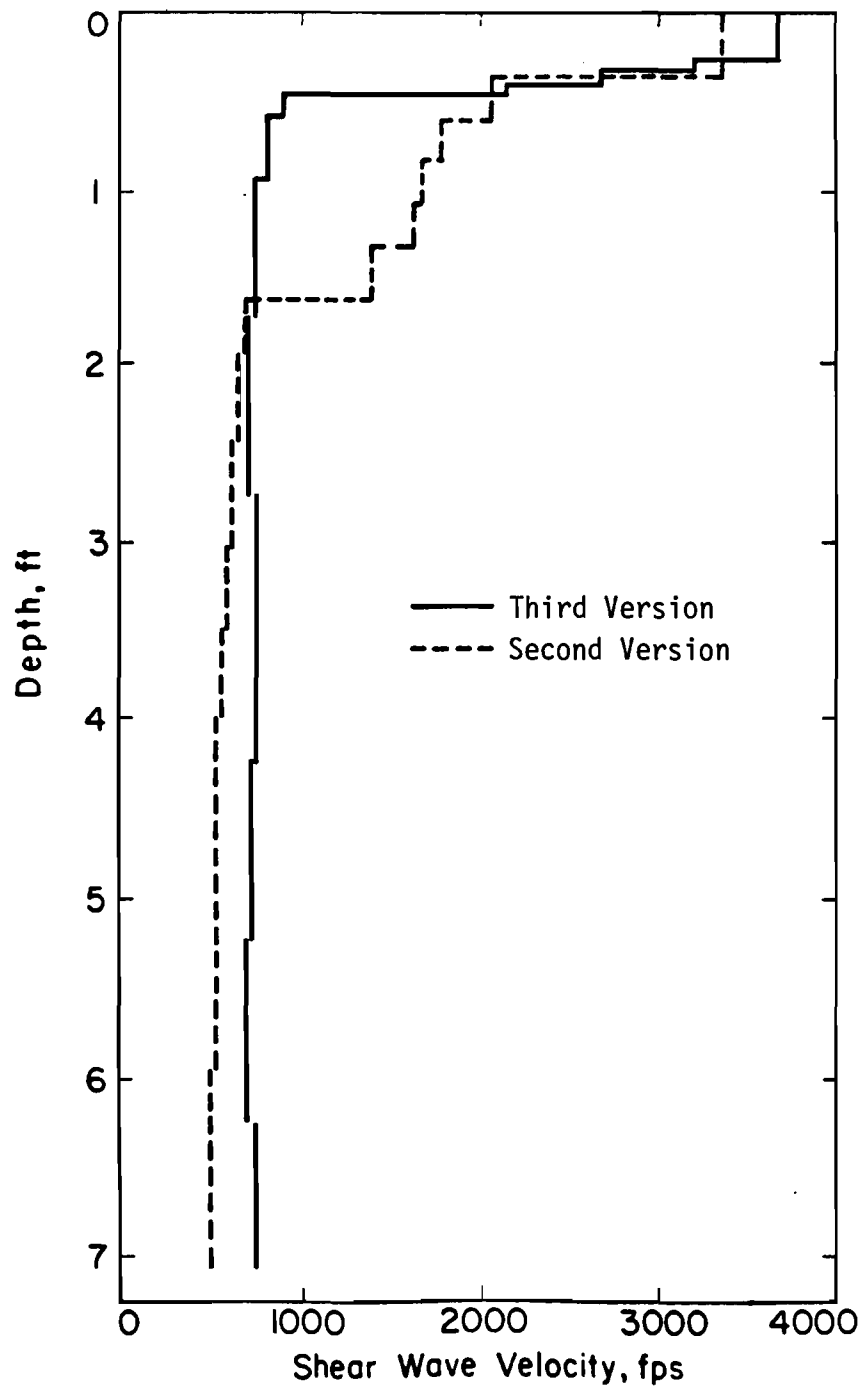


Figure 7.9 - Comparison of Shear Wave Velocity Profiles Based on the Second and Third Generations of the Inversion Process.

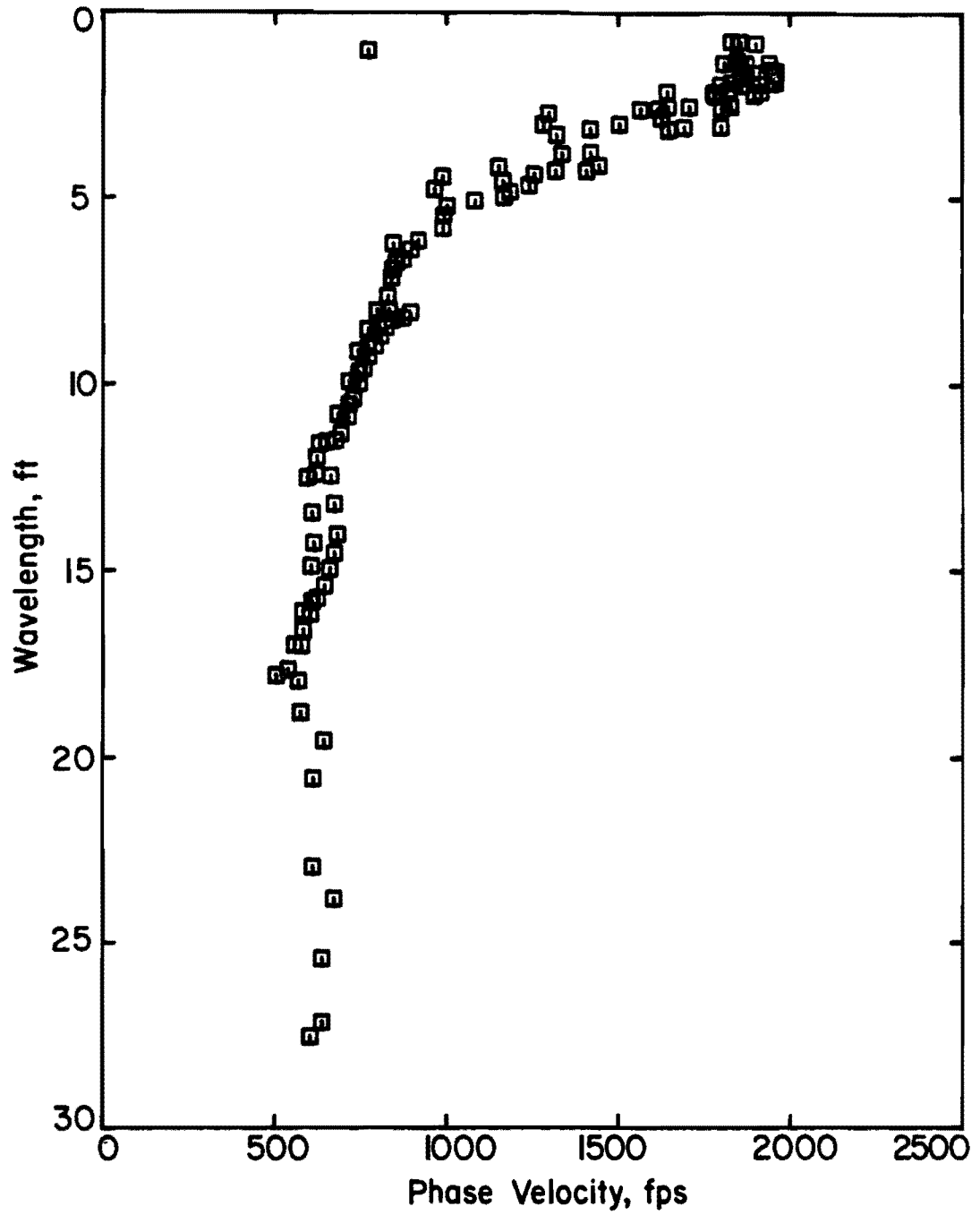


Figure 7.10 - Dispersion Curve from SASW Tests at Embankment Site.

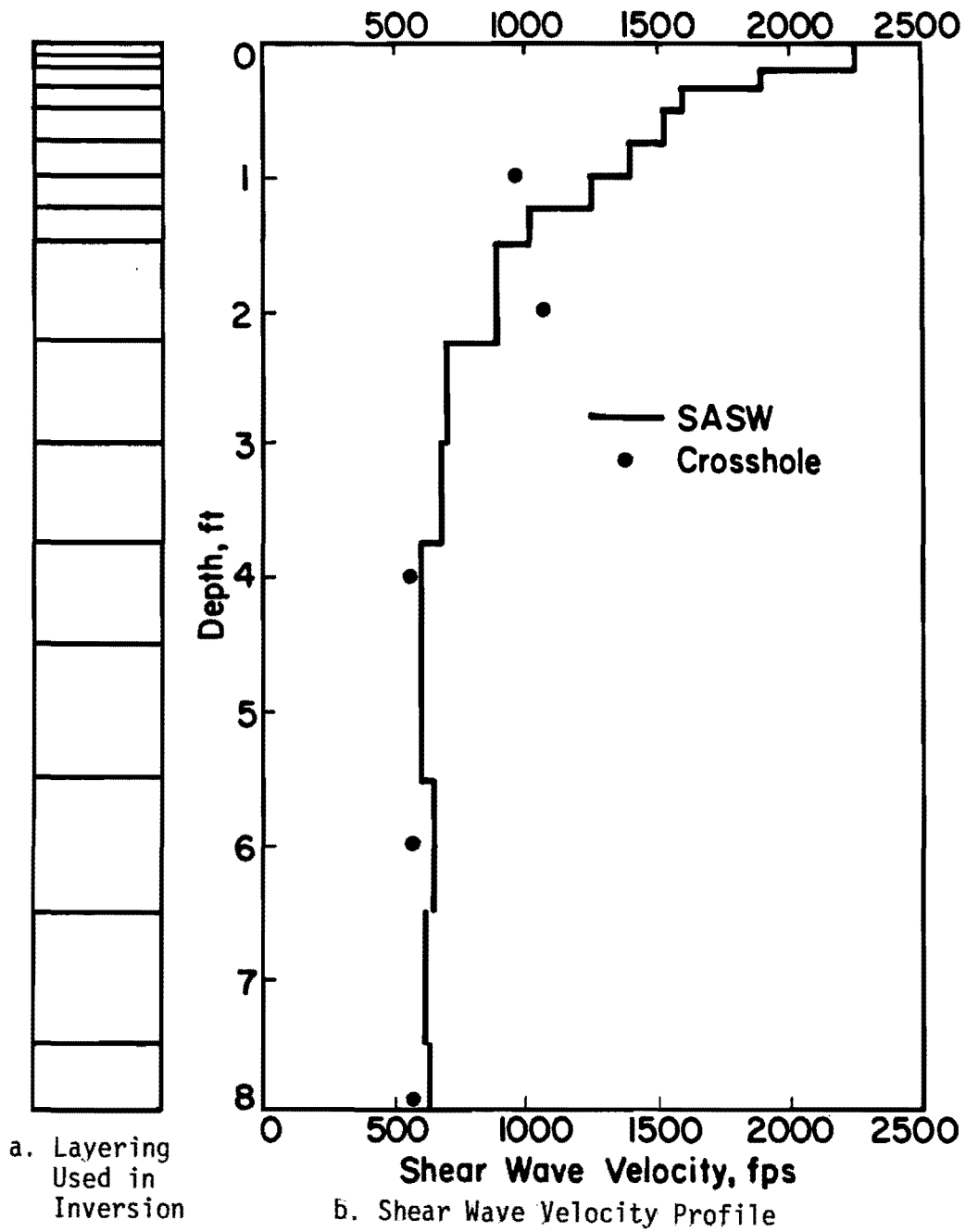


Figure 7.11 - Comparison of Shear Wave Velocity Profiles from SASW and Crosshole Tests at Embankment Site.

is immediately underlain by a much softer material. More research on this subject is required, and the inversion algorithm should be improved to solve this deficiency.

In May, 1983 a second set of the SASW tests was carried out at this site. In the period between the two experiments, the original pavement was removed and replaced by a new pavement. The new pavement consists of 2.5 in. (6.3 cm) of asphaltic concrete underlain by 15 in. (38 cm) of flexible base and then subgrade. The dispersion curve from this series of tests is presented in Fig. 7.12 and is compared with the curve obtained before replacement of the pavement in Fig. 7.13. The two curves follow each other quite well, within ten percent for wavelengths greater than 5 ft (1.5 m) within ten percent. Above this wavelength the dispersion curve from the old pavement lies below the curve from the new pavement, resulting in a higher stiffness for the old pavement. The shear wave velocity from the new pavement is presented and compared with the profile from the old pavement in Fig. 7.14. To accelerate the inversion process, the shear wave velocity profile from the first series of tests was input as the first estimate of the profile in the second set, because the thicknesses of the layers in both new and old pavements were equal. It is interesting to note that the asphalt layer is stiffer for the old pavement section, possibly due to an aging affect or temperature differences. The base material is stiffer in the first pavement as well, due to use of stabilized material as opposed to granular base material used for the new section.

Young's modulus profiles from the two series of SASW tests are shown in Fig. 7.15 and are compared in Table 7.2. Young's modulus of the asphalt layer is 20 percent higher in the old pavement section. The base material is on the average 15 percent stiffer for the old pavement. The subgrade moduli are within 20 percent, with a maximum difference of 40 percent at a depth of 4 ft (1.2 m). In the subgrade the moduli from the tests performed on the new pavement are consistently higher. However, the variation in the results from the two sets of tests is in the range of accuracy expected from this method. Therefore, it cannot, at this time, be determined if these differences in subgrade

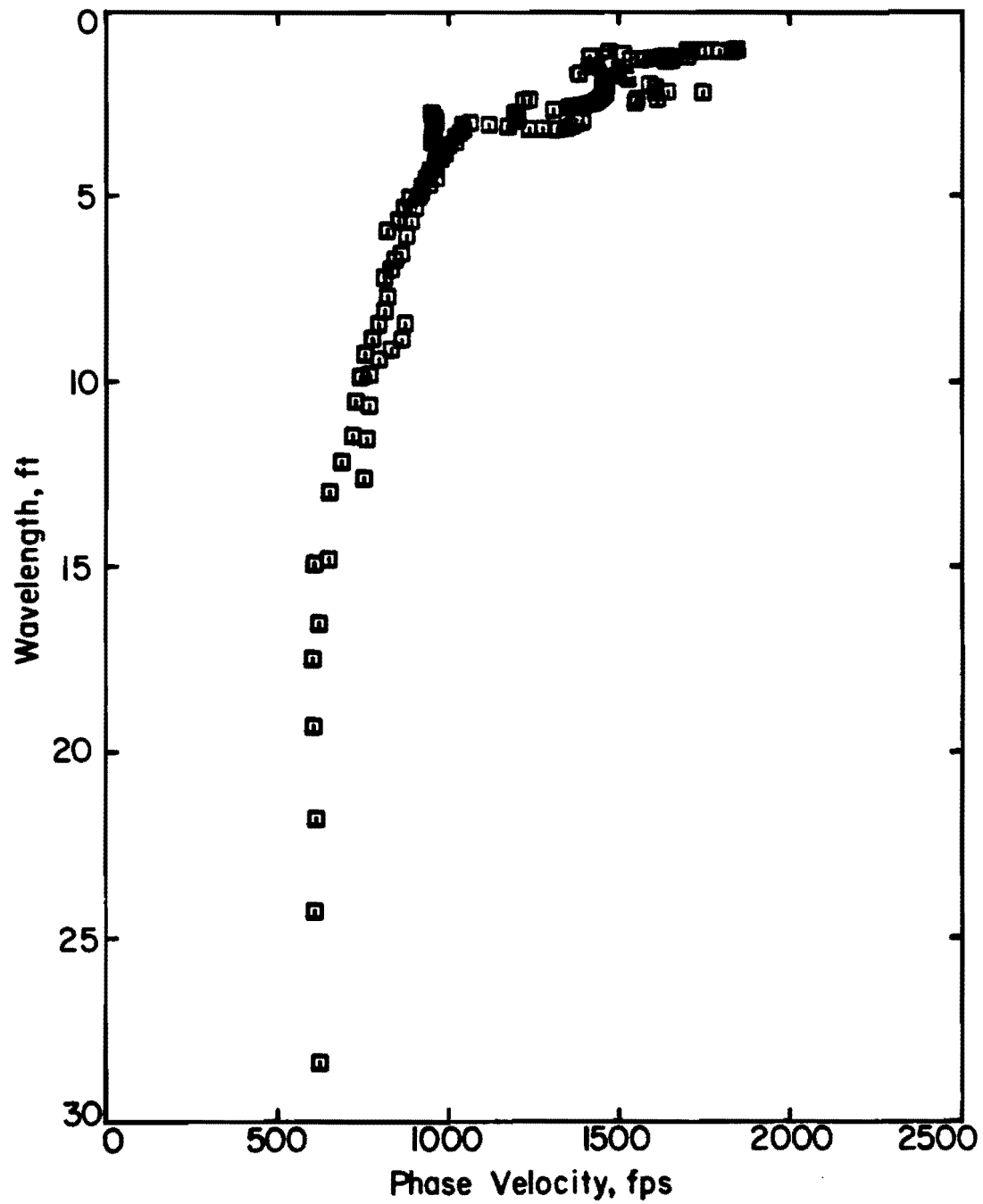


Figure 7.12 - Dispersion Curve from SASW Tests at Embankment Site after Replacement of the Pavement.

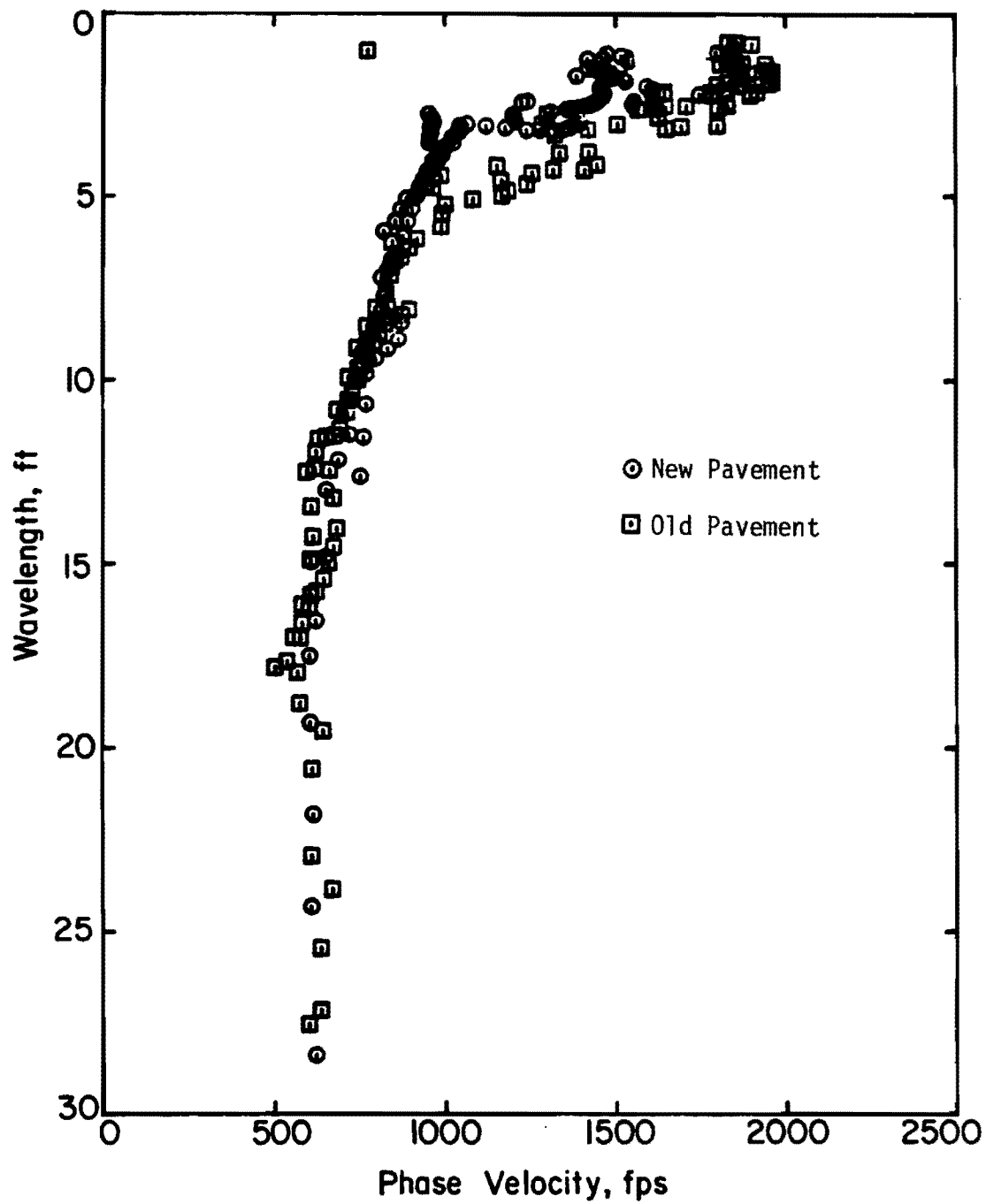


Figure 7.13 - Comparison of Dispersion Curves from SASW Tests Performed on Old and New Pavements.

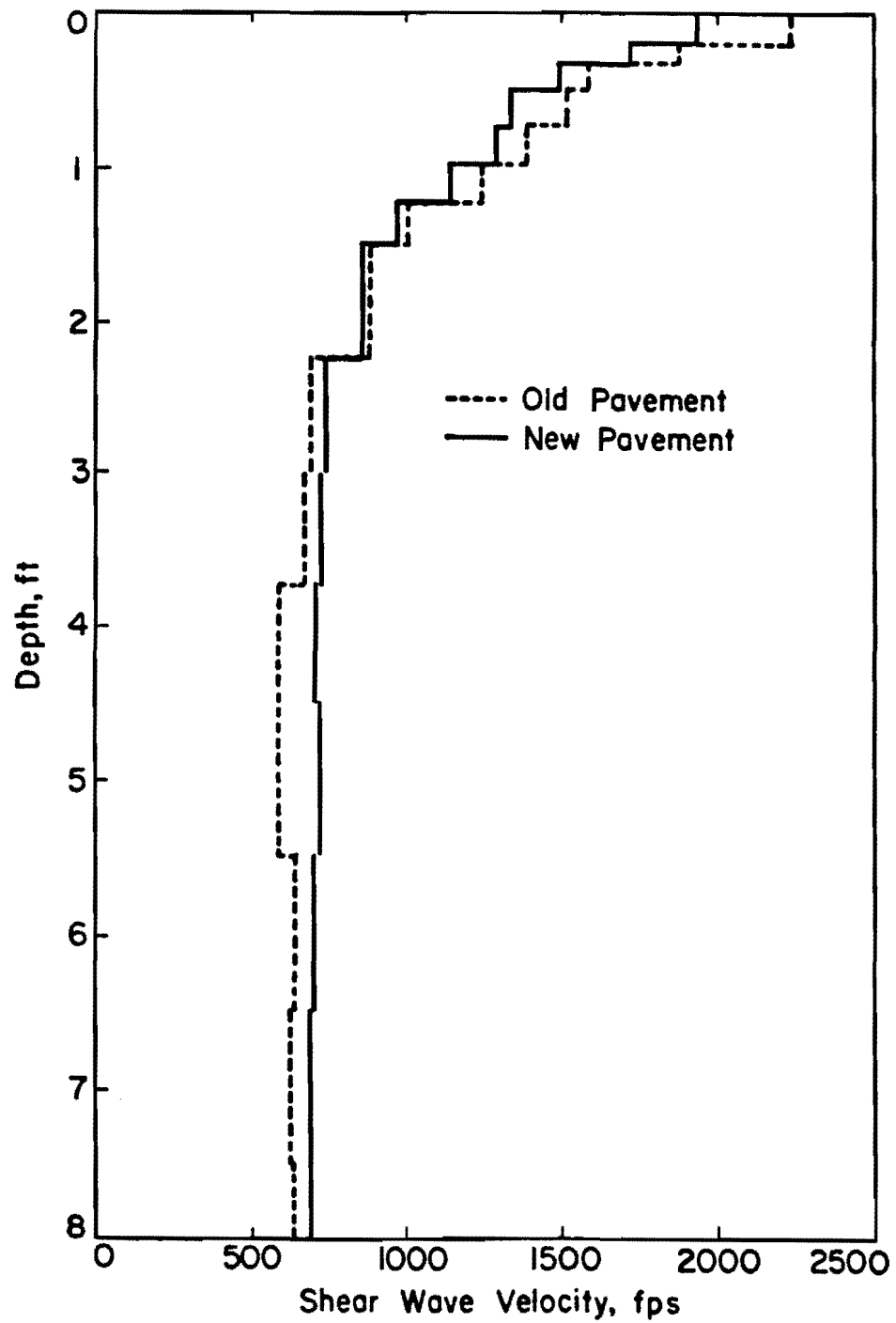


Figure 7.14 - Comparison of Shear Wave Velocity Profiles from SASW Tests Performed on Old and New Pavements at Embankment Site.

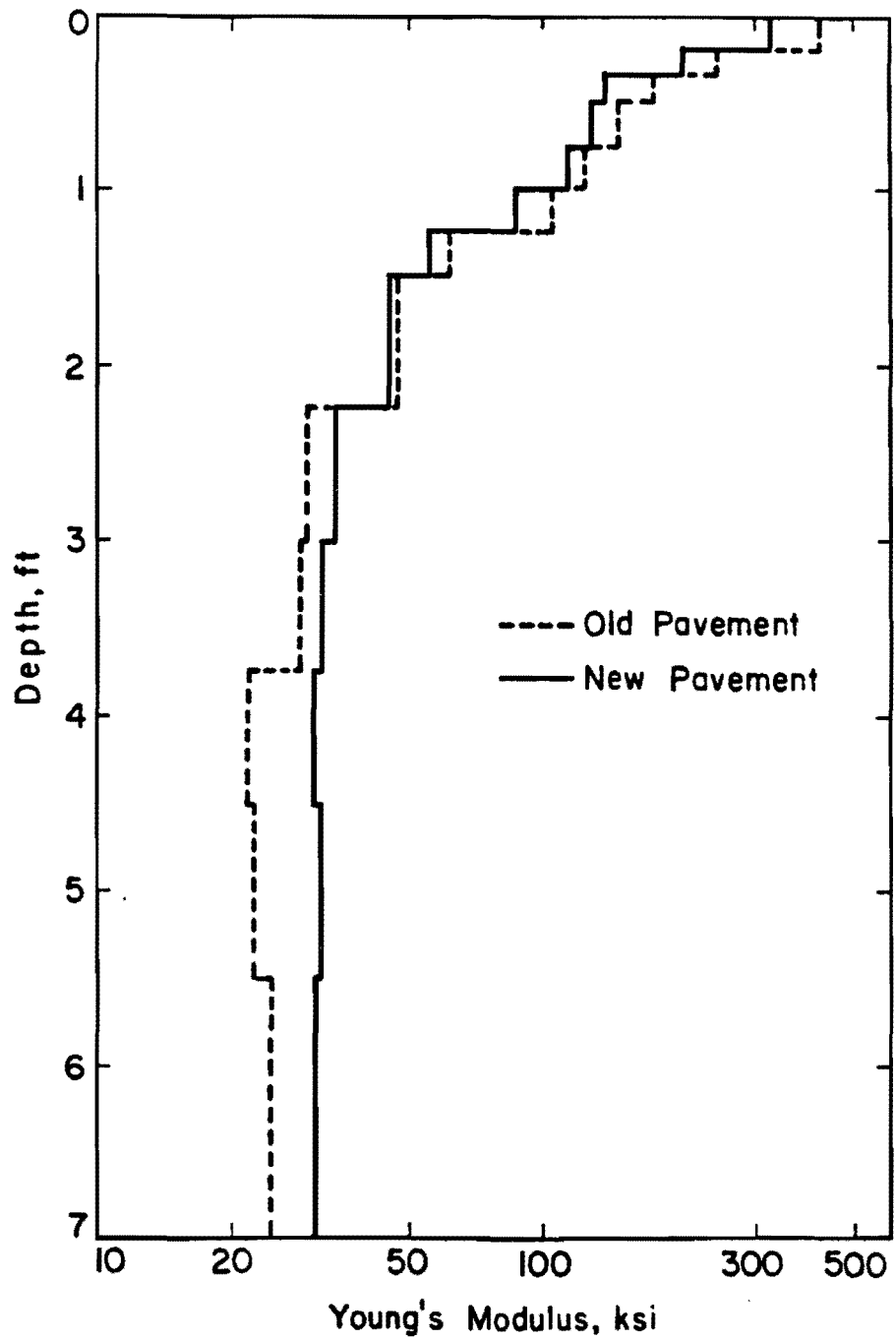


Figure 7.15 - Comparison of Young's Modulus Profile from SASW Tests on New and Old Pavements at Embankment Site.

Table 7.2. Comparison of Young's Moduli from SASW and Crosshole Methods at Embankment Site.

Layer	Depth, ft	Young's Modulus, ksi		
		SASW		Crosshole
		Old Pavement	New Pavement	
(1)	(2)	(3)	(4)	(5)
Asphalt	0.10	422	334	—
Base	0.28	246	210	—
	0.43	178	159	—
	0.63	163	125	—
	0.88	127	117	71.1
	1.13	105	87.6	—
	1.38	62.0	58.3	52.2
Subgrade	2.00	44.6	45.4	55.3
	3.00	29.2	34.4	32.5
	4.00	23.2	31.7	27.8
	6.00	26.6	32.2	27.2
	8.00	25.6	31.0	32.7
	10.00	26.3	31.8	32.7

with time are due to scatter in the testing technique or are partly or wholly real changes in stiffness.

## 7.4 RIGID PAVEMENTS

Rigid pavements contain layers with large contrasts in stiffness. As such, these systems represent the most difficult systems to invert. Fortunately, the thickness of the concrete layers used in pavements are normally relatively thick [more than 6 in. (15 cm)] which is desirable in the inversion process. Approximately 20 rigid pavements have been tested for this study. One such evaluation is presented.

### 7.4.1 Columbus Site

This site is located near Columbus, Texas, on State Highway (SH) 71, about 0.5 mile (800 m) south of the SH 71 overpass over US 90 as shown in Fig. 7.16. The longitudinal section of SH 71 along which testing was performed is illustrated in Fig. 7.17. The highway consists of two continuously-reinforced-concrete-pavement (CRCP) lanes, a 4-ft (1.2-m) wide asphaltic-concrete-pavement (ACP) shoulder and a soil median.

The soil profiles under the ACP shoulder and soil median determined from boreholes are shown in Fig. 7.18. No boreholes were drilled through the CRCP section due to the lack of required equipment. It is assumed that the soil profiles under the CRCP and ACP sections are identical below the subbase. The properties of the flexible pavement and soil median are presented elsewhere (Nazarian, et al, 1983) and are not included herein. The CRCP section consists of approximately 10 in. (25.5 cm) of continuously reinforced concrete, 4 in. (10 cm) of asphaltic-concrete base, 6 in. (15 cm) of lime-treated subbase and subgrade as shown in Fig. 7.18.

The dispersion curve from this site used for inversion is shown in Fig. 7.19. The dispersion curve was constructed by picking up points from cross power spectra manually, as at the time of data reduction the automated process of data reduction was not developed. About 20 points from each record were selected, and the phase associated with each

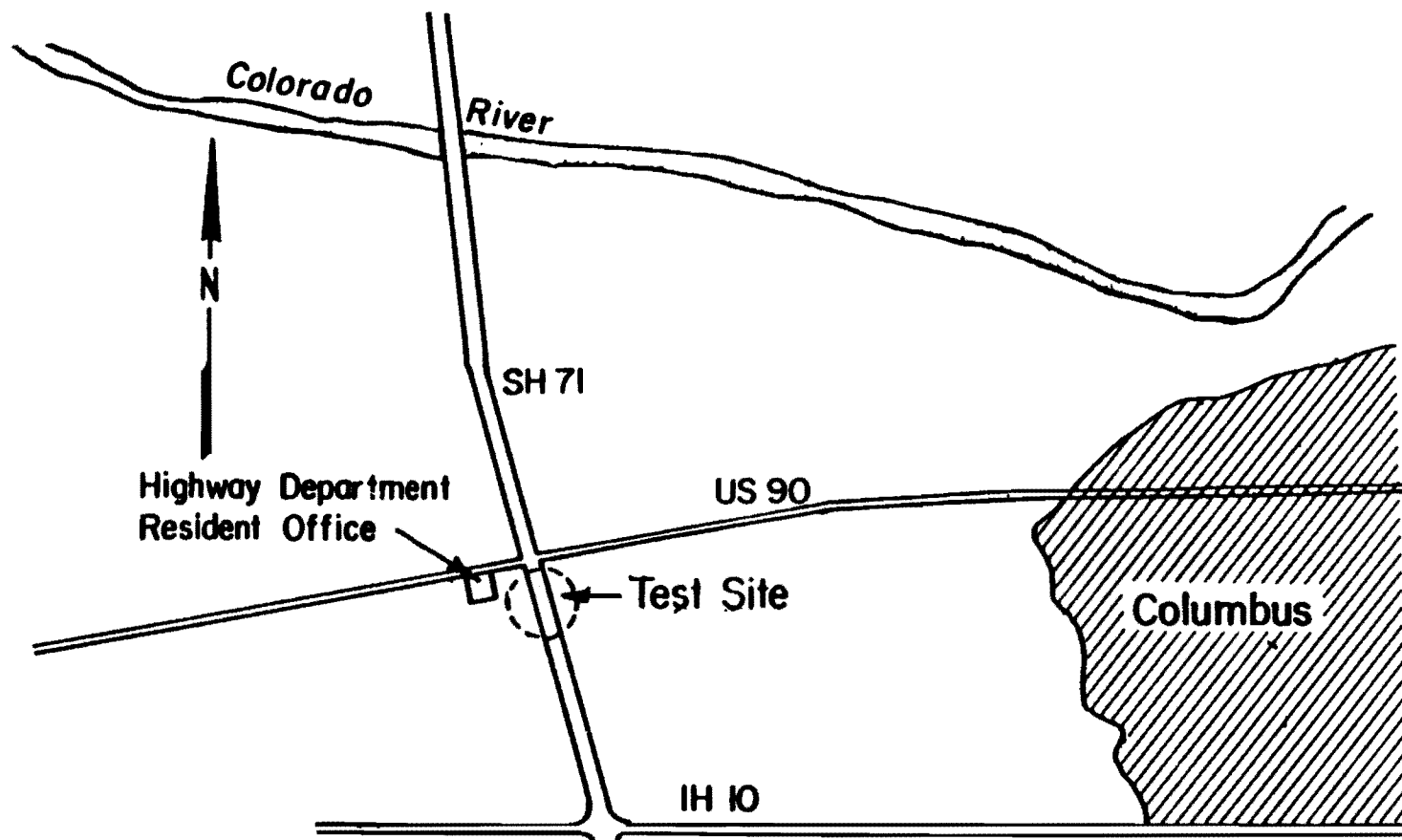


Figure 7.16 - Location of Sites on SH71.

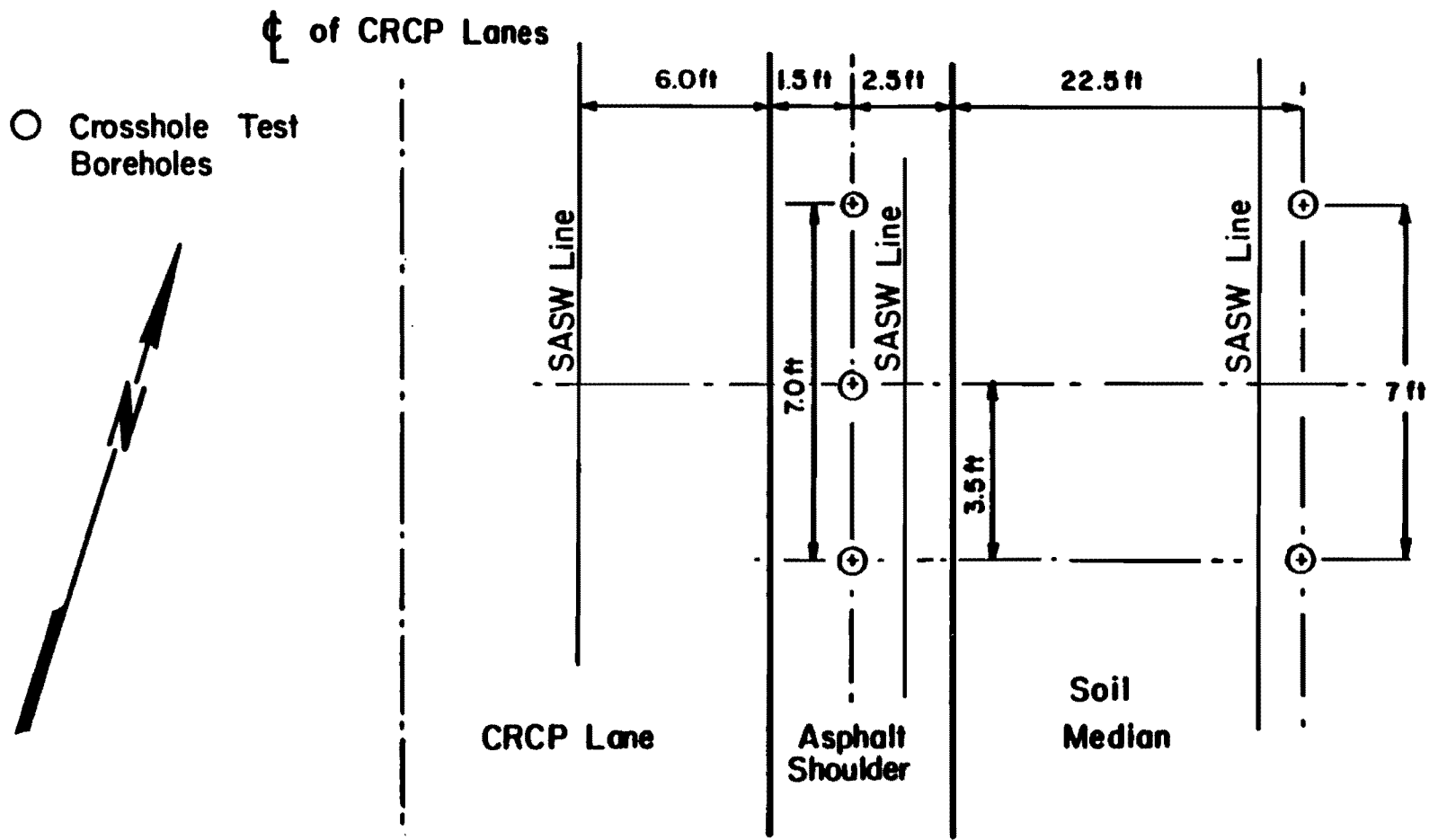
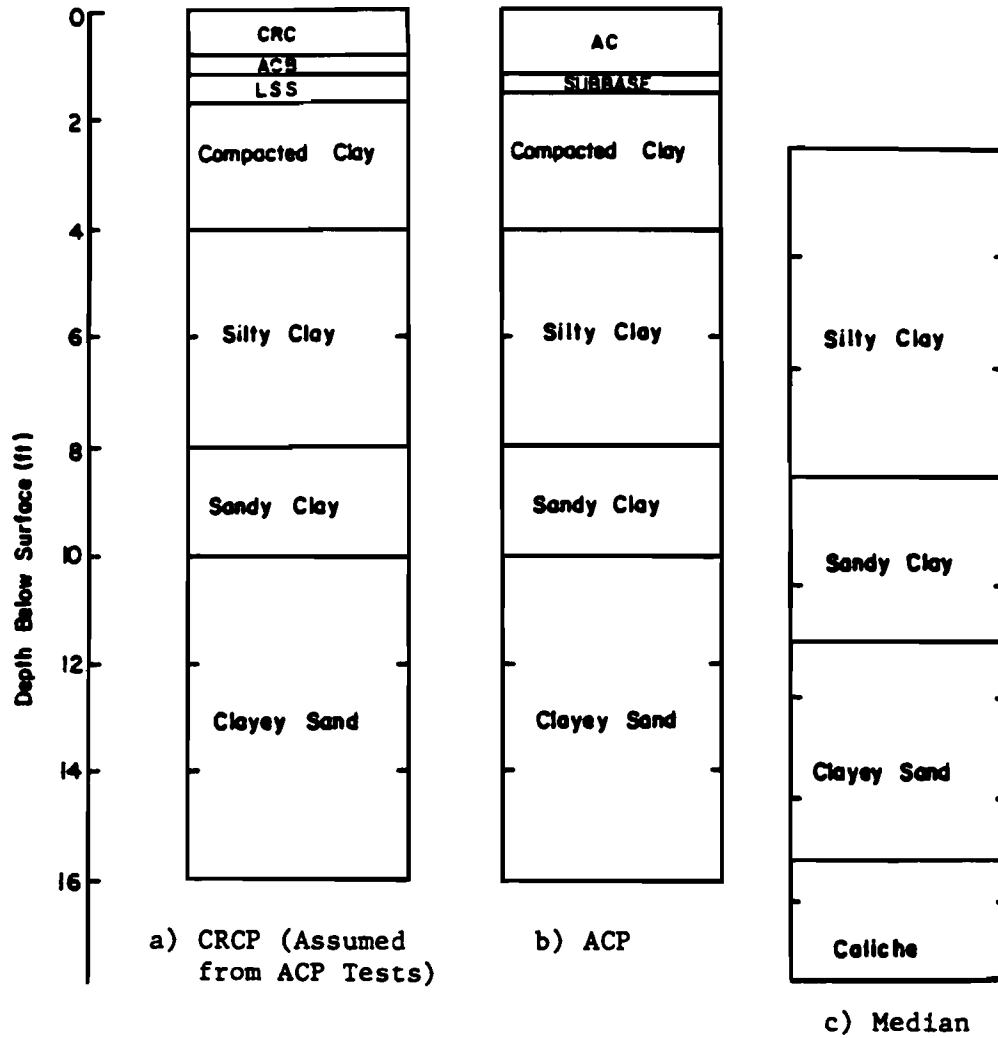


Figure 7.17 - Plan View of Testing Locations.



1. CRC = Continuous Reinforced Concrete
2. ACB = Asphalt-Concrete Base
3. LSS = Lime-stabilized Subbase
4. AC = Asphalt-Concrete

Figure 7.18 - Material Profile of Sites Tested at SH 71.

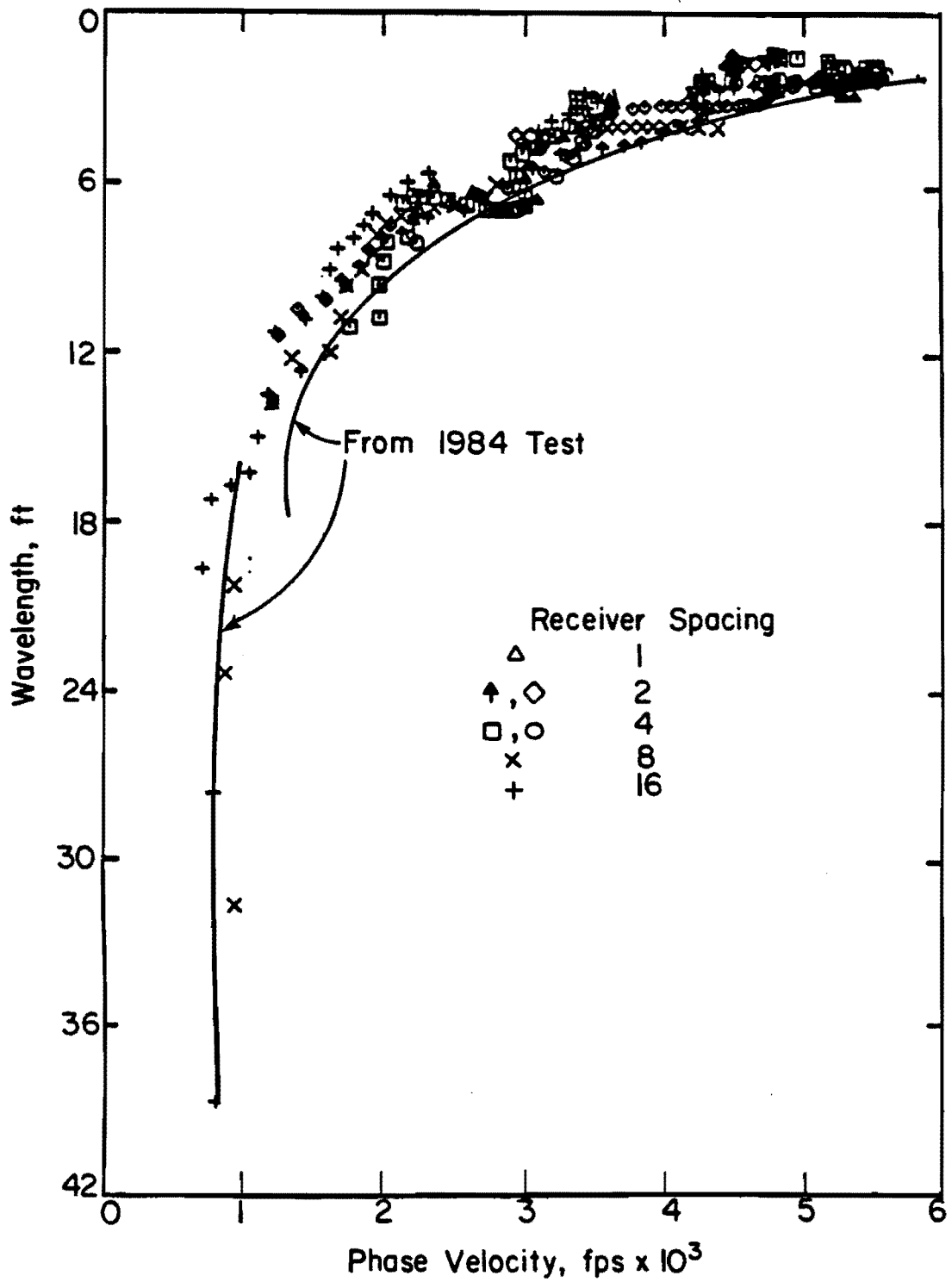


Figure 7.19 - Dispersion Curves from SASW Tests in May 1982 and August 1984 at CRCP Site.

frequency was read off the analyzer screen. The phases were then unfolded (proper number of cycles was added as discussed in Section 5.2 and illustrated in Fig. 5.3), and Eqs. 5.2 through 5.4 were employed to determine the wavelength and phase velocity associated with each data point by using a computer program coded by Heisey (1981). The criteria defined by Heisey for filtering the dispersion data (Eqs. 4.1 and 4.2) were utilized, and eventually, all the phase velocity-wavelength data from all the receiver-spacings were plotted, with no statistical manipulation. The first inversion process where the layers were added sequentially (discussed in Section 6.2) was utilized to obtain the  $V_s$  profile. The shear wave velocity profile determined by this process is shown in Fig. 7.20 and compared with the results of crosshole tests. Since no crosshole tests were performed at this section, wave velocities measured at the ACP section [about 7 ft (2.1 m) away] were assumed to be representative of the S-wave velocity profile in similar material beneath the CRCP. It can be seen from Fig. 7.20 that below a depth of 2.5 ft (75 cm) the profiles from the SASW and crosshole methods compare favorably with the velocities within 20 percent.

Recently (August, 1984) a series of SASW tests was performed at the same location. In the first series, geophones were employed as receivers. In this series, accelerometers were used so that higher frequencies (up to 12.5 kHz) would be measured. The dispersion curve obtained from the second attempt is presented in Fig. 7.21. The near-surface phase velocities are as high as about 9000 fps (2700 m/sec). The dispersion curve from the two series of tests are compared in Fig. 7.19. The solid lines in this figure represents the average dispersion curve from the 1984 attempt. The agreement between the two curves is excellent. However, the dispersion curve from recent tests suggests that the profile near the surface is stiffer than that of the 1982 profile. The importance of generating high frequencies during SASW tests can be realized by comparing of the dispersion curves. If high enough frequencies are not measured, the results may be in error (as is the case in the first set of tests). The shear wave velocity profile after inversion with program INVERT is shown in Fig. 7.22, and is com-

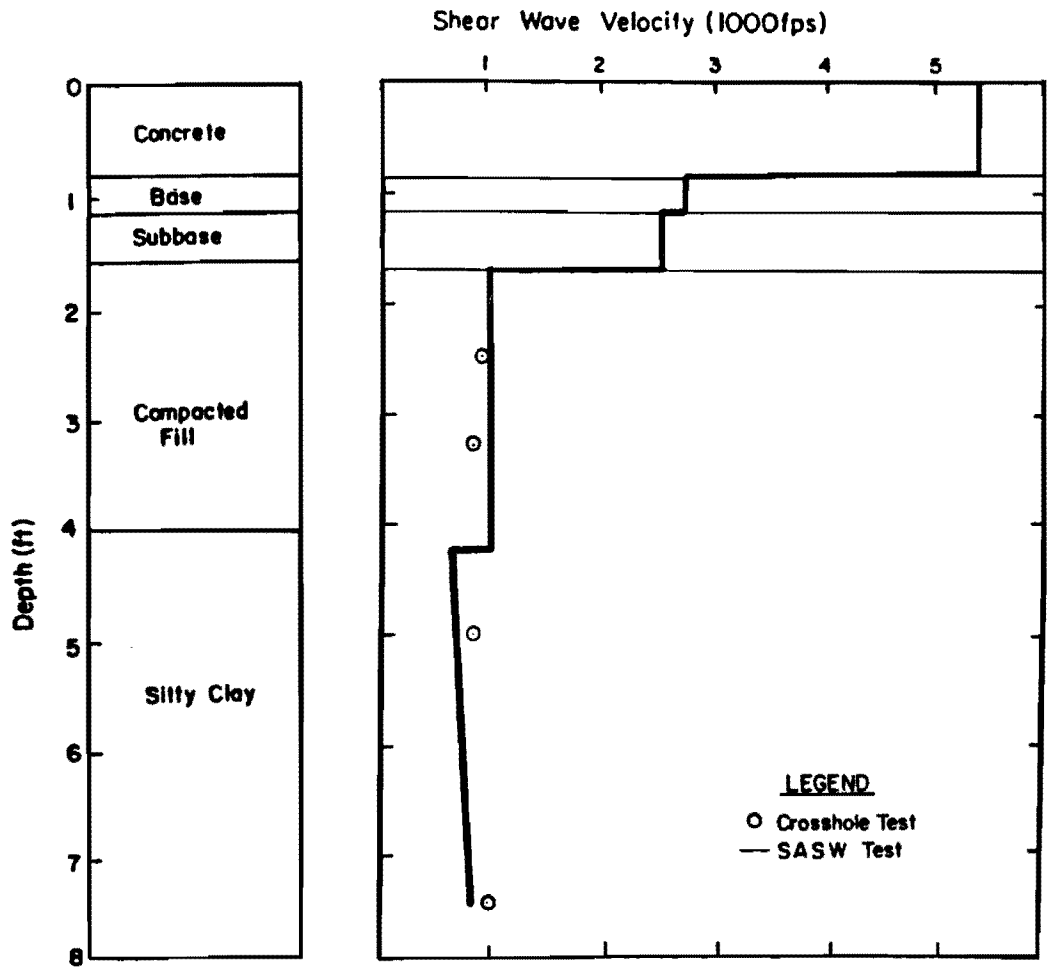


Fig. 7.20 - Shear Wave Velocity Profile at CRCP Site Determined by Initial Inversion Process.

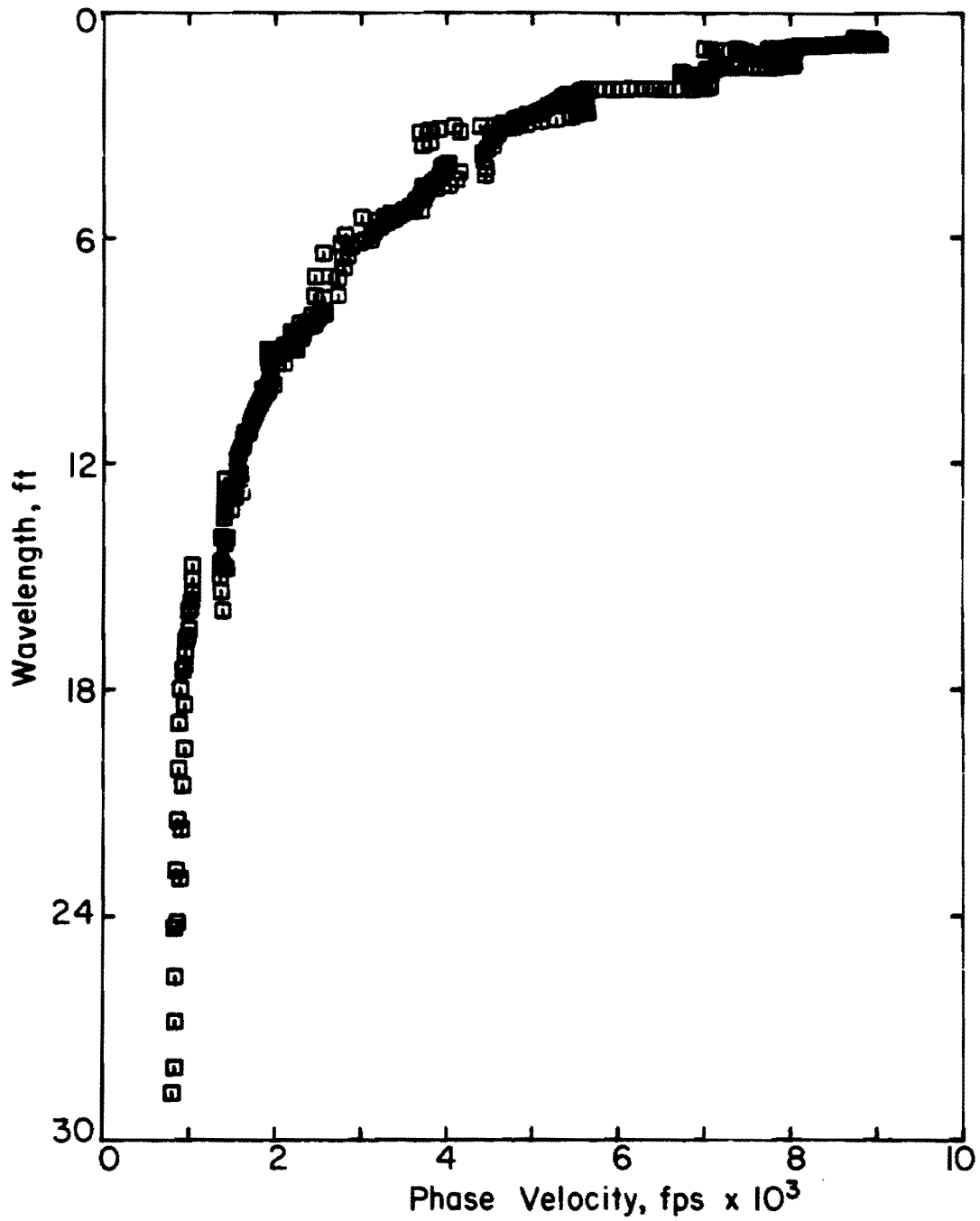


Figure 7.21 - Dispersion Curve from SASW Test on CRCP Section in August, 1984.

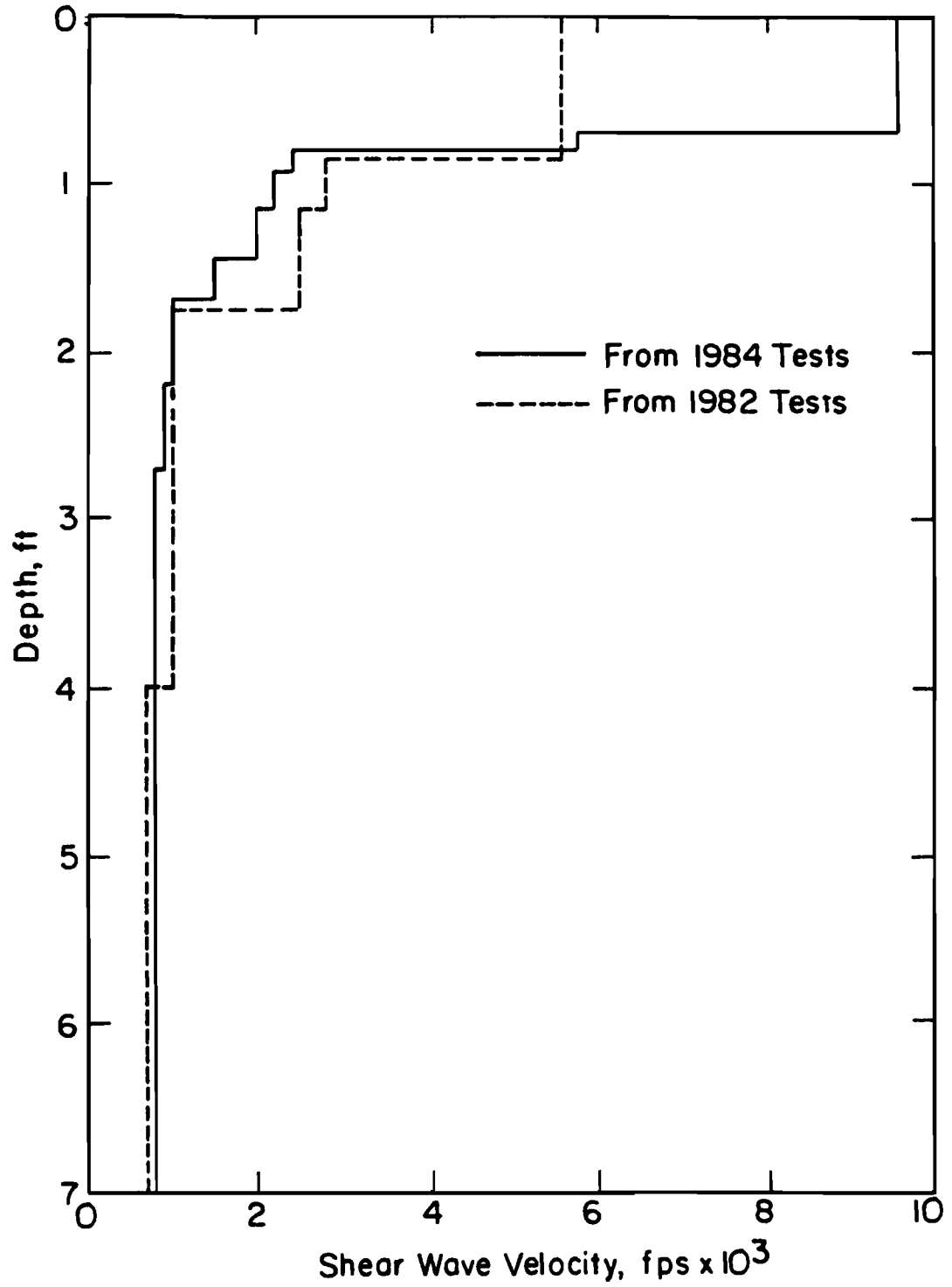


Figure 7.22 - Comparison of Shear Wave Velocities from 1982 and 1984 Tests at Columbus Site.

pared with the profile obtained from the 1982 tests. The shear wave velocity of the concrete from the recent tests is 9800 fps (2950 m/s) which is more representative of the stiffness of the good quality concrete used in construction of SH 71.

Young's modulus profiles from the two test series are shown in Fig. 7.23 and compared in Table 7.3. Poisson's ratios of 0.15, 0.25, 0.33 and 0.33 were assumed for the concrete, base and subbase, and subgrade, respectively. The mass densities used in calculation of Young's moduli were, 150, 125, 110 and 110 pcf ( 24.5, 20.4, and 18 kN/m<sup>3</sup>) for concrete, base and subbase, and subgrade, respectively. The stiffness of the concrete layer is much higher from the tests performed in 1984 (as it should be for such a high quality concrete). At the same time, Young's moduli of the base and subbase differ by almost a factor of two from the two series of tests. The profile from the 1982 tests was used as the first trial for the inversion of the 1984 tests. If the high-frequency waves were measured in the first series of tests, the deviation between the moduli of the base and subbase would be much greater. The moduli of the subgrade compare favorably (within 20 percent).

It should be mentioned that the first series of tests performed on this site was the first experience of the first author with pavements, and the 1984 testing was the last site tested for this study. The improvements in all aspects of data collection, reduction and inversion process is evident from this example. However, more research is required to extend all the aspects mentioned.

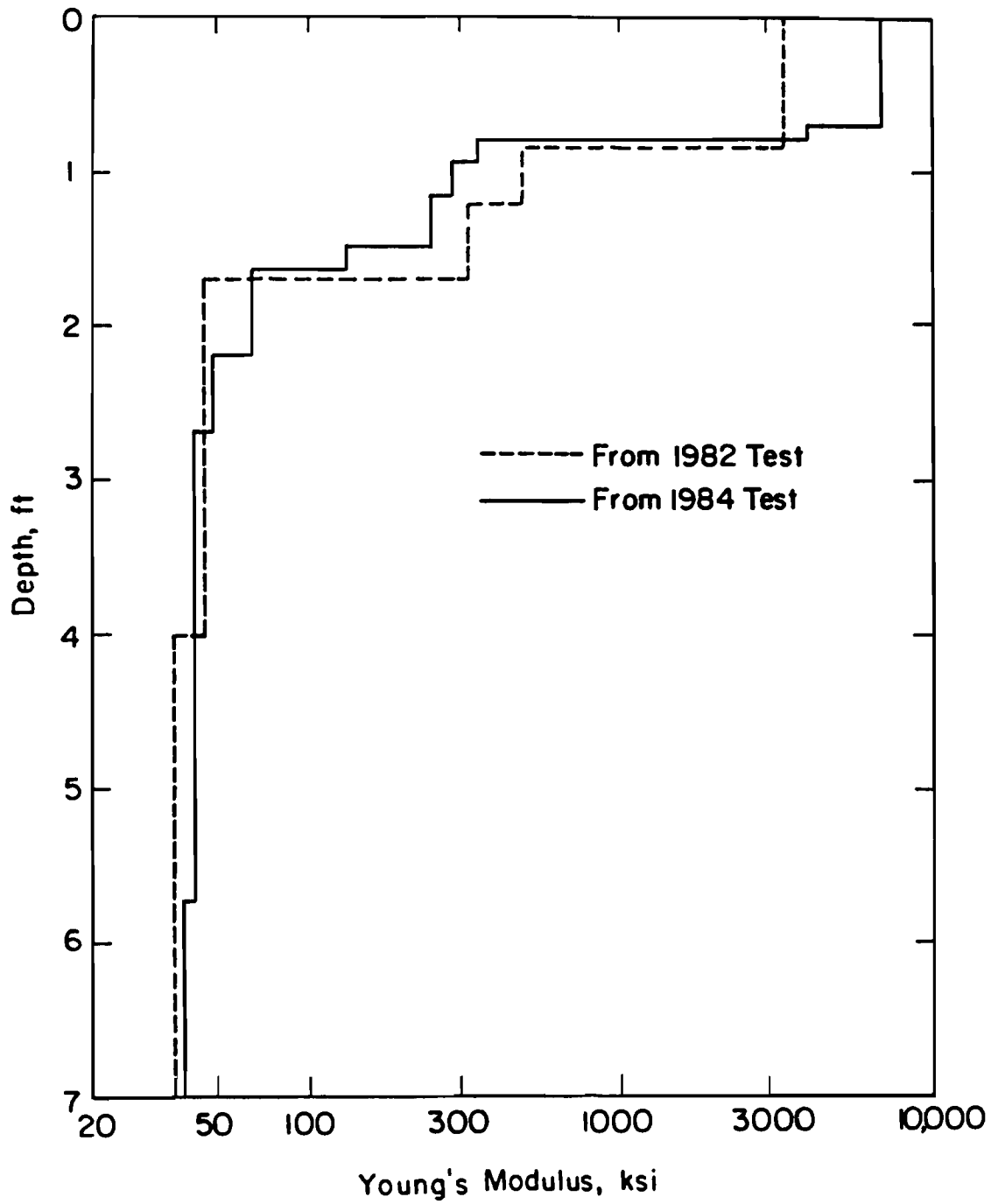


Figure 7.23 - Comparison of Young's Moduli from 1982 and 1984 Tests at Columbus Site.

Table 7.3. Comparison of Young's Moduli from SASW and Crosshole Tests at Columbus Site.

Layer	Depth, ft	Young's Modulus, ksi		
		SASW		Crosshole 1982
		1982	1984	
CRC <sup>1</sup>	0.83	3298	6870	—
ACB <sup>2</sup>	1.17	462	275	—
LSS <sup>3</sup>	1.67	321	133	—
Fill	2.50	47.5	47.9	37.6
	3.50	47.5	42.7	—
Subgrade	5.00	36.9	42.1	44.7
	7.50	37.9	39.6	42.8

1. Continuously Reinforced Concrete
2. Asphaltic-Concrete Base
3. Lime-Stabilized Subbase

This page replaces an intentionally blank page in the original.

-- CTR Library Digitization Team

## CHAPTER EIGHT

### SUMMARY, CONCLUSIONS AND RECOMMENDATIONS

#### 8.1 SUMMARY

The Spectral-Analysis-of-Surface-Waves (SASW) method is described herein. The method is used to determine the shear wave velocity and elastic modulus profiles of soil sites and pavement sections. With this method, a transient vertical impulse is applied to the surface, and a group of surface waves with different frequencies are generated in the medium. These waves propagate along the surface with velocities which vary with frequency and the properties of the different layers in the medium. Propagation of the waves are monitored with two receivers a known distance apart at the surface. By analysis of phase information from the cross power spectrum and by knowing the distance between receivers, phase velocity, shear wave velocity and moduli of each layer are determined. Measurement of the seismic waves are performed at strains below 0.001 percent where wave behavior is essentially elastic and independent of strain amplitude and strain rate.

#### 8.2 CONCLUSIONS

Based upon employment of this testing technique at many sites with substantially different profiles, the following conclusions are drawn.

1. The SASW method is well suited for determining moduli and thicknesses of pavement layers as well as shear wave velocity profiles of soil sites.
2. The results of SASW tests performed in situ are quite repeatable as dispersion curves from different tests performed at the same locations follow each other closely.
3. Use of the common-receiver-midpoint geometry reduces scatter in field data and, hence, is most accurate.
4. The simplified inversion process based upon scaling the dispersion curve is not suitable for determining shear wave

velocity profiles and a more rigorous inversion process such as the one presented herein should be utilized.

5. Shear wave velocities obtained with the SASW method are generally within 20 percent of those determined by other independent seismic methods.
6. Thicknesses of different layers are normally predicted with an accuracy of about 10 percent relative to layering reported from coring or construction plans.
7. When a large contrast exists in the stiffness of two layers in the profile, the inversion program used for construction of the theoretical dispersion curve is not sensitive to the stiffness of the layer immediately adjacent to the stiffer layer. Therefore, the results in this region are somewhat in error.

### **8.3 RECOMMENDATIONS FOR FUTURE RESEARCH**

This study is the start of an extensive research project on in situ nondestructive measurements of materials. More refinement is needed in the SASW method to develop fully the method. However, the study presented herein demonstrates the positive aspects and potential of the SASW method. The following are recommended for future research.

First, in situ data collection should be improved by:

1. adding a source capable of generating frequencies below 5 Hz so that deeper deposits can be sampled,
2. investigating the effect of distance between the source and near receiver to define the optimum distance for each set up,
3. fully automating the in situ data collection process to reduce testing time (greatly); design and construction of this type of equipment should be accelerated so that rapid collection of data can be performed at pavement sites open to traffic, and

4. updating the recording device with one capable of sampling data with a much higher resolution to achieve a more refined dispersion curve at lower frequencies (longer wavelengths).

Second, theoretical aspects of the SASW method also require some modifications as follows:

1. elimination of the nonuniqueness in the results at regions where a large velocity contrast exists in the profile, and
2. improvement in the statistical package for combining the dispersion curves is desirable for better definition of the final dispersion curve.

Finally, a series of model tests on materials with well known properties in the laboratory environment should be carried out for better understanding of the behavior of the waves, effect of receiver coupling, effect of shape and weight of sources, and configuration of source-receiver array.

This page replaces an intentionally blank page in the original.

-- CTR Library Digitization Team

## REFERENCES

1. Anderson, D.G., and Woods, R.D. (1975), "Comparison of Field and Laboratory Shear Moduli," Proceedings, Conference on In Situ Measurement of Soil Properties, ASCE, Vol. I, Raleigh, NC, pp. 69-92.
2. Baird, G.T. (1982), "Wave Propagation Method of Pavement Evaluation," New Mexico Engineering Research Institute, University of New Mexico, Albuquerque, NM.
3. Ballard, R.F., Jr. (1964), "Determination of Soil Shear Moduli at Depths by In Situ Vibratory Techniques," Miscellaneous Paper No. 4-691, U.S. Army Engineer Waterways Experiment Station, Vicksburg, MS.
4. Ballard, R.F., Jr., and Casagrande, D.R. (1967), "Dynamic Foundation Investigations, TAA-2A Radar Site, Cape Kennedy, Florida," Miscellaneous Paper 4-878, U.S. Army Engineer Waterways Experiment Station, Vicksburg, MS.
5. Ballard, R.F., Jr., and Chang, F.K. (1973), "Rapid Subsurface Exploration; Review of Selected Geophysical Techniques," Miscellaneous Paper No. S-69-30, U.S. Army Engineer Waterways Experiment Station, Vicksburg, MS.
6. Bennette, M.J., and Chen, A.T.F. (1982), "Site Characterization for Stations 6 and 7, El Centro Motion Array, Imperial Valley, California," Open File Report 82-1040, U.S. Geological Survey, Menlo Park, CA, 37 pages.
7. Bergstrom, S.G., and Linderholm, S. (1946), "Dynamisk Metod att Utrona Ultiga Marklagers Genomsnittliga Elasticitetsegenskaper," Handlingar No. 7, Svenska Forsknings-Institutet for Cement och Betong Vid. Kungl. Tekniska, Hogskolan.
8. Cunney, R.W., and Fry, Z.B. (1973), "Vibratory In Situ and Laboratory Soil Moduli Compared," Journal of the Soil Mechanics and Foundations Division, ASCE Vol. 99, No. SM12, pp. 1055-1076.
9. DEGEBO (1938), "Deutsche Gesellschaft fur Bodenmechanik," Vol. 4, Springer, Berlin.

10. Dunkin, J.W. (1965), "Computation of Modal Solutions in Layered, Elastic Media at High Frequencies," Bulletin of Seismological Society of America, Vol. 55, No. 2, pp. 335-358.
11. Eagleson, B., Heisey, J.S., Hudson, W.R., Meyer, A.H., and Stokoe, K.H., II (1981), "Comparison of Falling Weight Deflectometer and Dynaflect for Pavement Evaluation," Report No. 256-1, Center for Transportation Research, University of Texas, Austin, TX.
12. Engineer Manual 1110-1-1802 (1979), Geophysical Exploration, Department of the Army, Corps of Engineers, U.S.A.
13. Fry, Z.B. (1965), "Dynamic Soils Investigations Project Buggy, Buckboard Mesa Nevada Test Site, Mercury, Nevada," Miscellaneous Paper No. 4-666, U.S. Army Engineer Waterways Experiment Station, Vicksburg, MS.
14. Geological Survey (1982), "The Imperial Valley, California, Earthquake of October 15, 1979," Professional Paper 1254, U. S. Department of Interior, Washington, DC, 451 pages.
15. Haag, E.D. (1984), "Laboratory Investigation of the Static and Dynamic Soil Properties of Sands from the Imperial Valley, California after the 1981 Westmorland Earthquake," Master's Thesis, University of Texas, Austin, Texas.
16. Haag, E.D., Stokoe, K.H., II, and Nazarian S. (1984), "Seismic Investigation of Five Sites in the Imperial Valley, California after the 1981 Westmorland Earthquake," Geotechnical Engineering Center, University of Texas, Austin, Texas.
17. Haas, R., and Hudson, W.R. (1978), Pavement Management Systems, McGraw Hill Book Co., New York, NY, 456 pages.
18. Haskell, N.A. (1953), "The Dispersion of Surface Waves on Multilayered Media," Bulletin of Seismological Society of America, Vol. 43, No. 1, pp. 17-34.
19. Hardin, B.O., and Drnevich, V.P. (1972), "Shear Modulus and Damping in Soils: Measurement and Parameter Effects," Journal of the Soil Mechanics and Foundations Division, ASCE, Vol. 95, No. SM6, pp. 603-624.
20. Heisey, J.S. (1982), "Determination of In Situ Shear Wave Velocity from Spectral Analysis of Surface Waves," Master's Thesis, University of Texas, Austin, TX, 300 pages.
21. Heukelom, W., and Klomp, J.G. (1962), "Dynamic Testing as a Means of Controlling Pavements during and after Construction,"

- Proceedings, International Conference on Structural Design of Asphalt Pavements, Ann Arbor, MI, pp. 495-510.
22. Hoar, R.J. (1982), "Field Measurement of Seismic Wave Velocity and Attenuation for Dynamic Analyses," Ph.D. Dissertation, The University of Texas, Austin, TX, 479 pages.
  23. Krohn, C.E. (1984), "Geophone Ground Coupling," Geophysics, Vol. 49, No. 6, pp. 722-731.
  24. Lamb, H. (1904), "On the Propagation of Tremors Over the Surface of an Elastic Solid," Philosophical Transactions of the Royal Society of London, Vol. A203, pp. 1-42.
  25. Lytton, R.L., Moore, W.M., and Mahoney, J.P. (1975), "Pavement Evaluation: Phase I, Pavement Evaluation Equipment," Report No. FHWA-RD-75-78, Federal Highway Administration, Washington, D.C.
  26. Mark Products (1981), "Geophone General Information," Marks Products, Inc., Houston, TX., 17 pages.
  27. Maxwell, A.A., and Fry, F.B. (1967), "A Procedure for Determining Elastic Moduli of In Situ Soils by Dynamic Techniques," Proceedings, International Symposium on Wave Propagation and Dynamic Properties of Earth Materials, Albuquerque, NM, pp. 913-920.
  28. Miller, I., and Freund, J.E. (1977), Probability and Statistics for Engineers, Prentice-Hall, Inc., Englewood Cliffs, NJ, 529 pages.
  29. Nazarian, S. (1984), "In Situ Determination of Elastic Moduli of Soil Deposits and Pavement Systems by Spectral-Analysis-of-Surface-Waves Method," Doctoral Dissertation, The University of Texas, Austin, Texas, 452 pages.
  30. Nazarian, S. and K.H. Stokoe, II (1982), "Evaluation of Moduli and Thicknesses of Pavement Systems by SASW methods," Report No. 256-4, Center for Transportation Research, The University of Texas, Austin, TX.
  31. Nazarian, S., Stokoe, K.H., II and W.R. Hudson (1983), "Use of Spectral Analysis of Surface Waves for Determination of Moduli and Thicknesses of Pavement Systems," Transportation Research Record, No. 954, Washington, D.C.
  32. Nazarian, S., and K.H. Stokoe, II (1984a), "Nondestructive Testing of Pavements Using Surface Waves," Transportation Research Record, 993, Washington, D.C.

33. Nazarian, S., and K.H. Stokoe, II (1984b), "In Situ Shear Wave Velocities from Spectral Analysis of Surface Waves," Proceedings, Eighth World Conference on Earthquake Engineering, San Francisco, California.
34. Nazarian, S. and K.H. Stokoe, II (1984c), "Investigation of Five Pavement Sections at Homestead Air Force Base, Florida by Surface Wave Technique," Geotechnical Engineering Center, The University of Texas, Austin, TX.
35. Nazarian, S. and K.H. Stokoe, II (1985a), "In Situ Determination of Elastic Moduli of Pavement Systems by Spectral-Analysis-of-Surface-Waves Method (Theoretical Aspects)," Report No. 437-1, Center for Transportation Research, The University of Texas, Austin, TX (in press).
36. Nazarian, S. and K.H. Stokoe, II (1985b), "User's Guide for Interactive Program "INVERT" Used in Inversion of Dispersion Curves," Report No. 437-2, Center for Transportation Research, The University of Texas, Austin, TX (in press).
37. Nazarian, S., W. Uddin, K.H. Stokoe, II and A.H. Meyer (1984), "Moduli and Thicknesses of Pavement Systems from Spectral Analysis of Surface Waves," Proceedings, Tenth World Meeting of International Road Federation, Brazil.
38. Neilson, J.R., and Baird, G.T. (1975), "Air Force System for Non-destructive Testing of Pavements," Presented at, Symposium on Nondestructive Test and Evaluation of Airport Pavements, Vicksburg, MS.
39. Neilson, J.P., and Baird, G.T. (1977), "Evaluation of an Impulse Testing Technique for Nondestructive Testing of Pavements," Research Report CEEDO-TR-77-46, Tyndall AFB, Panama City, FL.
40. Nijober, L.W., and Van der Poel, C. (1953), "A Study of Vibration Phenomena in Asphaltic Road Construction," Proceedings, Association of Asphaltic Pavement Technology, pp. 197-231.
41. PCB Piezotronics (1983), "Quartz Piezoelectric Transducers," (from) Catalog No. 375, PCB Piezotronics, Inc., Depew, NY.
42. Rayleigh, L. (1887), "On Waves Propagated along the Plane Surface of an Elastic Solid," Proceedings, London Mathematical Society, Vol. 17, pp. 4-11.
43. Richart, F.E., Jr. (1978), "Field and Laboratory Measurement of Dynamic Soil Properties," Proceedings of the Conference on Dynamical Methods in Soil and Rock Mechanics, Karlsruhe, Germany, Vol. I, pp. 3-36.

44. Richart, F.E., Jr., Hall, J.R., Jr., and Woods, R.D. (1970), Vibrations of Soils and Foundations, Prentice-Hall, Inc., Englewood Cliffs, NJ, 414 pages.
45. Schwab, F., and Knopoff, L. (1970), "Surface Wave Dispersion Computations," Bulletin of Seismological Society of America, Vol. 60, No. 2, pp. 321-344.
46. Stokoe, K.H., II (1980), "Field Measurement of Dynamic Soil Properties," presented to the Specialty Conference on Civil Engineering and Nuclear Power, ASCE, Sept. 15-17, Knoxville, Tennessee, 31 pp.
47. Stokoe, K.H., II, and Chen, A.T.F. (1980), "Effects on Site Response of Methods of Estimating In Situ Soil Behavior," Proceedings, Seventh World Conference on Earthquake Engineering, Turkey.
48. Stokoe, K.H., II, and Hoar, R.J. (1978), "Variables Affecting in Situ Seismic Measurements," Proceedings, Conference on Earthquake Engineering and Soil Dynamics, ASCE, Pasadena, CA, Vol. II, pp. 919-939.
49. Stokoe, K.H., II, and Lodde, P.F. (1978), "Dynamic Response of San Francisco Bay Mud," Proceedings, Conference on Earthquake Engineering and Soil Dynamics, ASCE, Pasadena, CA, Vol. II, pp. 940-959.
50. Stokoe, K.H., II and S. Nazarian (1983a), "Effectiveness of Ground Improvement from Spectral Analysis of Surface Waves," Proceedings, Eighth European Conference on Soil Mechanics and Foundation Engineering, Helsinki, Finland, Vol. 1, pp. 91-95.
51. Stokoe, K.H., II and S. Nazarian (1983b), "Comparative Study of Two Pavement Sections at Tyndall Air Force Base, Florida," Report No. GR83-23, Geotechnical Engineering Center, The University of Texas, Austin, TX.
52. Stokoe, K.H., II and S. Nazarian (1984a), "Investigation of Stability of Debris Blockage Impounding Lakes of Mt. St. Helens, Washington, by Surface Wave Method," Report No. GR84-2, Geotechnical Engineering Center, The University of Texas, Austin, TX.
53. Stokoe, K.H., II and S. Nazarian (1984b), "Determination of Moduli and Thicknesses of Five Pavement Sections, McDill Air Force Base, Florida by Different In Situ Seismic Tests," Report No. GR84-7, Geotechnical Engineering Center, The University of Texas, Austin, TX.

54. Stokoe, K.H., II and S. Nazarian (1984c), "Investigation of Two Earth Dams in California Acqueduct System by Surface Wave Technique," Report No. GR84-4, Geotechnical Engineering Center, The University of Texas, Austin, TX.
55. Stokoe, K.H., II, and Woods R.D. (1972), "In Situ Shear Wave Velocity by Cross-Hole Method," Journal of Soil Mechanics and Foundations Division, ASCE, Vol. 98, No. SM5, pp. 443-460.
56. Thomson, W.T. (1950), "Transmission of Elastic Waves through a Stratified Solid Medium," Journal of Applied Physics, Vol. 21, pp. 89-93.
57. Thrower, E.N. (1965), "The Computation of the Dispersion of Elastic Waves in Layered Media," Journal of Sound Vibration, Vol. 2, No. 3, pp. 210-226.
58. Uddin, W. (1984), "A Structural System for Pavements Based on Dynamic Deflections," Ph.D. Dissertation, The University of Texas, Austin, TX.
59. Uddin, W., Nazarian, S., Hudson, W.R., Meyer, A.H., and Stokoe, K.H., II (1983), "Investigation into Dynaflect Deflections in Relation to Location/Temperature Parameters and In Situ Material Characteristics of Rigid Pavements," Research Report No. 256-5, Center for Transportation Research, The University of Texas, Austin, TX, 273 pages.
60. Van der Poel, C. (1951), "Dynamic Testing of Road Construction," Journal of Applied Chemistry, Vol. 1, No. 7, pp. 281-290.
61. Van der Poel, C. (1954), "A General System Describing the Visco-Elastic Properties of Bitumens and its Relation to Routine Test Data," Shell Bitumen Reprint No. 9, Shell Laboratories-Kominklikike.
62. Woods, R.D. (1978), "Measurment of Dynamic Soil Properties," Proceedings of the Conference Placement and Improvement of Soil to Support Structures, ASCE, Cambridge, Massachusetts, pp. 407-435.
63. Woods, R.D., and Richart, F.E., Jr. (1967), "Screening of Elastic Surface Waves by Trenches," Proceedings, International Symposium on Wave Propagation and Dynamic Properties of Earth Materials, Albuquerque, NM, pp. 275-290.
64. Yoder, E.J., and Witczak, M.W. (1975), Principles of Pavement Design, John Wiley & Sons, Inc., New York, NY, 2nd Edition, 711 pages.

## APPENDIX A

### EQUIPMENT USED IN SASW TESTING

#### A.1 SOURCE

The source should be able to generate surface waves over a wide range in frequencies with adequate amplitude so that they can be detected by the receivers. Simultaneously, the source should generate minimal P- and S-wave energy. Near the surface, P- and S-waves (body waves) attenuate much more rapidly than surface waves. The distance between the first receiver (receiver closer to the source) and the source should be large enough so that a significant amount of the energy associated with the body waves dies out before arrival at the first receiver. On the other hand, if the source is too far from the first or second receiver, another problem arises. The energy (amplitude) associated with different frequencies may not be sufficient to be detected by the receivers, and background noise dominates the records. The optimum distance between the source and first receiver is being studied in a separate investigation.

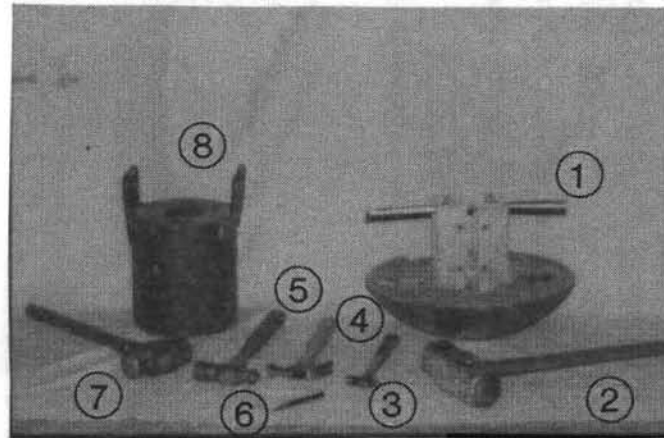
For sampling shallow depths, the maximum frequency excited is of utmost importance. For shallow sampling, the receivers and source are placed close to one another; therefore, it is not necessary to transfer much energy to the medium. High frequencies translate to short wavelengths, which correspond to shallower depths of sampling. The highest frequency required in an experiment depends on the stiffness of the material near the surface as well as the particle size of this material. For a constant wavelength, the maximum frequency required in testing will increase as the stiffness of the layer increases. However, it cannot be expected to measure meaningful velocities for wavelengths shorter than about the maximum aggregate size. For a typical soil deposit, the highest frequency necessary is on the order of 200 to 800 Hz; for a flexible pavement, the source should generate frequencies up to 6 kHz, and, for a rigid pavement, this upper boundary is on the order of 10 to 20 kHz.

For determination of properties of relatively deep layers, the energy coupled into the medium is of greater importance. Excitation of low frequencies (as low as 8 to 10 Hz) is relatively simple. However, the amplitude of these low-frequency waves should be large enough so that they can be detected by the receivers. One of the limiting factors in the lowest frequency being detected is the natural frequency of the receiver which will be discussed in the next section.

Different sources used in this study are shown in Fig. A.1. For experiments in which the properties of shallow layers are of primary concern, a light-weight source capable of exciting high frequencies, such as a chisel and hammer or 2-oz (56 gr) hammer, etc., is desirable. The size of the hammer is increased gradually until, for sampling deep layers, a relatively heavy and bulky source, such as a Standard Penetration Test (SPT) hammer, or other large drop weights have been used with some success.

With sources shown in Fig. A.1, waves with wavelengths up to 150 ft (45 m) have been generated and detected [corresponding to sampling depths of up to 50 ft (15 m)]. To investigate deeper deposits, a source capable of generating lower frequencies is necessary. The significance of low-frequency waves can be clarified by the following example. Assume that a series of tests is being performed on an ideal half-space consisting of uniform material with an R-wave velocity of 1000 fps (300 m/sec). If the lowest frequencies generated are 10, 5, and 2 Hz, the maximum wavelengths measured would be 100, 200, and 500 ft (30, 60, 150 m), respectively. Reducing the minimum frequency from ten to five Hz, will only include wavelengths in the range of 100 to 200 ft (30 to 60 m). However, when the frequency is lowered from five to two Hz, the maximum wavelength is increased from 200 to 500 ft (60 to 150 m).

To generate waves of lower frequencies (on the order of 2 to 5 Hz) a source which can generate an impulse with long duration is required. Preliminary studies show that this period should be on the order of 100 msec or more. Research on designing and building such a source is being conducted in a separate study.



- |                        |  |
|------------------------|--|
| 1. *150-1b Drop Weight | 5. 2-1b Hammer                         |
| 2. 10-1b Sledge Hammer | 6. Chisel                              |
| 3. 8-oz Hammer         | 7. *15-1b Sledge Hammer                |
| 4. 1-1b Claw Hammer    | 8. *150-1b Standard Penetration Hammer |

\*Used only on Soil Sites

Figure A.1 - Sources Used in SASW Tests.

## A.2 RECEIVERS

Selection of appropriate receivers is necessary in any seismic test. Two types of receivers are usually used: velocity transducers (geophones) or acceleration transducers (accelerometers).

Geophones are coil-magnet systems as shown in Fig. A.2. A mass is attached to a spring and a coil is connected to the mass (which becomes part of the total mass). The coil is located such that it crosses the magnetic field. Upon impact the magnet moves but the mass remains more or less stationary causing a relative motion between the coil and magnet. This relative motion generates a voltage in the coil which is proportional to the relative velocity between the coil and magnet.

The geophone system can be considered as a one-degree-of-freedom system. To design a geophone, the natural frequency, transductivity, and damping properties should be determined (like any other dynamic system). The natural frequency is the undamped natural frequency of the system. Transductivity is the factor of proportionality between the actual velocity and the output voltage and can be considered as a calibration factor. Damping of the system indicates the attenuation of the (free-vibration) motion with time.

The response of a typical geophone used in this study is shown in Fig. A.3 for several damping ratios. The nominal natural frequency of the geophone is 4.5 Hz. For each damping ratio, three zones can be distinguished. For example, consider curve A corresponding to a damping ratio of 28 percent. Up to a frequency of about 4 Hz, the response of the geophone increases linearly. In the frequency range of say 4 to 30 Hz, the response goes through a peak and then decreases. The third portion of the curve, which encompasses frequencies over 30 Hz, exhibits a constant output (independent of frequency). This is the desirable range for seismic measurements. Another important point illustrated in Fig. A.3 is that as the damping ratio increases from low values the amplitude of the peak decreases, and, for all practical purposes, the output is constant over a larger range of frequencies. For example, if a damping ratio of 60 percent is selected, the curve is quite constant above 5 Hz, while, for a damping ratio of 28 percent the

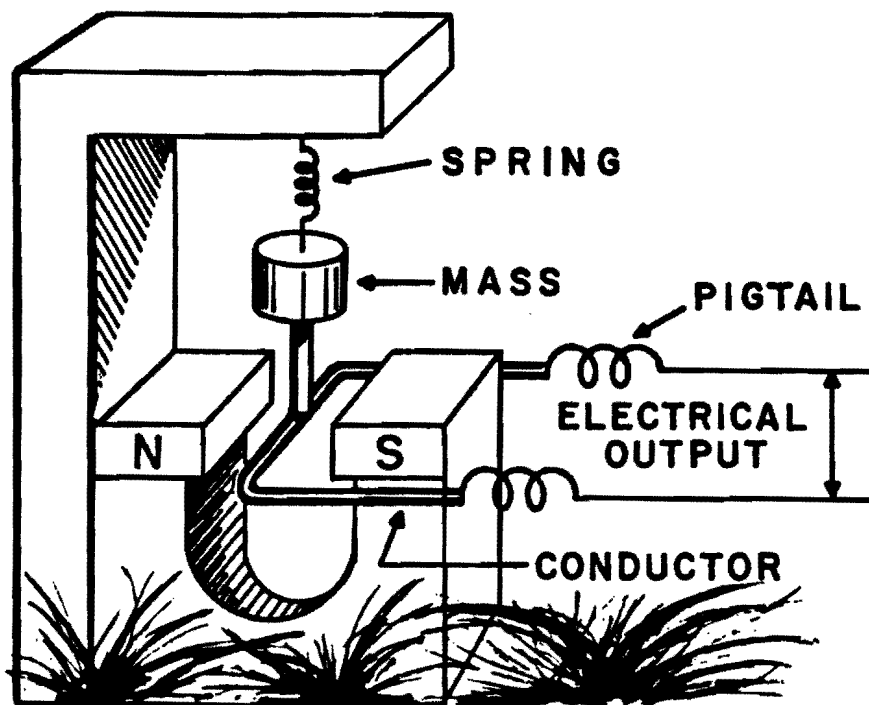


Figure A.2 - Elements of a Geophone.

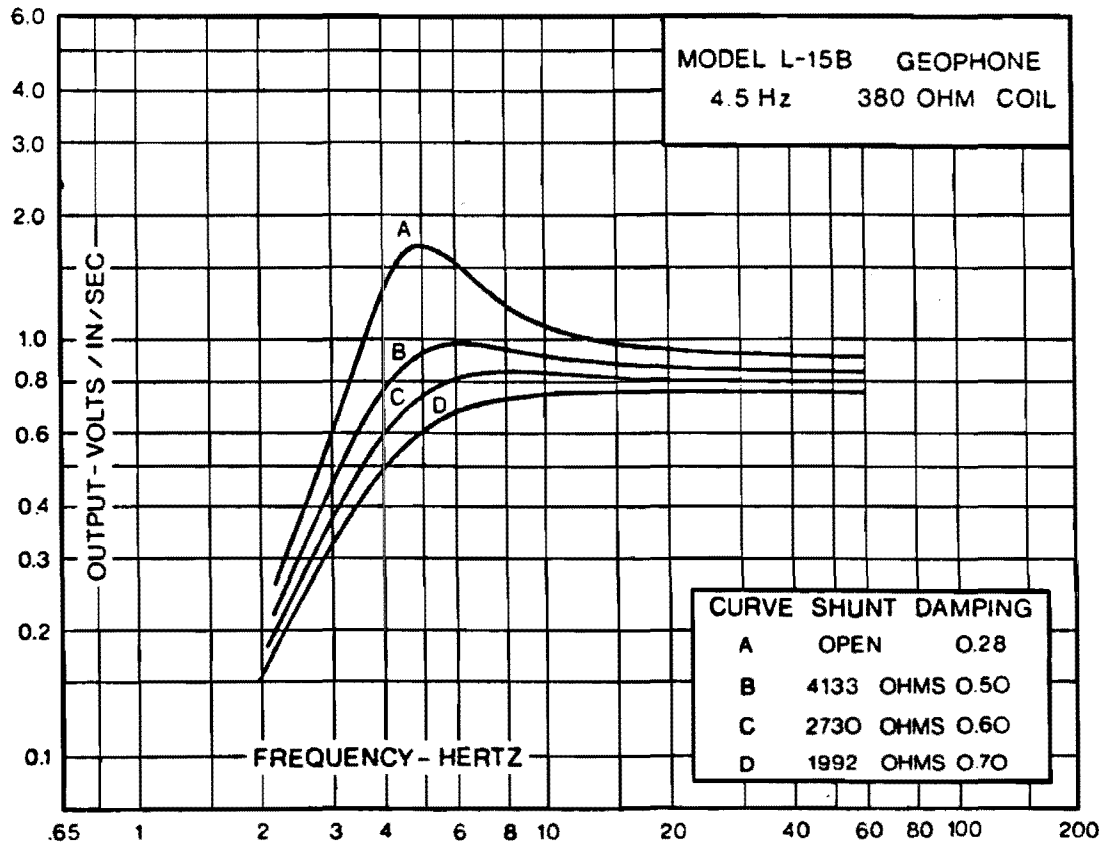


Figure A.3 - Typical Responses of Geophones with Different Damping Ratios

frequency-independent portion starts at about 20 Hz. For this geophone, 60 percent damping is the optimum value.

The geophones used in this study had either a natural frequency of 4.5 Hz (Model L-15B, manufactured by Mark Products Inc.) and a damping ratio of 60 percent; or a natural frequency of 2 Hz (Model L-22D of Mark Products Inc.) and a damping ratio of 50 percent.

In summary, the limit of lower frequencies which translates to sampling of deeper layers is limited by the natural frequency of the receivers as well as the lowest frequencies being generated by the source.

The other type of transducer used was a piezoelectric accelerometer. The principle of operation of this type of accelerometer is based upon the piezoelectric properties of a quartz crystal. Due to the passage of seismic waves, the crystal is strained, which in turn generates electric charges that accumulate on major opposing surfaces of the crystal. These charges create a voltage signal which is proportional to the acceleration of the disturbance. The crystal element has a dual function. First, it acts as a spring to oppose the applied movement; secondly, it supplies an electrical signal proportional to acceleration. The response of a typical accelerometer used in this study is shown in Fig. A.4. The response is quite constant for any practical purposes. Natural frequencies of accelerometers are quite high (30 to 100 kHz). Therefore, they perform much more accurately than geophones at higher frequencies. In addition, accelerometers are much smaller than velocity transducers (as such, they are more appropriate for measurements at close spacings). However, the transductivity of the accelerometers used in this study are less than the geophones, so that it is quite difficult to pick up high quality signals at spacings of 8 ft (2.5 m) and more. Also, during the course of this study it was found that accelerometers are more apt to reduce the effect of environmental noise.

On soil sites geophones were used exclusively. However, on pavement sites either geophones or a combination of accelerometers and geophones were employed. On soil sites the receivers were secured in

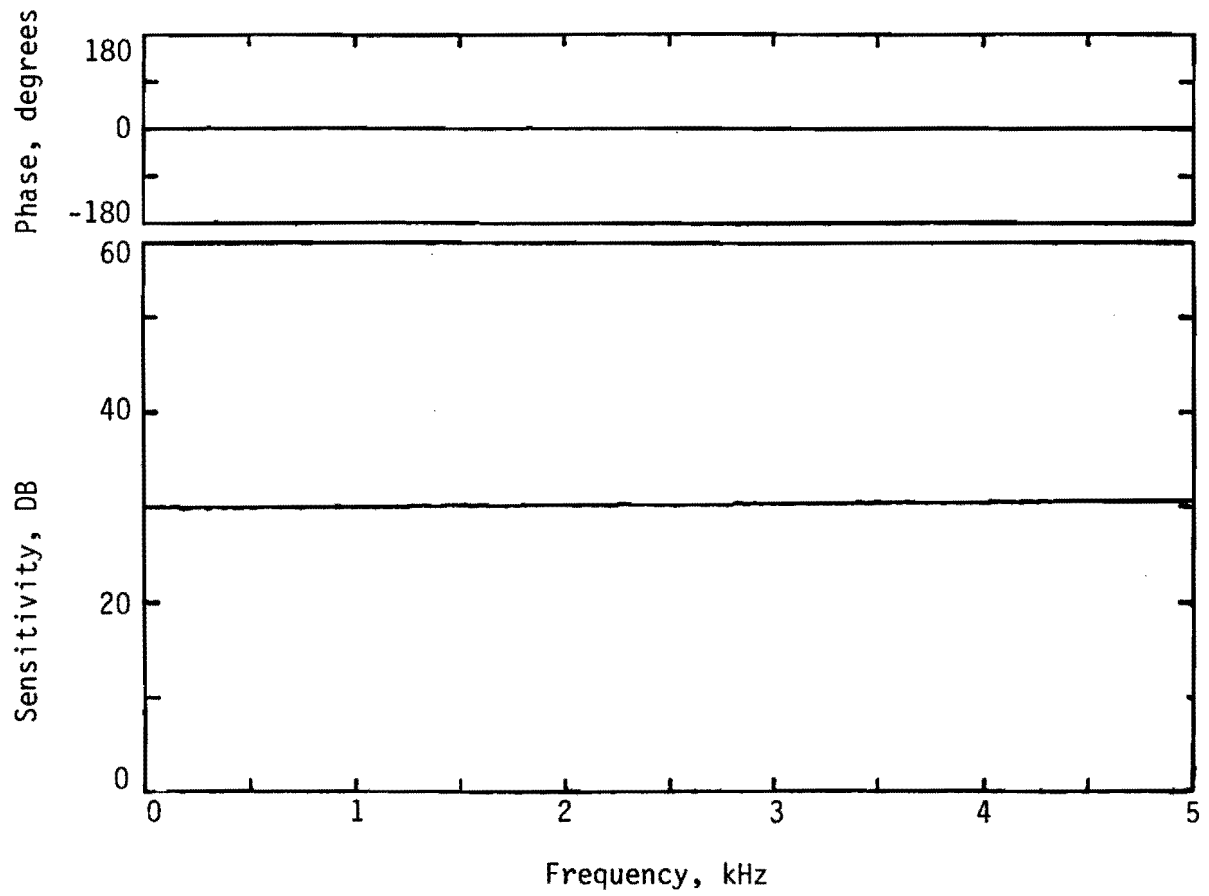


Figure A.4 - Typical Response of an Accelerometer.

place by means of spikes approximately 2-in. (5-cm) long. Accelerometers were mounted on the pavement surface with bees-wax, and geophones were epoxied to the surface with 5-minute epoxy glue. The accelerometers and geophones used are shown in Fig. A.5. It should be mentioned that the casings of the geophones were built at the in-house machine shop.

Good coupling between the receivers and the material being tested is essential. Recently Krohn (1984) studied the geophone-ground coupling in detail in the laboratory and the field. He concluded that for very loose soils the geophones should be buried for better coupling. For firm soils he indicated that use of the conventional method of using spikes is adequate.

### A.3 RECORDING DEVICE

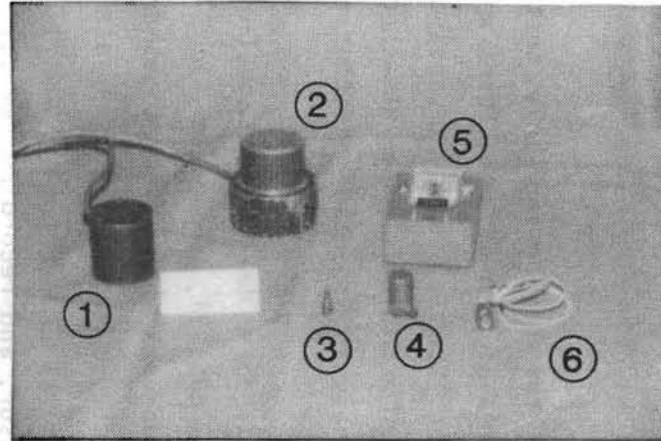
A convenient recording device for performing SASW tests is a spectral analyzer. An in-depth review of Fourier transforms and spectral analyses is presented in Chapter Three. A spectral analyzer is a digital oscilloscope that, by means of a microprocessor attached to it, has the ability to perform signal analysis directly in either the time or frequency domain.

The analyzer used in this study is a Hewlett-Packard (HP) 5423A structural dynamics analyzer. The HP5423A, shown in Fig. A.6, is portable and consists of three components which stack together vertically during operation and are connected by means of appropriate cables. The three units are:

- (1) oscilloscope, microprocessor, and recording device,
- (2) control panel, and
- (3) analog-to-digital/digital-to-analog convertors.

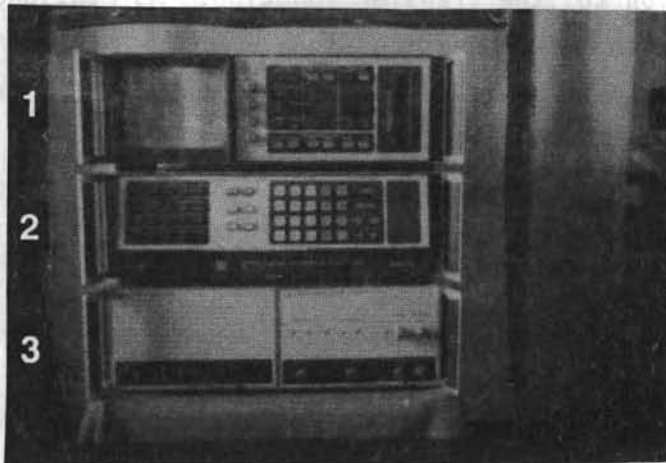
This analyzer is hard wired and dual channel (i.e., only two receivers can be recorded simultaneously).

The procedure used in the field to test with the analyzer is as follows. Upon turning on, a menu similar to one shown in Fig. A.7 appears on the screen which indicates the default features of the device. Each of these items can be changed quite easily. The menu usually used



- |                        |                                   |
|------------------------|-----------------------------------|
| 1. 4.5-Hz Geophone     | 4. Large Accelerometer            |
| 2. 2-Hz Geophone       | 5. Power Supply for Accelerometer |
| 3. Small Accelerometer | 6. Cables Used with Accelerometer |

Figure A.5 - Receivers Used in SASW Tests.



1. Oscilloscope and Microprocessor
2. Control Panel
3. Analog-to-Digital Converter

Figure A.6 - Hewlett-Packard 5423A Structural Dynamics Analyzer.

for the SASW test on a soil site at the initial receiver spacing is shown in Fig. A.8.

The "TRANSFER FUNCTION" is chosen as the measurement type. In this state, the coherence function, cross power spectrum between the two signals, and auto power spectrum of each signal is determined by the analyzer, in addition to the transfer function. As mentioned before, five averages are used to enhance the signals. The average is simply the arithmetic average of the signals denoted by "STABLE" on the menu illustrated in Fig. A.8.

The type of signal is selected as "IMPACT" which means that the signals are expected to be transient. By indicating "IMPACT" the operator has the option of discarding signals which are of poor quality. This option is quite beneficial in the field as a tool to further enhance the signals.

As the relative phase of the two signals is of interest (as opposed to absolute phase) the signals are triggered internally; that is the records are captured at about the time the first half sine wave of the impulse passes by the first receiver. A pretriggering delay, for inspection of a small portion of the record before the arrival of the actual signal is chosen as discussed later in this section. The range of the frequencies (bandwidth) is also selected. As a rule of thumb, for each measurement the optimum bandwidth is obtained when more than three-fourth of the frequency range is of good quality (generally, identified by a coherence value greater than 0.90).

The HP5423A digitizes each record into 256 points. Time length, T, and frequency bandwidth, F, are related by the number of points digitized, N, by:

$$N = F \cdot T \quad (A.1)$$

So that if either the bandwidth or time length is set, the other will be set automatically by the analyzer. This matter is of importance because if good resolution in the frequency domain is sought, the resolution in the time domain may be poor and vice versa. For SASW

MEASUREMENT STATE

MEASUREMENT :	TRANSFER FUNCTION		
AVERAGE :	20	, STABLE	
SIGNAL :	RANDOM		
TRIGGER :	FREE RUN	, CHNL 1	

CENT FREQ :	0.0 HZ	AF :	100.000 HZ
BANDWIDTH :	25.0000 KHZ		
TIME LENGTH :	10.0000 $\mu$ S	AT :	0.70582 $\mu$ S

CHAN #	RANGE	AC/DC	DELAY	CAL (EU/V)
* 1	10 V	DC	0.0 S	1.00000
* 2	10 V	DC	0.0 S	1.00000

Figure A.7 - Default Measurement State of Analyzer.

MEASUREMENT STATE

MEASUREMENT :	TRANSFER FUNCTION		
AVERAGE :	5	, STABLE	
SIGNAL :	IMPACT		
TRIGGER :	INTERNAL	, CHNL 1	

CENT FREQ :	0.0 HZ	AF :	1.56250 HZ
BANDWIDTH :	400.000 HZ		
TIME LENGTH :	040.000 $\mu$ S	AT :	025.000 $\mu$ S

CHAN #	RANGE	AC/DC	DELAY	CAL (EU/V)
* 1	1 V	DC	-20.0000 $\mu$ S	1.00000
* 2	1 V	DC	-20.0000 $\mu$ S	1.00000

Figure A.8 - A Typical Measurement State Used in SASW Tests.

testing, good resolution in the frequency domain is important. Therefore, good resolution in the time domain is often not achieved. The analyzer is programmed to prevent frequency aliasing (i.e. distortion of the frequency domain functions obtained from the time domain records which are digitized with large sampling intervals) so that the resolution of the time domain records is adequate for Fourier transforming.

The phase information of cross power spectra of a series of tests performed on a pavement site with three different bandwidths are shown in Fig. A.9. The curves are quite similar as illustrated in the figure. Thus, the bandwidth selected did not significantly affect the record in the frequency domain. However, as the bandwidth increases, the resolution in the frequency domain decreases which results in loss of resolution in the dispersion curve. For a record with a long time length (relative to the duration of the signal), if a time signal is transformed into the frequency domain and then inverse-transformed back into the time domain, the results are usually of no value and may be significantly aliased.

As an example of transforming the signal between the time and frequency domains, an accelerometer was set on a concrete floor, and signals generated by a drop hammer were monitored as shown in Fig. A.10. In Fig. A.10a the time record was obtained by setting the time length to 100 msec. The lower record, Fig. A.10b, corresponds to the inverse-transform of the linear spectrum of a time record with a time length of 1 sec. The reproduceability of the original signal was assured by repeating the test several times and by controlling the height and location of the drop. The difference between the two signals is quite evident.

The voltage range expected to be generated by the receivers also has to be set. Generally, this range should be set as low as possible to gain the best resolution possible. In fact, if the range is set too high relative to the magnitude of the signal, either the machine will not be able to trigger or the record will be somewhat erroneous. To demonstrate this point, the signals from one accelerometer connected to both channels of the recorder are shown in Fig. A.11. The voltage

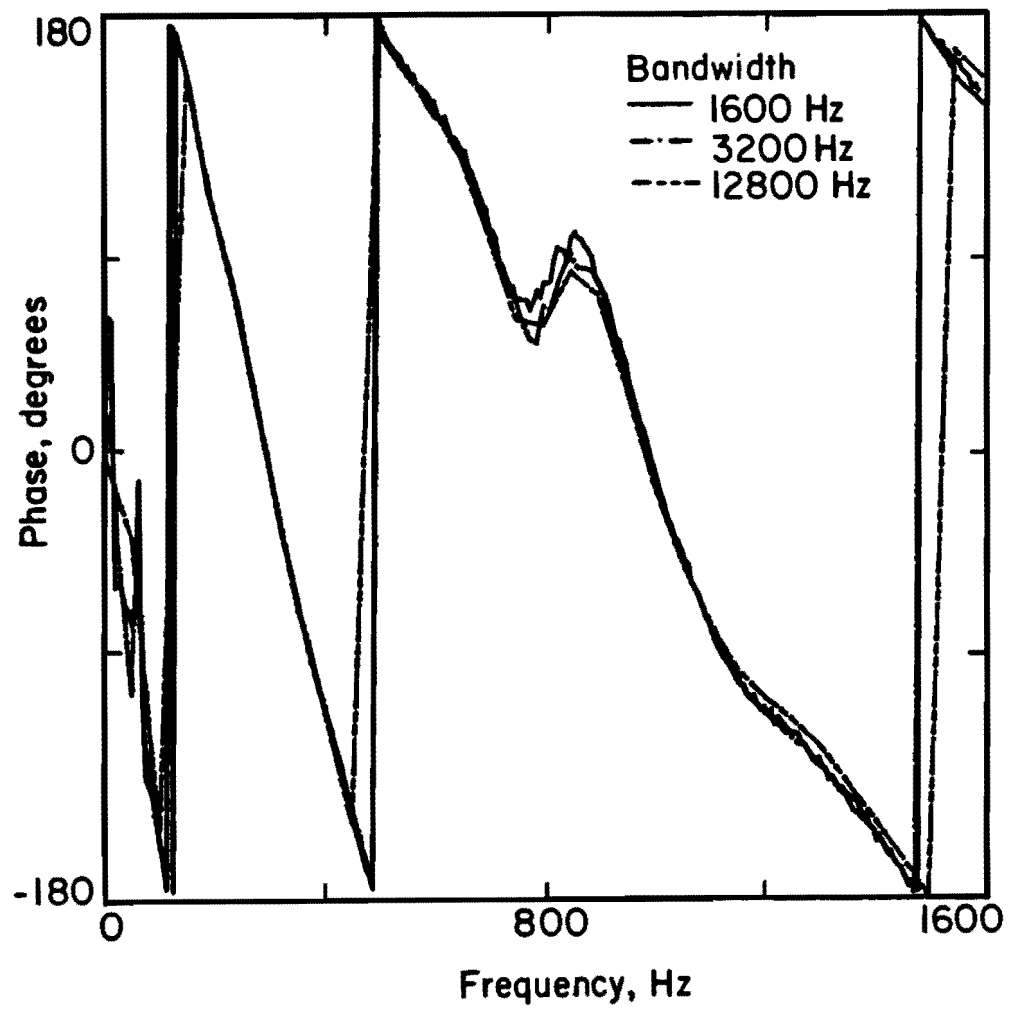
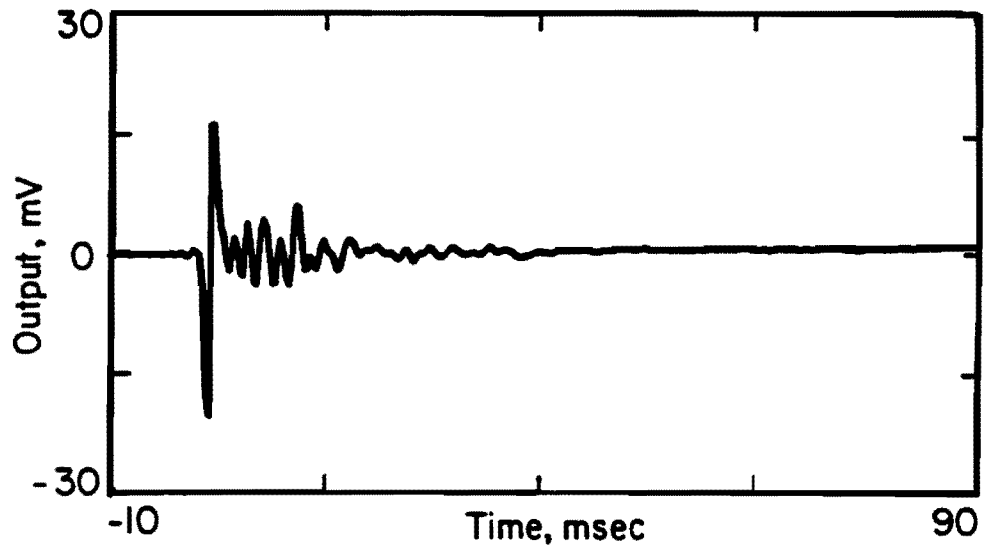
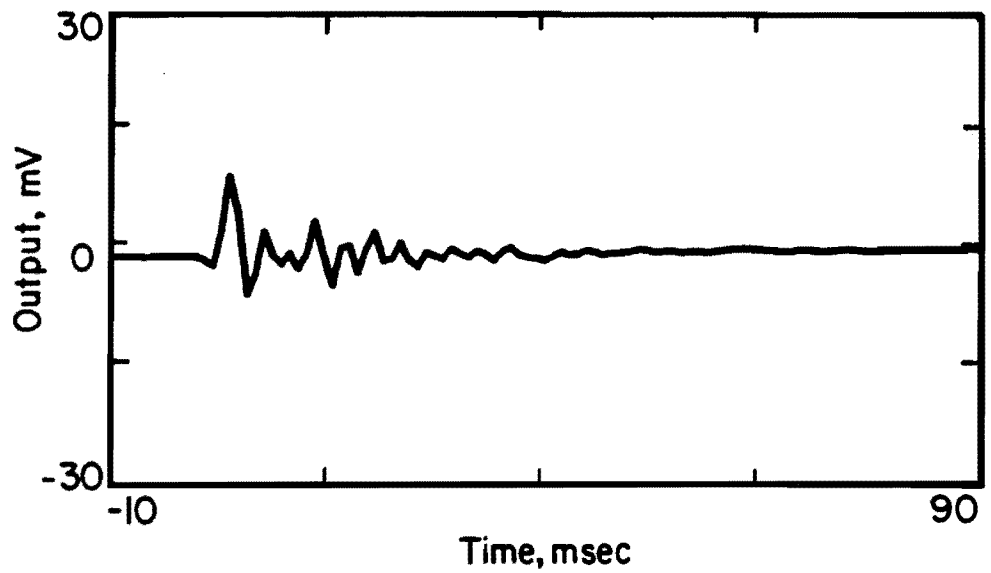


Figure A.9 - Phase Information of Cross Power Spectra from Different Bandwidths.

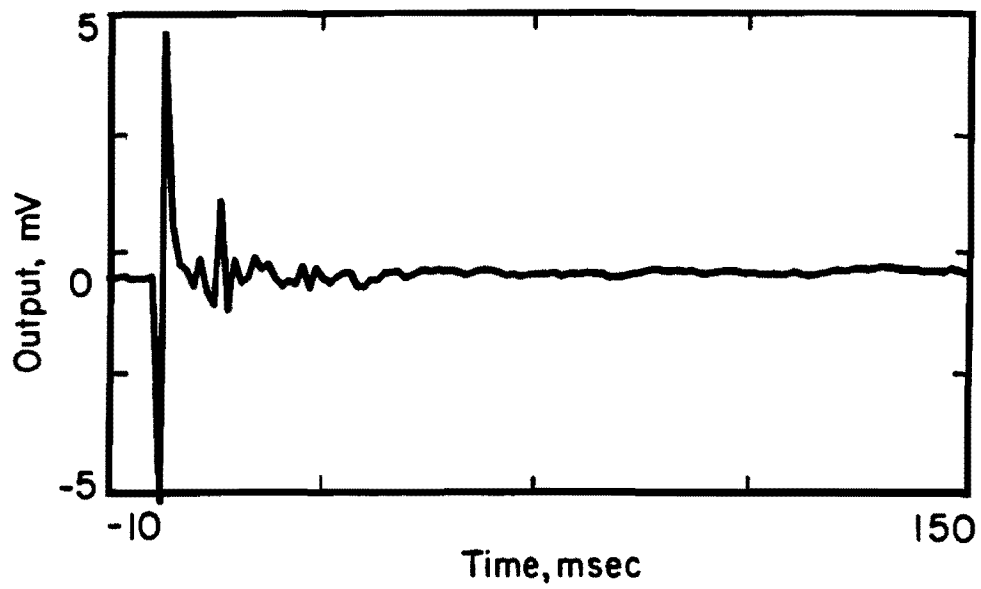


a. Bandwidth of 800 Hz.

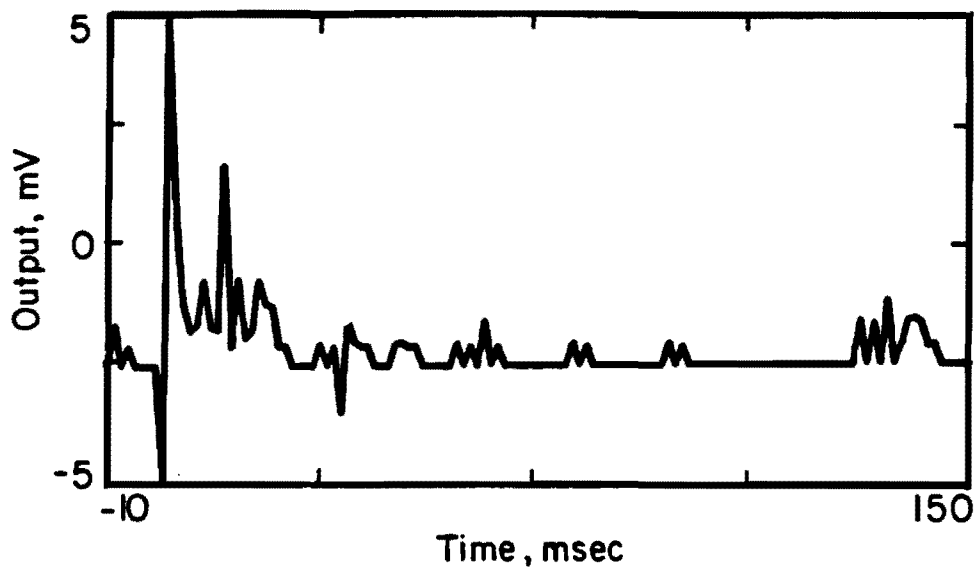


b. Bandwidth of 128 Hz.

Figure A.10 - Effect of Bandwidth on Time Domain Records.



a. Sensitivity of 100 m Volts



b. Sensitivity of 5 Volts.

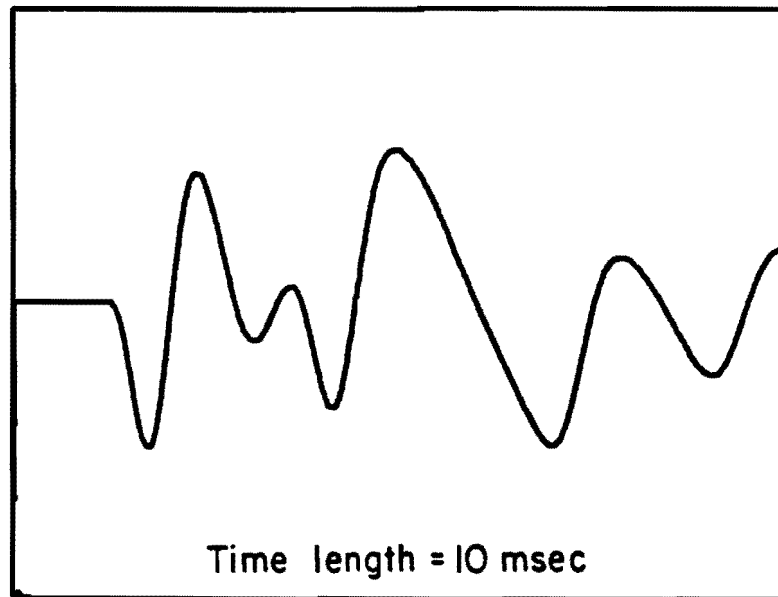
Figure A.11 - Effect of Sensitivity of Recording Channels on Time Records.

range for channel one (Fig. A.11a) and channel two (Fig. A.11b) were 0.1 and five volts, respectively. The record from the second channel contains sharp peaks and troughs because of loss of resolution during digitization of the output voltage. Upon using identical ranges on both channels, the outputs were identical.

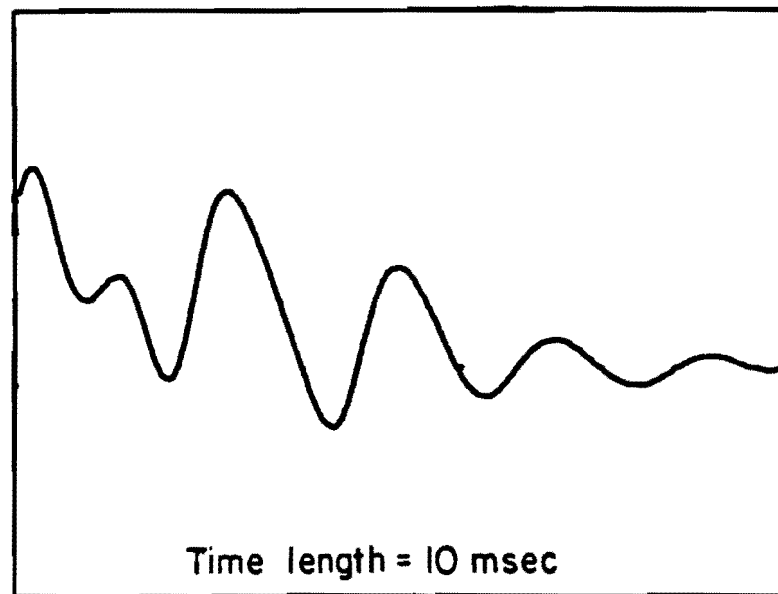
A negative time delay, also called a pretrigger delay, imposed on a signal allows the operator to inspect a small portion of the record before the arrival of the actual signal at the first receiver. For triggering a signal, the voltage and slope of the first major event to be captured are set. The effect of voltage is discussed above. If the slope is too flat, the recorder may not be able to trigger. However, if the slope is too steep, part of the major signal may be lost during testing. Travel time records from a geophone set on a concrete floor are shown in Fig. A.12. In the first case (Fig. A.12a), a pretriggering delay was imposed on the signal. In the lower trace (Fig. A.12b), the delay was omitted, and the test was repeated. By comparing these two records it can be seen that a major portion of the travel time record in the second case is lost. The importance of the pretrigger delay is that the operator can detect this undesirable loss of signal and can make the appropriate adjustments. Pretriggering should be identical for both channels or a false internal phase will be introduced between the two signals. Also, experience has shown that the duration of the pretriggering delay should be on the order of ten percent of the time length sampled.

#### **A.4 POWER SUPPLY**

The power supply used is a portable generator with a maximum power of two kva. A signal conditioner is placed between the generator and recorder to minimize voltage fluctuations so as to regulate the voltage before entering the analyzer. The frequency and voltage of the current generated by the power supply should be checked before the test, as the performance of digital recorders are quite sensitive to the quality of the input power.



a. With Pretriggering



b. Without Pretriggering

Figure A.12 - Effect of Pretriggering Delay on Signal.

### A.5 SUMMARY

The practical aspects and equipment used in SASW testing were discussed in this chapter. It is shown that:

1. seismic signals can be effectively enhanced by averaging,
2. many external parameters having undesirable effects on testing can be minimized by reversing the source, and
3. the CRMP geometry reduces scatter in the dispersion curve.

Equipment necessary for performing SASW tests are an appropriate source, high quality receivers and a spectral analyzer. The source should be able to generate surface waves over a wide range of frequencies. Two types of receivers can be used, geophones and accelerometers, depending on receiver spacing. A spectral analyzer accelerates substantially the testing time and has essential features such as rapid determination of the coherence function which can ensure the quality of the signals in the field and the ability to trigger the signals internally.

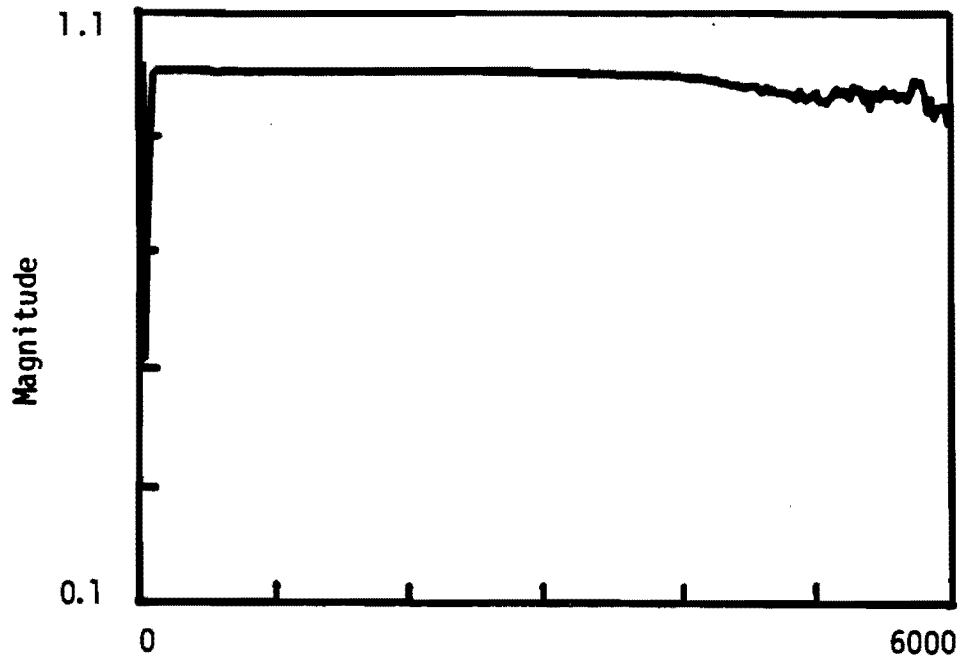
## APPENDIX B

### CONSTRUCTION OF A DISPERSION CURVE FOR A FLEXIBLE PAVEMENT SITE

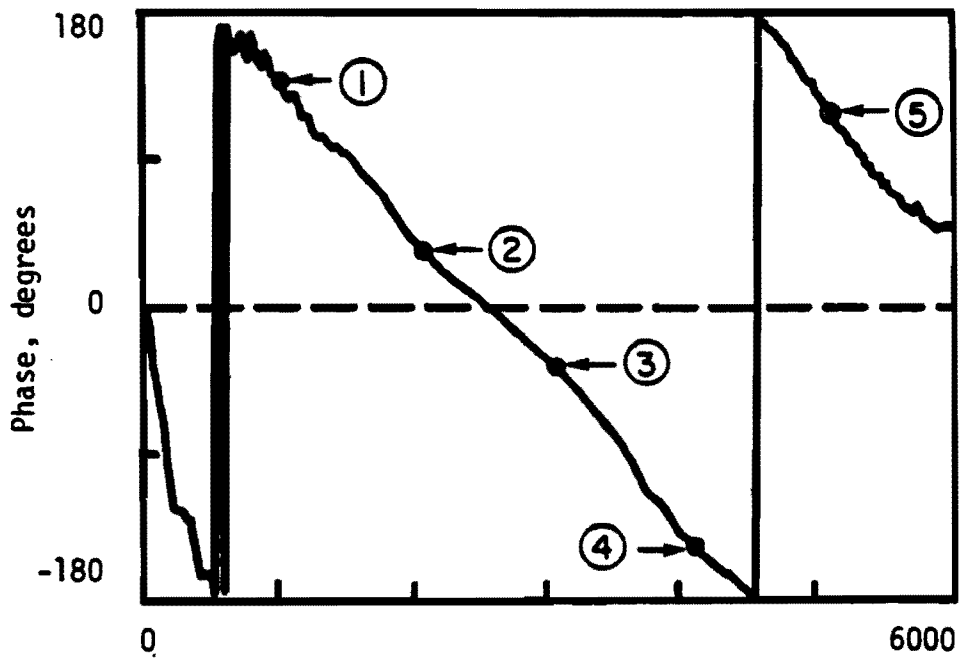
A typical coherence function and phase information from the cross spectrum measured with a receiver spacing of one ft (30 cm) on a flexible pavement site are shown in Fig. B.1. The dispersion curve from the cross power spectrum shown in Fig. B.1b is given in Fig. B.2. Every sixth data point is plotted so that the five points marked 1 to 5 in Fig. B.1b can be clearly illustrated in Fig. B.2. The higher resolution for higher frequencies can easily be appreciated in Fig. B.2.

Figure B.3 shows the actual dispersion curve with all points included after Heisey's criteria is applied. Also shown is the reverse profile and average profile actually being used in construction of the final dispersion curve. The forward and reverse profiles are in good agreement and do not deviate by more than about five percent over the range of wavelengths shown.

Following the general procedure presented in Section 5.3, the final dispersion curve is obtained as illustrated in Fig. B.4.



a. Coherence Function



b. Cross Power Spectrum

Figure B.1 - Typical Spectral Analysis Measurements on a Flexible Pavement.

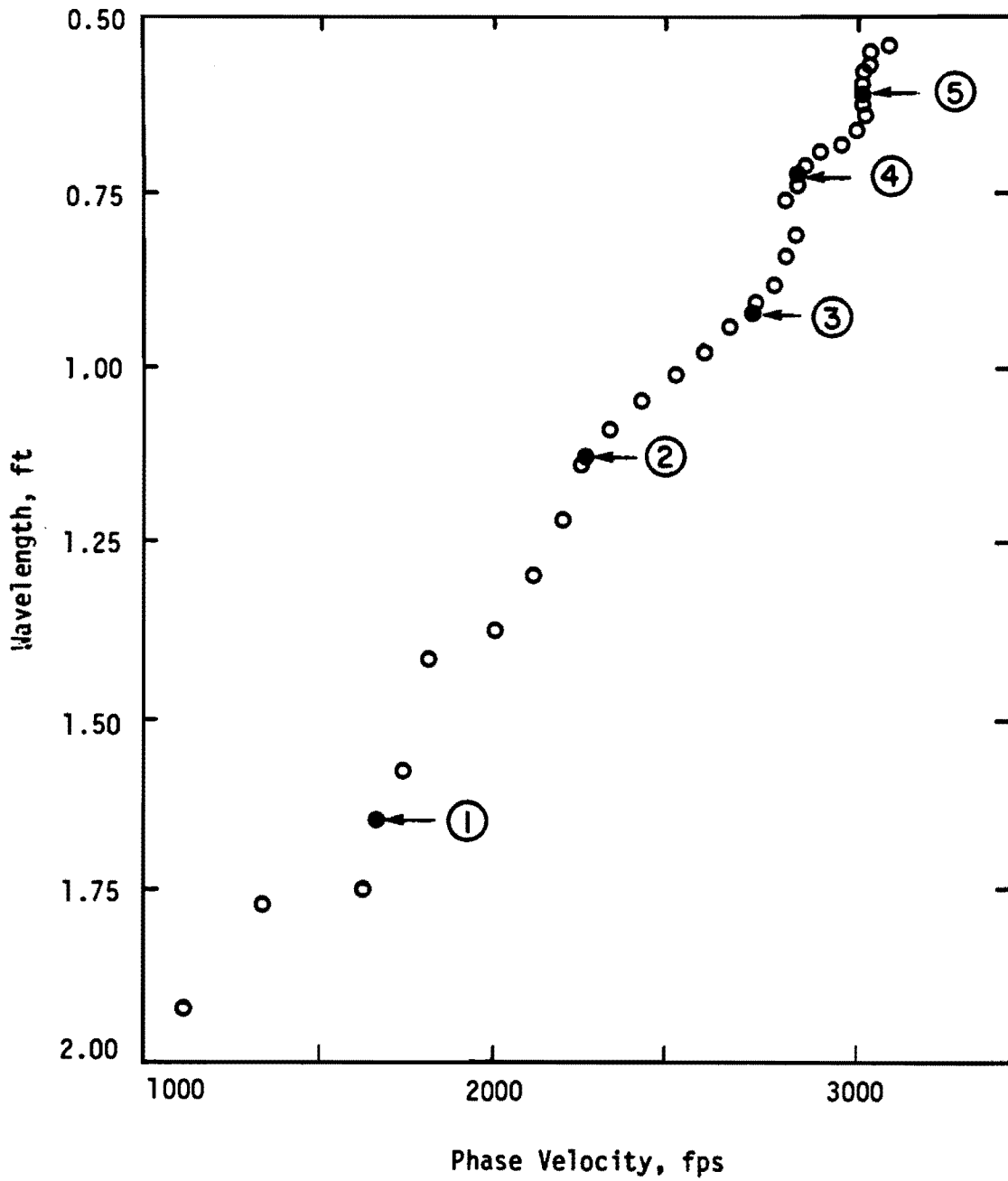


Figure B.2 - Dispersion Curve Constructed from Phase Information of Cross Power Spectrum at Pavement Site (from Figure B.1b).

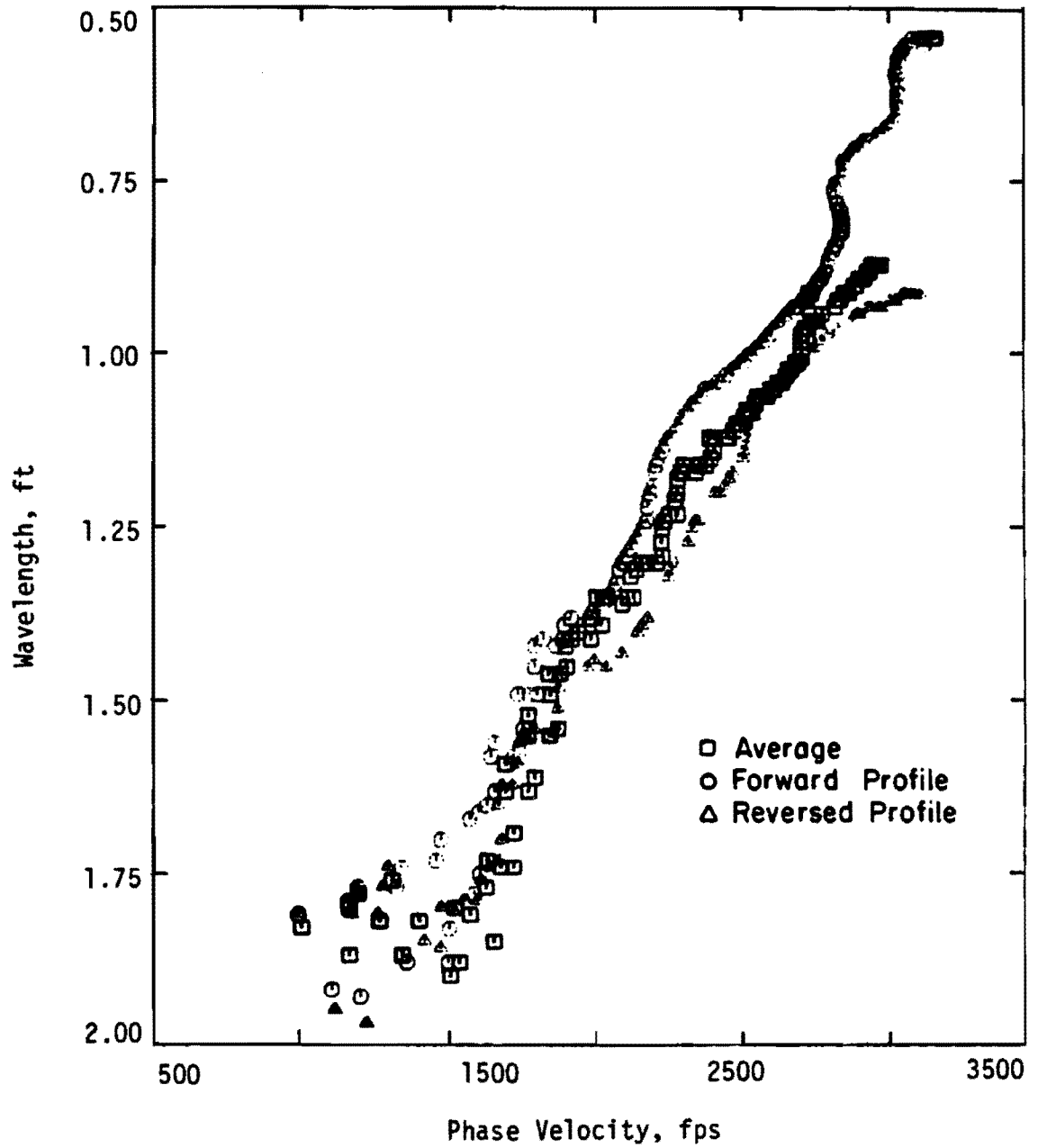


Figure B.3 - Comparison of Dispersion Curve from Forward and Reverse Profiles at Pavement Site.

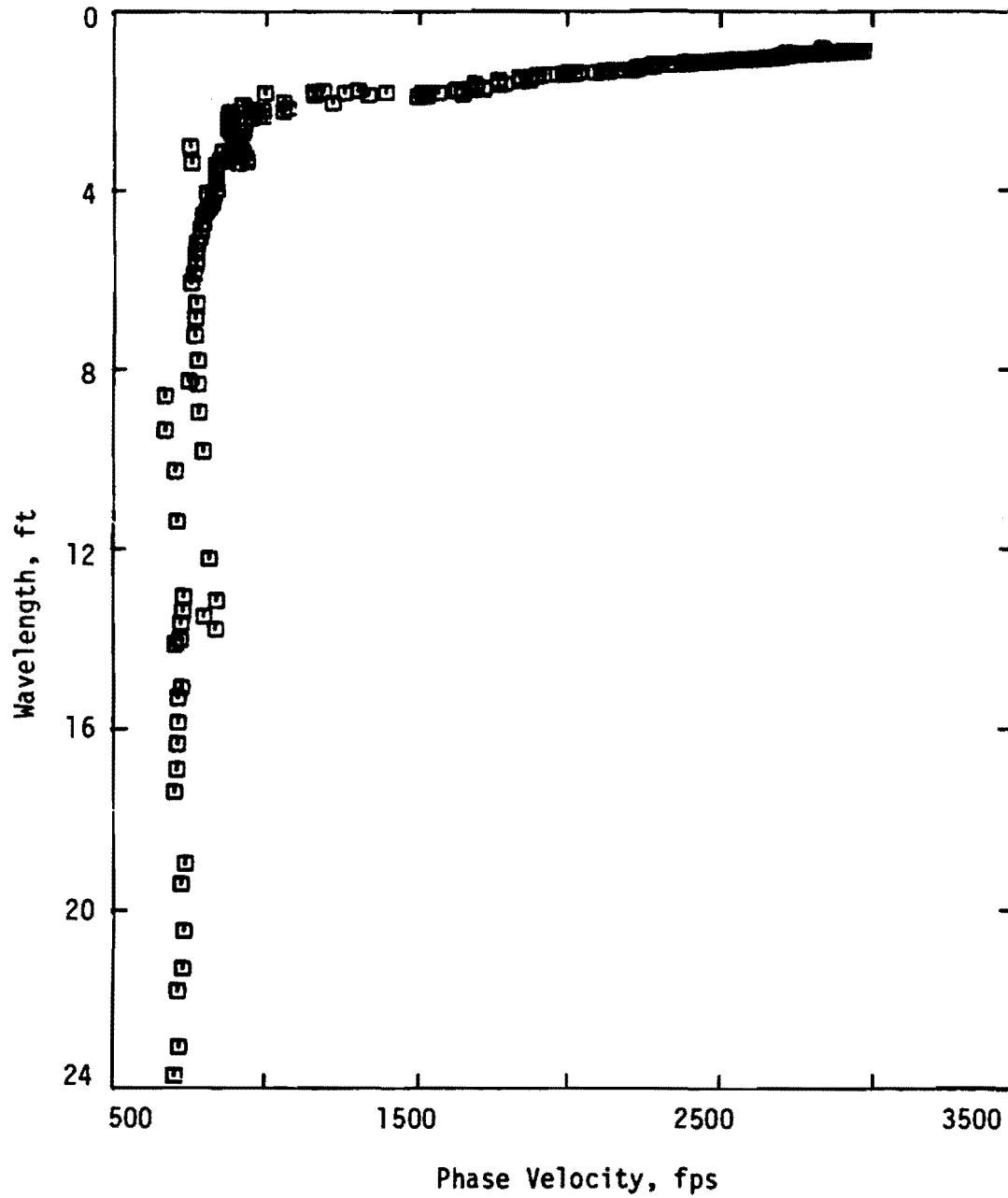


Figure B.4 - Dispersion Curve from All Receiver Spacings for Flexible Pavement Site.

This page replaces an intentionally blank page in the original.

-- CTR Library Digitization Team

**APPENDIX C**

**COMPARISON OF THEORETICAL AND EXPERIMENTAL DISPERSION  
CURVES AFTER COMPLETION OF INVERSION PROCESS AT WILDLIFE  
SITE**

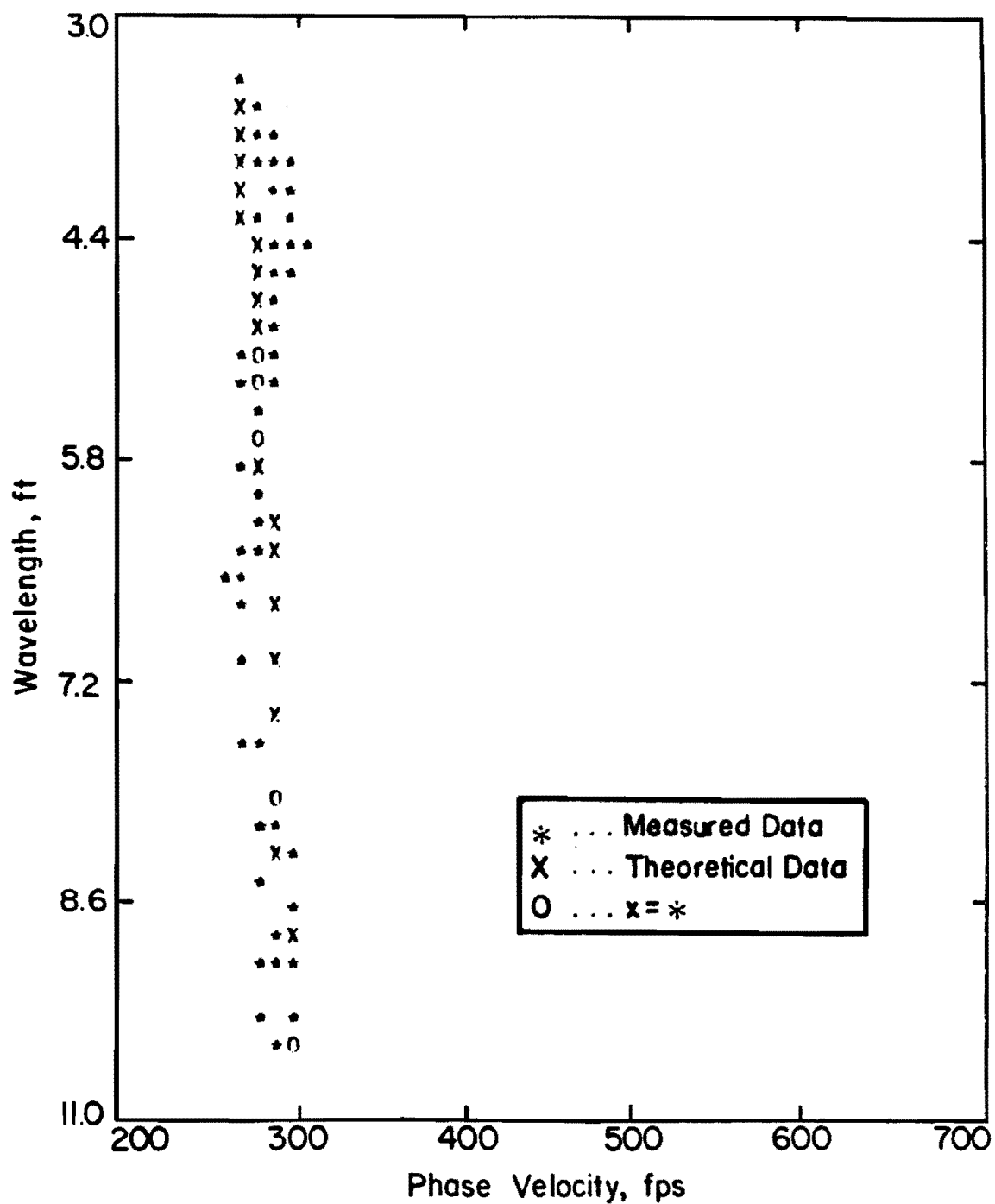


Figure C.1 - Comparison of Theoretical and Experimental Dispersion Curves after Completion of Inversion Process at Wildlife Site (Range of Wavelengths of 3 to 10 ft).

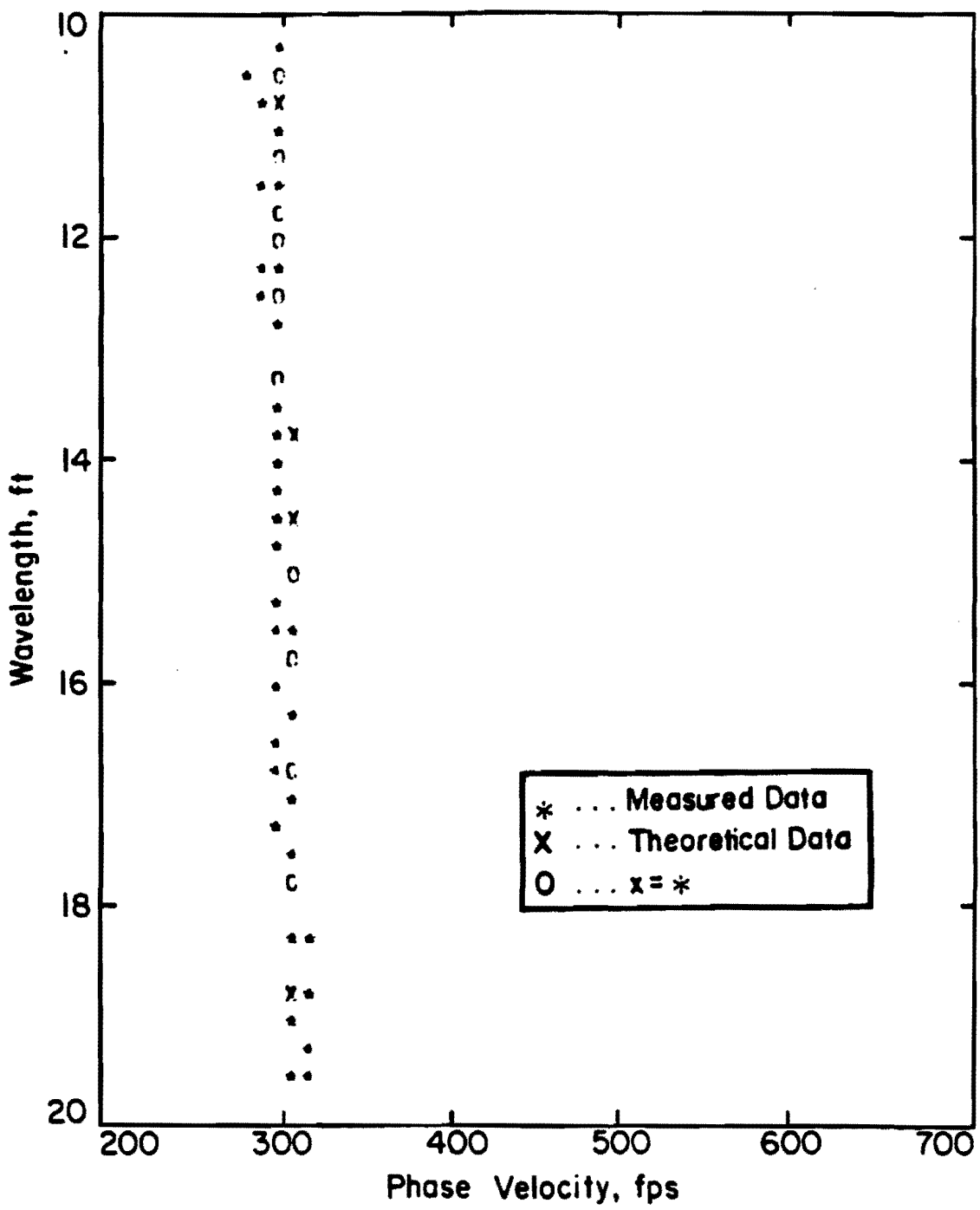


Figure C.2 - Comparison of Theoretical and Experimental Dispersion Curves after Completion of Inversion Process at Wildlife Site (Range of Wavelengths of 10 to 20 ft).

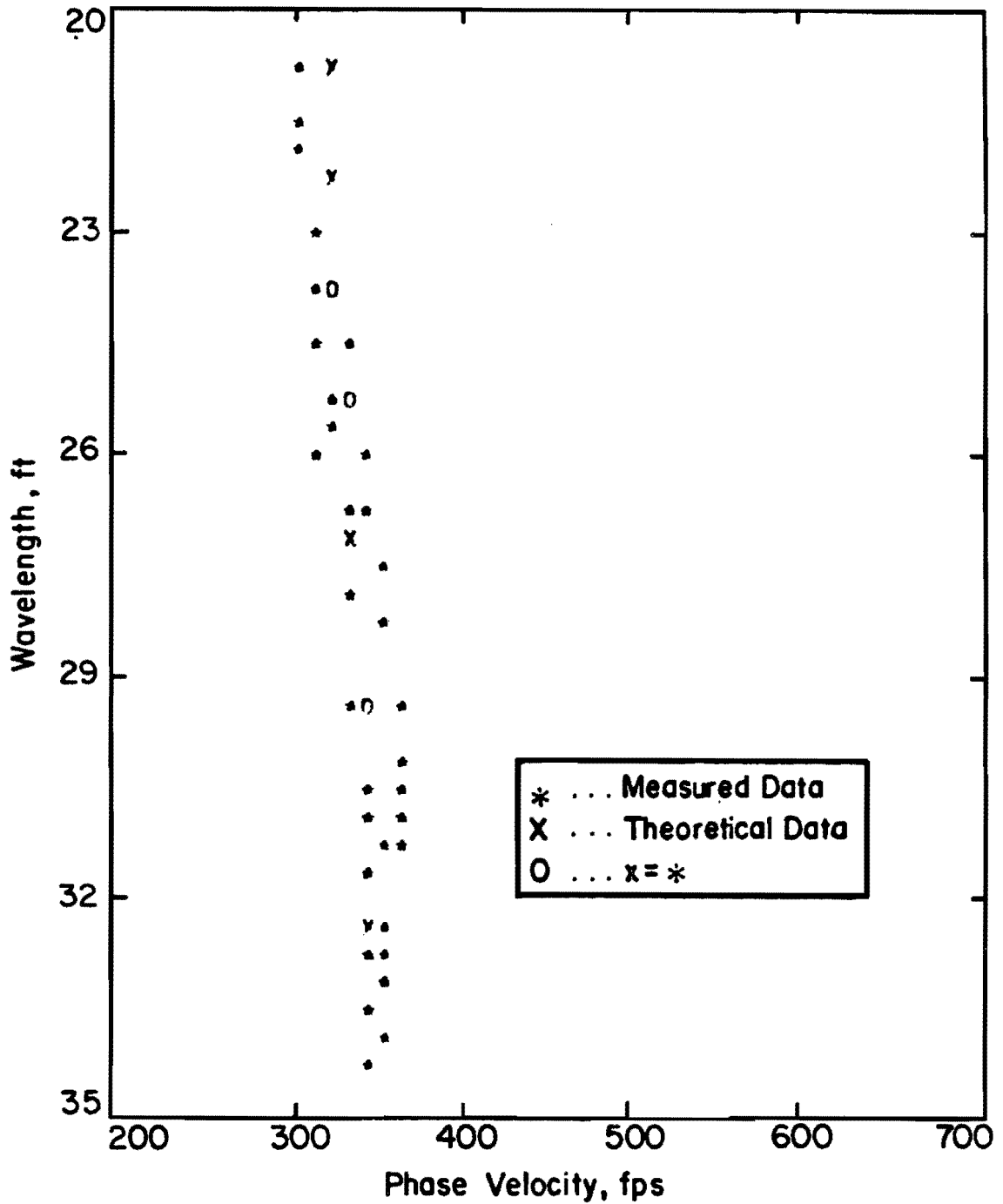


Figure C.3 - Comparison of Theoretical and Experimental Dispersion Curves after Completion of Inversion Process at Wildlife Site (Range of Wavelengths of 20 to 35 ft).

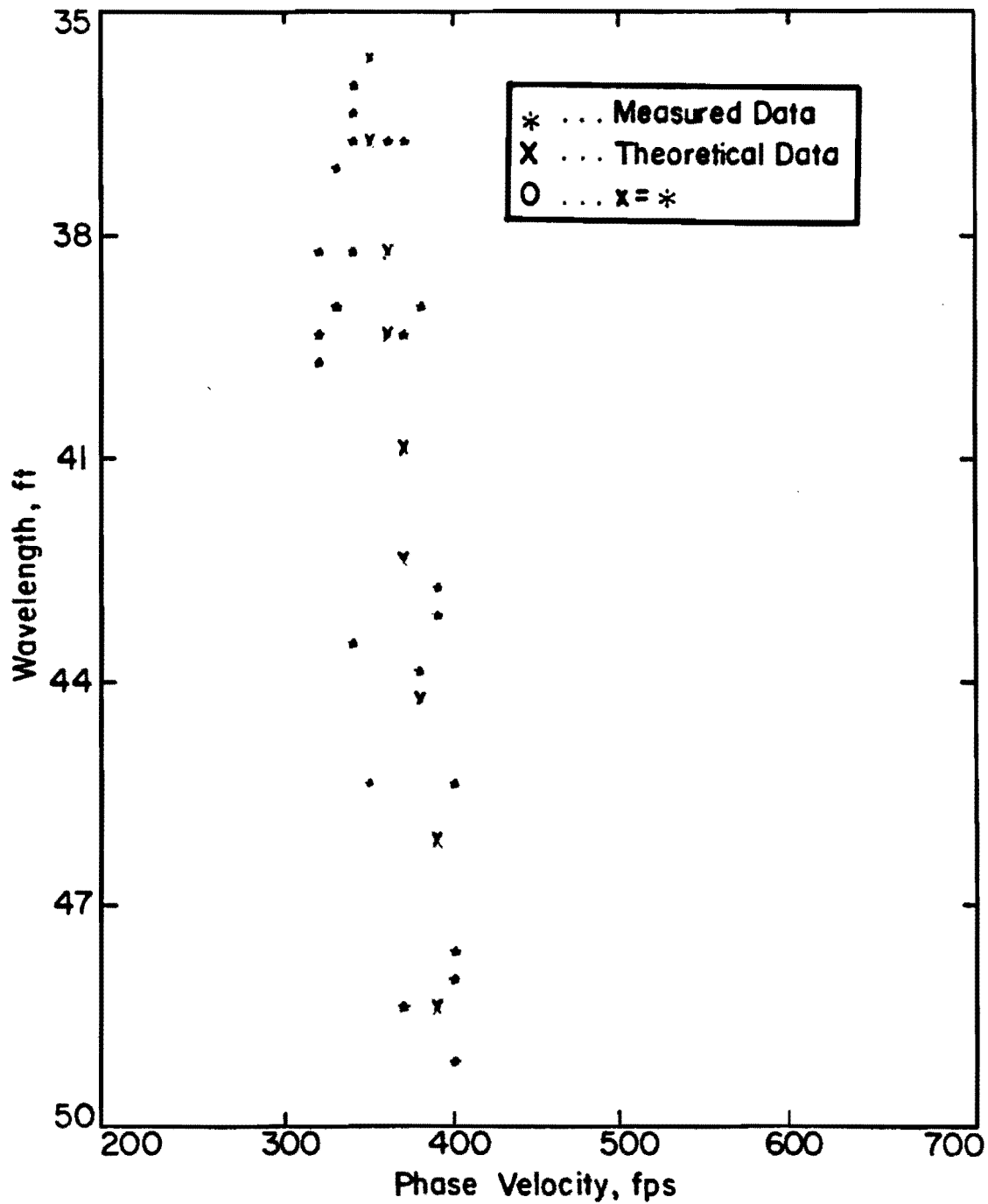


Figure C.4 - Comparison of Theoretical and Experimental Dispersion Curves after Completion of Inversion Process at Wildlife Site (Range of Wavelengths of 35 to 50 ft).

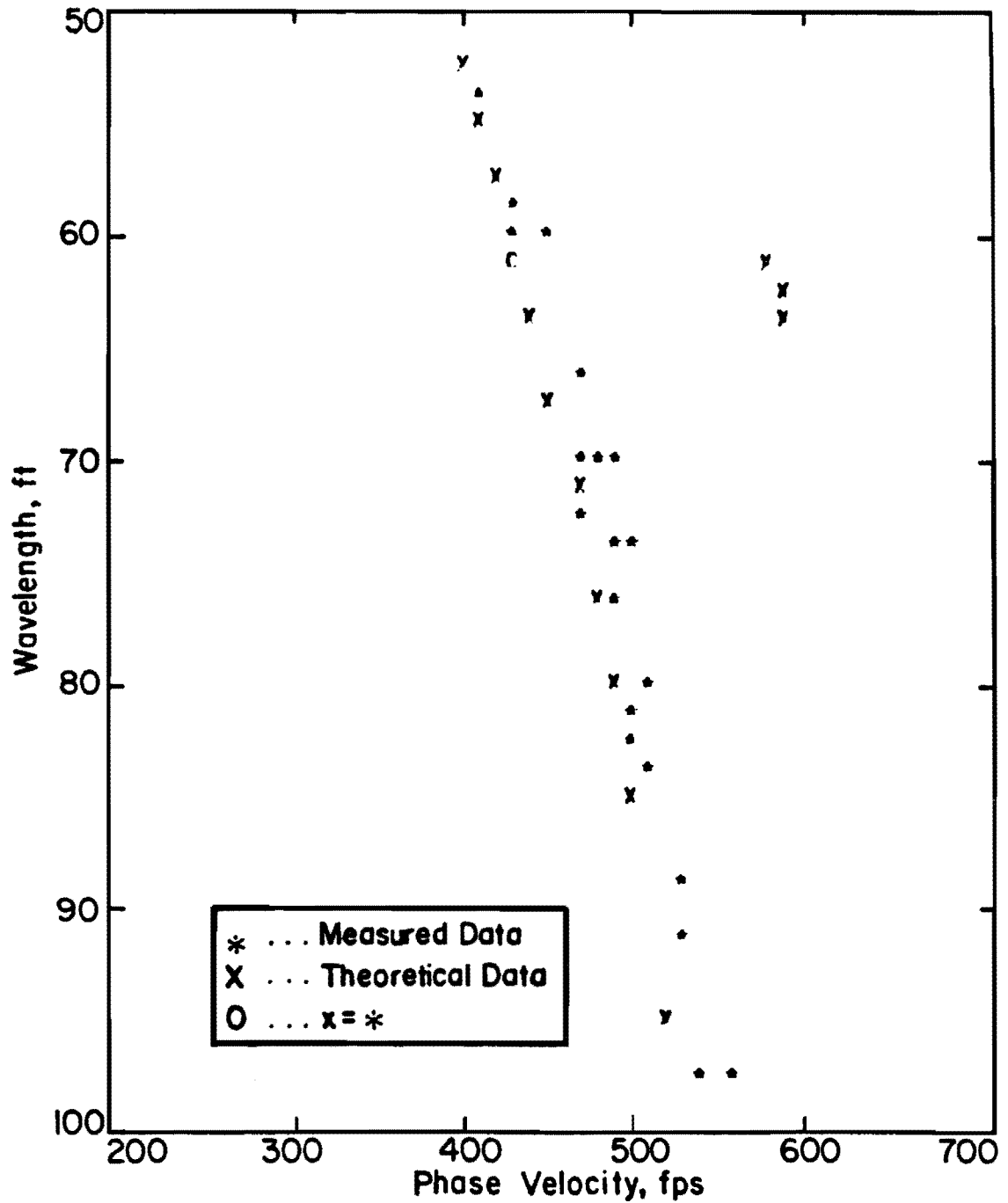


Figure C.5 - Comparison of Theoretical and Experimental Dispersion Curves after Completion of Inversion Process at Wildlife Site (Range of Wavelengths of 50 to 100 ft).

**APPENDIX D**  
**COMPARISON OF THEORETICAL AND EXPERIMENTAL DISPERSION**  
**CURVES AFTER COMPLETION OF INVERSION PROCESS AT A FLEXI-**  
**BLE PAVEMENT SITE**

The experimental and theoretical dispersion curves after the matching process has been completed are shown in Figs. D.1 through D.6. These curves are presented on expanded scales to show the accuracy of the match. This site is the one shown in Appendix B where development of the dispersion curve is illustrated.

It can be seen that the experimental and theoretical curves are in good agreement, with the average difference on the order of plus or minus five percent. However, around wavelengths of 1.8 to 2.0 ft (54 to 60 cm) where the transition between the pavement system and subgrade is expected, a portion of the curve cannot be matched due to a sharp change in the velocity. This is a typical characteristic of transition zones and occurs universally in dispersion curves of pavement systems measured in this study. Practically speaking, these transition zones appear either as a step in the dispersion curve or as data which is so erratic that, during construction of the dispersion curves, the data points in this range do not fulfill the statistical criterion discussed in the last section. Scatter in the data in the upper part of Fig. D.3 illustrate the erraticness in the transition zone.

Another point of interest is the presence of jumps in the theoretical curve like the one shown in Fig. D.4. These jumps occur in the vicinity of shear wave velocities of layers when a big contrast in velocities is present. This is due to a weakness in the program, and, at these boundaries phase velocities are somewhat inaccurate.

The shear wave velocity profile after inversion is presented in Fig. D.6. More discussion of this site is presented in Section 7.3.1.

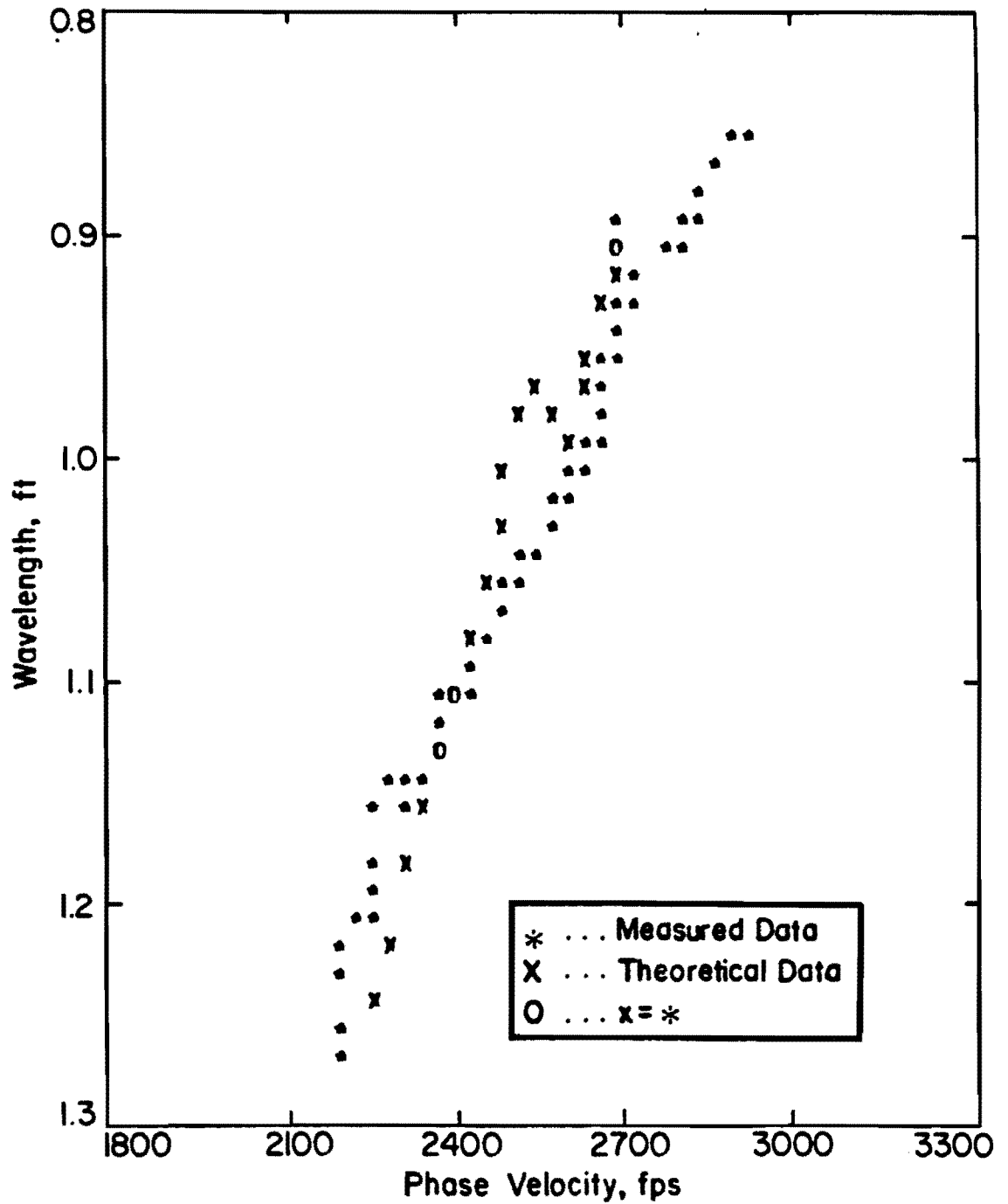


Figure D.1 - Comparison of Theoretical and Experimental Dispersion Curves after Completion of Inversion Process at Pavement Site (Range of Wavelengths of 0.80 to 1.30 ft).

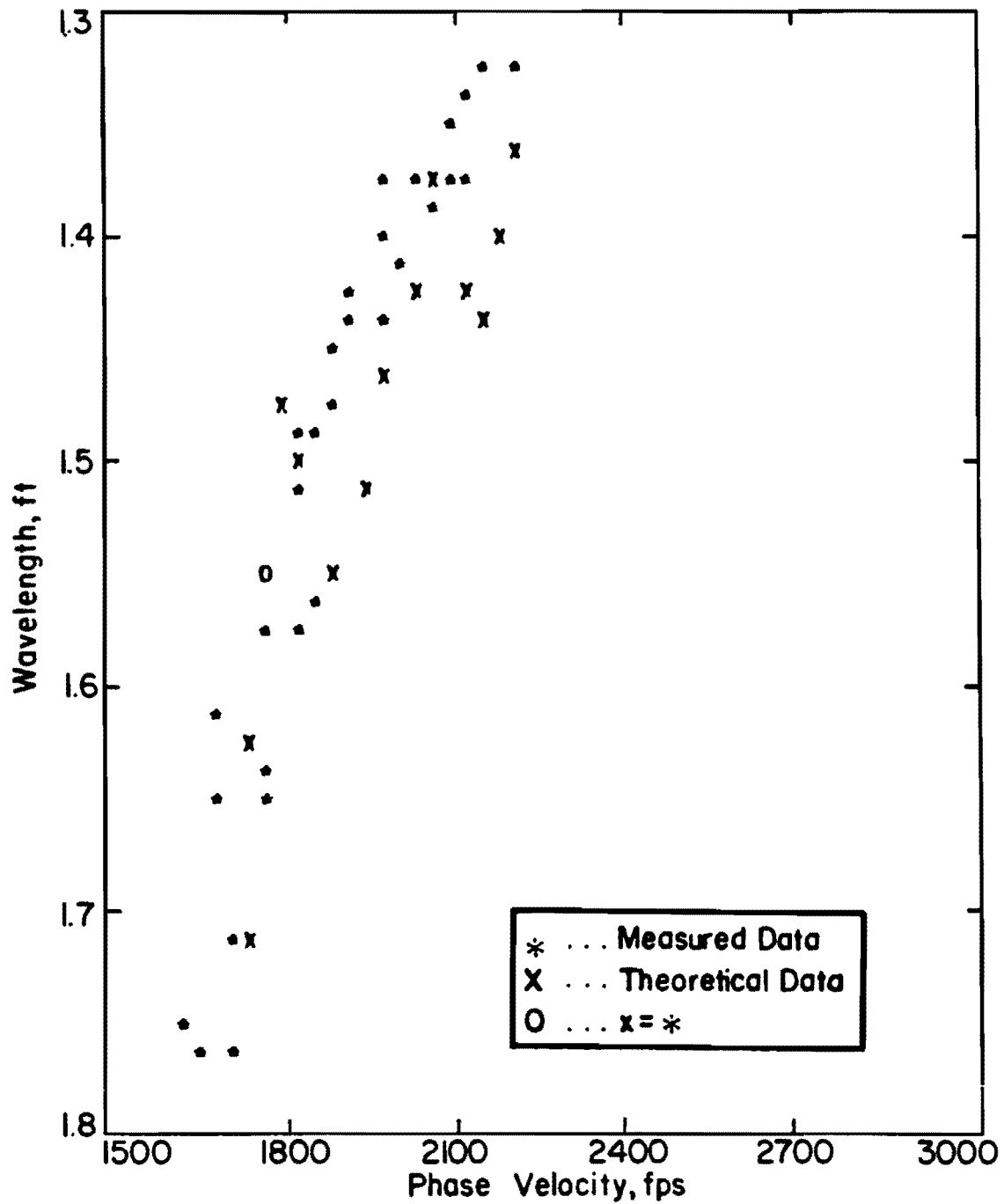


Figure D.2 - Comparison of Theoretical and Experimental Dispersion Curves after Completion of Inversion Process at Pavement Site (Range of Wavelengths of 1.30 to 1.80 ft ).



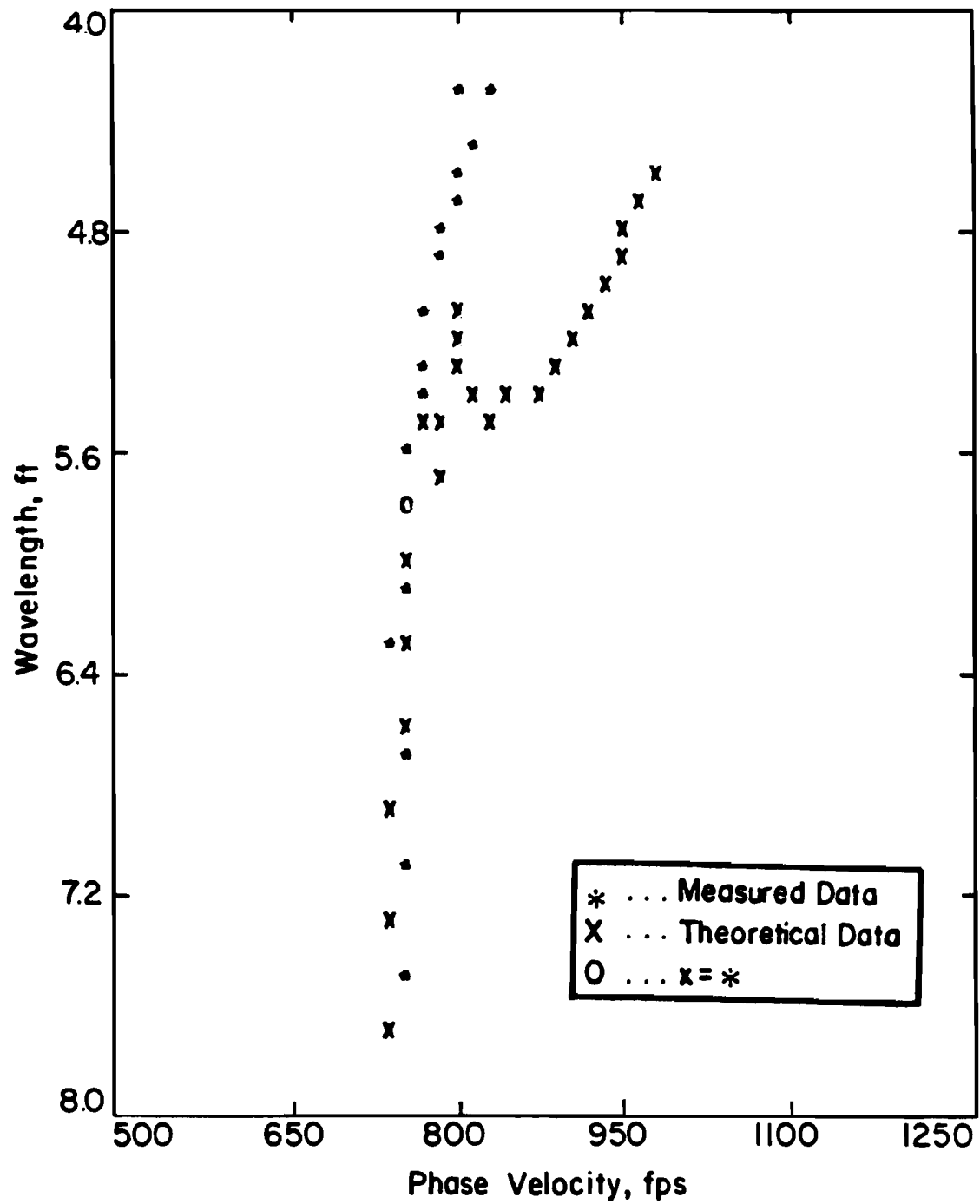


Figure D.4 - Comparison of Theoretical and Experimental Dispersion Curves after Completion of Inversion Process at Pavement Site (Range of Wavelengths of 4 to 8 ft).

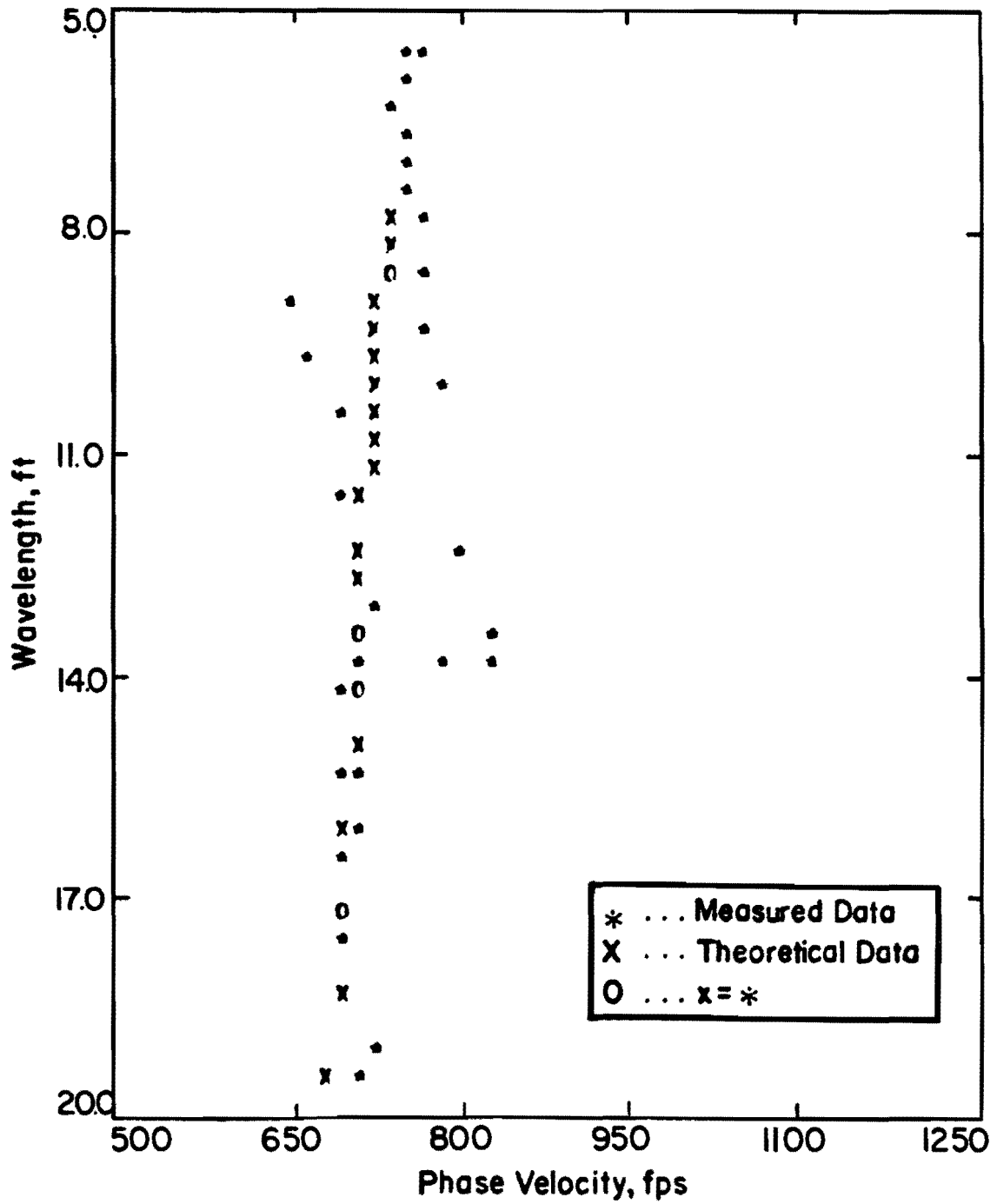


Figure D.5 - Comparison of Theoretical and Experimental Dispersion Curves after Completion of Inversion Process at Pavement Site (Range of Wavelengths of 5 to 20 ft).

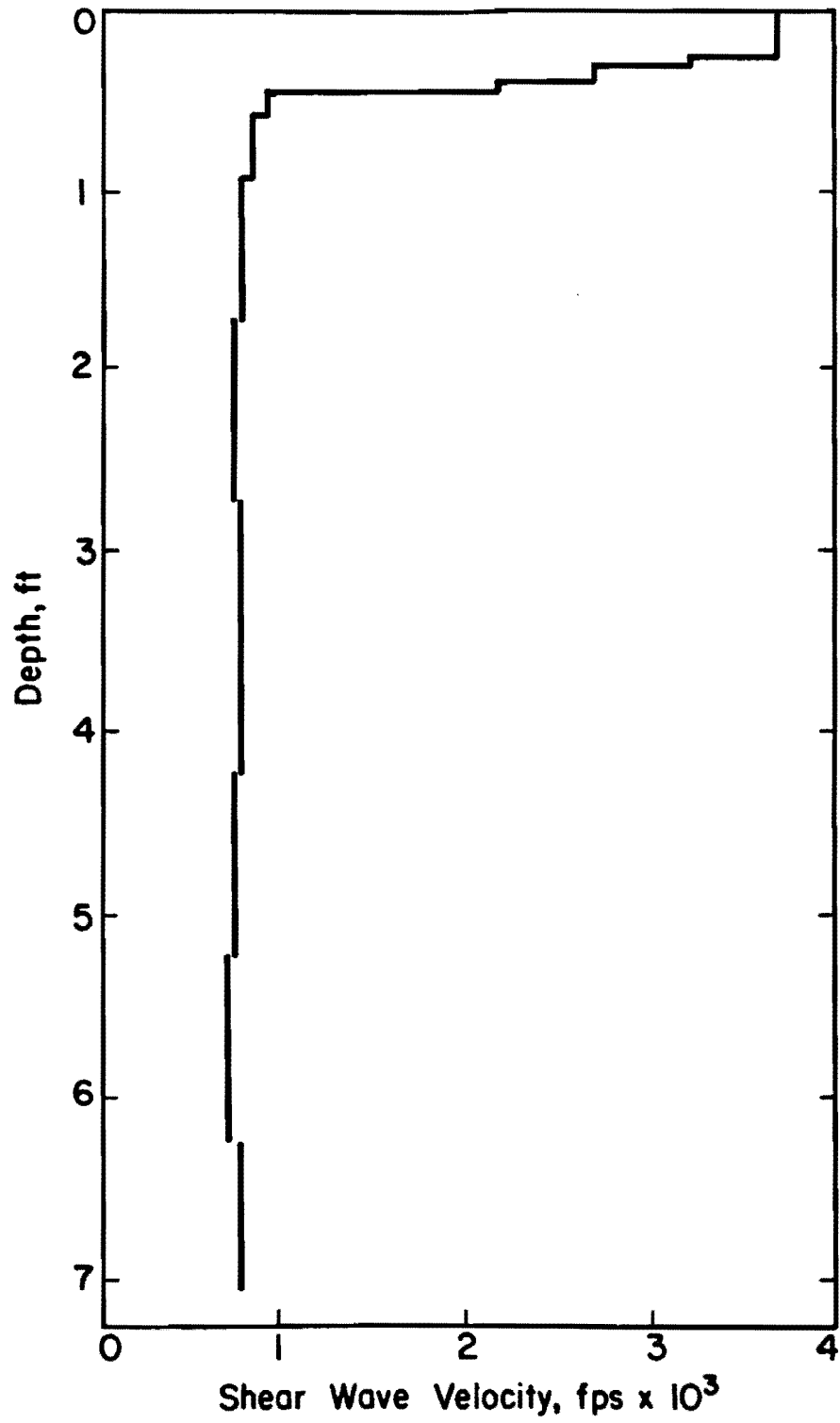


Figure D.6 - Shear Wave Velocity Profile of the Flexible Pavement Site after Completion of Inversion.